University of Stavanger

Faculty of Science and Technology

MASTER'S THESIS

Study program/ Specialization: Petroleum Engineering	Spring semester, 2011 Open
Writer: Harald Frette Litlehamar	…… (Writer's signature)
Faculty supervisor: Professor Kjell Kåre Fjelde External supervisor(s): Helge Saure (Transocean)	
Title of thesis: Well Control Procedures and Simulations	
Credits (ECTS): 30	
Key words: - Well control - Kick - Kick simulator - AUSMV	Pages: 97 + enclosure: 20 Stavanger, June 15th 2011 Date/year

Abstract

A brief introduction is given to a range of well control procedures. It was found that many of the procedures rely on a set of simplifying assumptions. This is particularly true in the hand calculations for designing a well kill. This set of assumptions was used to define an analytical model. The premises of the analytical model and some of the procedures were tested in a crude kick simulator. The main objective of this thesis was to verify some of the well control procedures, and to shed light on their limitations. Particular attention was given to driller's method for a vertical and horizontal well. Additionally, simulations were run to investigate the worst case scenarios which a well might be subjected to if well control is lost.

As a means for achieving this, the previously implemented explicit numerical AUSMV scheme was used as a basis for simulations on a kicking well. However, in order to conduct realistic simulations some modifications to the scheme had to be introduced. The most important modification was the implementation of a PI-regulator, as it proved impossible simply to set the bottomhole pressure to a defined constant value in the numerical scheme. Extensive tuning of the regulator was necessary for it to perform satisfactory. In this process, a novel alternative to the classical PI-regulator was discovered.

Further modifications deemed necessary:

- Improved accuracy in reading of bottomhole and choke pressures.
- Implementation of additional topside parameters (pit gain, drillpipe pressure)
- A more realistic friction model.
- Changing the liquid component of the system from water to drilling fluid (altering the liquid density).
- A chokeline and riser for simulation on subsea wells.
- Opening up for wellbore deviation.
- A Darcy relation for influx where influx size and mass rate depends on downhole pressure differential. This is important for drilled kicks or connection kicks.
- Additionally, a choke model was implemented in the model, but it has not been used in the simulations. The choke model depicts the backpressure as a function of fluid density, flow rate and choke opening.

By use of the crude kick simulator, simulations were run for a vertical and a horizontal well. The results obtained by the kick simulator were compared to hand calculations. The main discovery was that although the hand calculations produce slight errors, the errors exclusively functions as additional safety margins with respect to downhole pressure differential.

It was also found that a gas bubble migrating in a shut-in annulus subjects the well to higher loads than the gas filled well scenario.

Acknowledgement

I would like to thank professor Kjell Kåre Fjelde for outstanding help and guidance in the work with my thesis. He has kept his office door open at all times. Thank you for sharing your insight in the well control discipline, for helping out with Matlab programming and for being a great conversation partner.

Further, I am very grateful to toolpusher Helge Saure and Transocean. He sent me to an IADC well control course, which was very helpful. I was also allowed to use Transocean's well control handbook. He was also partially responsible for the subject of the thesis. "It is all about the procedures," he said.

Some of my friends at the university also require particular attention. Stian Molvik has been writing a thesis on the theoretical aspects of the AUSMV scheme. Thank you for the inspiring discussions and for enlightening me! Andreas Davidsen, Kim Øvstebø, Ørjan Tveteraas and Johan Helleren have been keeping me with company when working long hours at the university. Thank you!

Finally, I would like to thank my family for all help, support and patience along the way.

Table of contents

1. Introduction

Classical well control is based on decades of experience from worldwide drilling operations. In the early days of offshore drilling, most wells were drilled in shallow water with simple wellbore geometries. Over the years, the boundaries of drilling have continuously been pushed towards new extremes. The wells are getting deeper along with higher downhole pressures and temperatures, the waters are getting deeper and the wellbore geometries are getting more adventurous. Yet, there has been little change in the actual well control procedures and methods in use. In the aftermath of the recent events of the Macondo well in the Gulf of Mexico, there has been an increasing focus on safety and well control. Great effort has been made to investigate what went wrong, and to take lessons from the tragic accident.

This thesis aims at giving an introduction to a range well control methods presently in use. Further, the objective is to validate or shed light on the limitations of some of the procedures, using models and computer simulations on a kicking well. It will particularly be focused on well kill operations during conventional drilling operations from floating drilling units with subsea BOP.

The first sections of this thesis give a general overview of well control as a whole, and present a range of well control procedures and methods. The information is gathered from a variety of sources, and the objective is to briefly summarize the present status of the well control discipline. In the following sections, attempts are made to model a wellbore, both analytical and numerical. Having accurate wellbore models is important in order to understand the processes taking place during a well control situation. The presented analytical model is the basis for most of the classical well control formulas. However, some of the assumptions and implications of the analytical model may not be realistic. These are put to the test by the more advanced numerical two phase model.

As a means for well control related simulations, it was decided to use the previously implemented AUSMV scheme. This scheme has to be modified in order to make it more realistic and suitable for well control simulations. The most important extension to the numerical scheme is the implementation of a PI-regulator to control the bottomhole pressure, as it is not possible to simply set the bottomhole pressure to a constant value. Further necessary extensions and modifications are:

- Improved accuracy in reading of bottomhole and choke pressures.
- Implementation of additional topside parameters (pit gain, drillpipe pressure)
- A more realistic friction model.
- Changing the liquid component of the system from water to drilling fluid (altering the liquid density).
- A chokeline and riser for simulation on subsea wells.
- Opening up for wellbore deviation.
- A Darcy relation for influx where influx size and mass rate depends on downhole pressure differential. This is important for drilled kicks or connection kicks.
- Additionally, a choke model was implemented in the model, but it has not been used in the simulations. The choke model depicts the backpressure as a function of fluid density, flow rate and choke opening.

2. What is well control?

NORSOK D-010[1] defines well control as a «collective expression for all measures that can be applied to prevent uncontrolled release of well bore effluents to the external environment or uncontrolled underground flow».

API RP 59[2] defines a kick as an "intrusion of formation fluids into the wellbore."

This might not sound very dramatic. However, a kicking well may develop into a full scale blowout, if not handled properly. This may injure or kill people, and will damage the environment and property. Keeping a well in control at all times is therefore utterly important.

In conventional drilling, the well is controlled by balancing the formation pressure with the hydrostatic pressure exerted by a column of drilling fluid. This is called primary well control. If the drilling fluid for any reason fails to provide an overbalance against the formation, the formation fluids may flow into the well bore, i.e. a kick is taken. By the means of secondary well control, the influx can be detected, contained and removed from the well bore in a controlled manner. In this way, primary well control is re-established. Thus, well control involves:

- Testing and verification of well barriers
- Kick prevention, monitoring and maintenance of primary barrier
- Kick detection upon failure of primary barrier
- Influx containment, activation of secondary barrier
- Removal of influx, re-establishment of primary barrier

Well control depends on both equipment and operational procedures.

2.1. The barrier philosophy

In most literature on the subject well control, one may encounter a barrier philosophy. The intention is that no single equipment failure or operational mistake shall lead to a well control situation. This is insured by sets of independent tested well barriers.

"There shall be two well barriers available during all well activities and operations, including suspended or abandoned wells, where a pressure differential exists that may cause uncontrolled outflow from the borehole/well to the external environment. "[1]

"If the well is considered to have potential to flow, maintenance a two-barriers –barriers-to-flow system should be considered."[2]

“After setting the initial casing string (...) a minimum of two independent and tested barriers must be in place at all times. Upon failure of a barrier, normal operations must cease and not resume until a two barrier position has been restored. “[3]

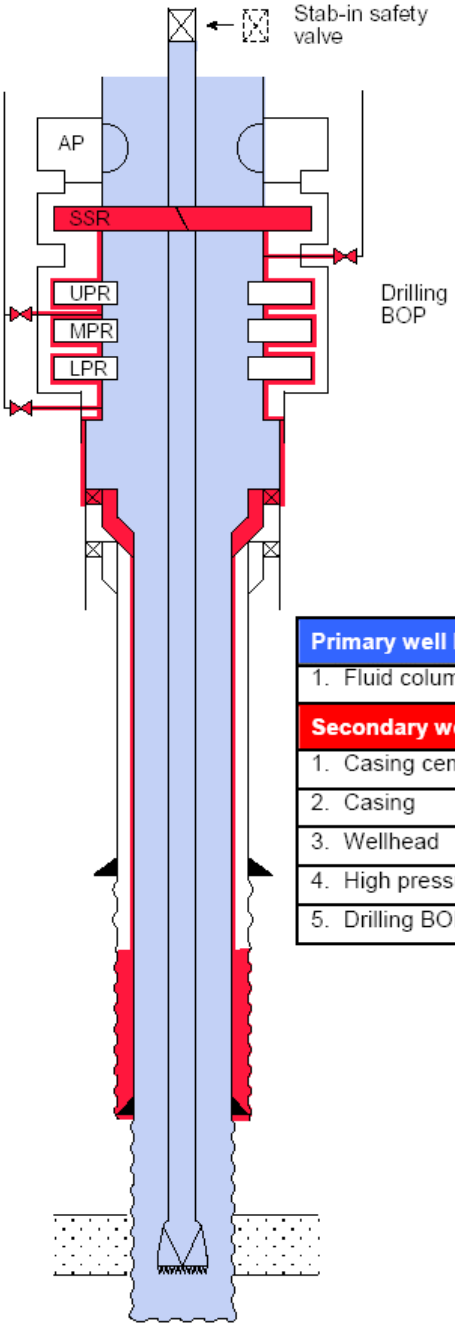

Primary well barrier		
1. Fluid column	1	
Secondary well barrier		
1. Casing cement	22	
2. Casing	2	Last casing set.
3. Wellhead	5	
4. High pressure riser	26	If installed.
5. Drilling BOP	4	

Figure 2-1: Well Barrier Schematic[1].

Figure 2-1 illustrates the well barrier philosophy. The figure gives an overview of the well barriers in place during ordinary drilling activities. The drilling fluid is defined as the primary barrier. The secondary barrier consists of a set of barrier elements, with the objective of being able to shut in the well in the occurrence of a kick.

2.1.1. The primary barrier

The intention of the primary well barrier is to prevent a kick from occurring. The drilling fluid is during normal operations defined as the primary barrier. The mud must be heavy enough to exert a pressure overbalance with respect to the formation pressure. In this way influx of formation fluids can be avoided and wellbore stability ensured. On the other hand, the mud should also be light enough not to fracture the formation or loose circulation.

The mud has a variety of other functions, and design of the drilling fluid is given careful thought. The final drilling fluid is a compromise between the required properties.

In order to maintain the correct downhole pressures, the well must be kept full at all times. This is achieved by constant monitoring of the fluid levels in the trip tank and active pits. It is also important to verify that the mud weight is correct. The mud weight is measured at regular intervals, both going in and coming out from the wellbore.

For further elaboration on acceptance criteria reference is made to[1].

2.1.2. The secondary barrier

The secondary barrier acts as a backup system. When a kick has occurred, the primary barrier has failed. A secondary independent barrier or set of barrier elements should be able to contain the influx. This is generally achieved by mechanical measures. In the occurrence of an influx, the well control equipment must be able to contain the influx before it reaches the surface. This is achieved by shutting in the well by means of the blowout preventer stack, BOP.

The BOP prevents the influx from reaching the surface. Below the BOP other well barrier elements (primarily casing and cement) prevents underground blow-outs and subsurface cross flow.

Some literature also uses the term tertiary barrier. This refers to contingency plans if both the primary and secondary barriers should fail. This often involves pumping heavy and highly viscous fluids or cement to shut off the kicking formation.

2.2. Killing a well

Killing a well refers to a re-establishment of the primary barrier. After successful containment of an influx, the kick fluids should be removed in a controlled manner. The shut-in influx should be removed from the wellbore without causing further influx of formation fluids, and without fracturing the formation. After a well is killed, the wellbore will be free from influx fluids, and the original drilling fluid displaced to kill mud, which balances the formation pressure. There exists a variety of methods for killing wells. Some methods are based on circulating a kick out of the wellbore. Other methods can be used when circulation is not possible. An example of the latter is bullheading, where the influx is squeezed back into the formation, with no returns to surface.

3. Kick prevention and preparation

A range of precautions are made in order to prevent kicks from occurring and to be prepared for a well control situation. In the subsequent sections some of these precautions are mentioned.

3.1. Well design and planning

"Well design is a process with the objective of establishing, verifying and documenting the selected technical solutions that fulfils the purpose of the well, complies with requirements and has an acceptable risk of failure (by means of risk analysis) throughout the defined life cycle of the well." [1]

The objective of the well design process is to obtain a usable well at minimized cost and at a high level of safety[4]. In the following, a brief summary of the well design process as described in [5] will be presented. For further elaboration reference is made to [4, 5]. It will particularly be focused on the subjects regarding well control and well integrity, mainly casing design and design of mud weight schedule. Formation and fracture pressure prognoses are vital when it comes to designing a mud weight schedule and casing program. These prognoses are produced using seismic and correlation of geological data and well logs from offset wells.

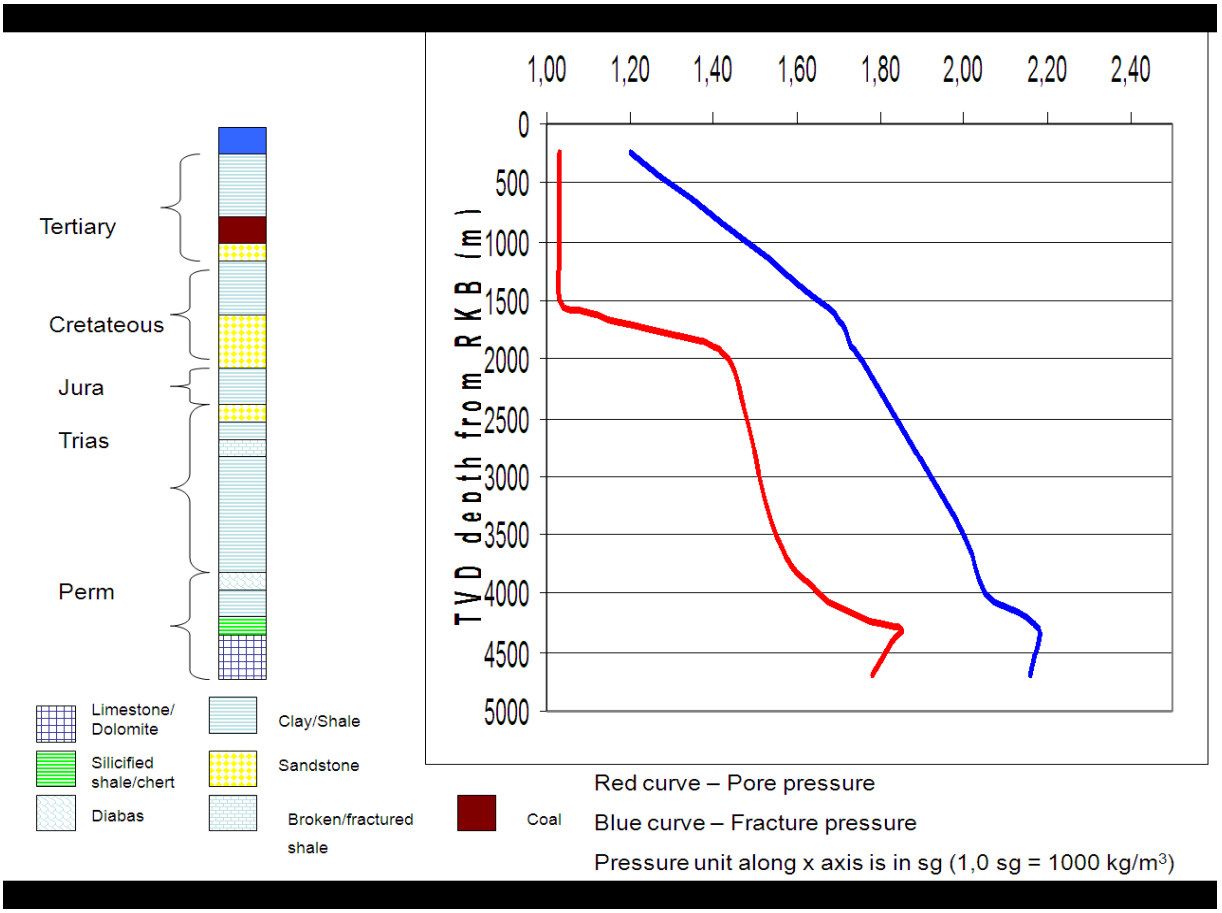

Figure 3-1: Example of downhole pressure prognosis[6].

In the figure a fictive pressure prognosis is shown. However, these pressure profiles are typical. This may be used as an illustration for the sections to come.

3.1.1. Mud weight schedule

The optimal mud weight for the various hole sections is determined as a compromise between a range of different considerations. Although most literature suggests using a mud weight close to the formation pressure in order to increase the drilling rates, [5] recommends using a relatively high mud weight. Use of a median line principle when designing a mud weight program is suggested. The median line is obtained as the arithmetic average of the pore pressure and the fracture pressure. This is said to have positive effect with regards to a range of borehole problems. A summary of the principle is given as follows:

"

1. Establish a pore pressure gradient curve and a fracturing gradient curve for the well. The fracture gradient curve should be corrected for known effects like wellbore inclination and tectonic stresses.
2. Draw the median line between the pore and the fracture gradient curve.
3. Design the mud weight gradient to start below the median line immediately below the previous casing shoe.
4. Mark out depth intervals prone to lost circulation and differential sticking, and their acceptable mud weight limits, if known.
5. Design a stepwise mud weight schedule around the median line that also takes into account limitations from 3 and 4 above.
6. Avoid reducing the mud weight with depth. If a median line reversal occur, keep the mud weight constant." [5]

Safety margins as trip- and riser margins should be included when determining the correct mud weight. There should also be a margin towards the fracture pressure. Often the safety margins are set to a minimum of 2 points SG. Thus, the mud density should lie between the equivalent mud weight of the formation added a safety margin of 0,02 SG and equivalent mud weight fracture pressure subtracted a safety margin of 0,02 SG. If the median line principle is used, these safety margins are often already included in the mud weight schedule.

3.1.2. Casing design

Casing design and setting depth relies on a range of different factors and considerations. In this section however, only considerations related to burst will be presented, as this is most important with respect to well control.

The ordinary casing dimensions used at the NCS is as follows:

- 30 inch conductor
- 20 inch surface casing
- 13 3/8 inch intermediate casing
- 9 5/8 inch production casing
- 7 or 5 inch liner

When designing a casing program load cases have to be defined. The casing strings have to withstand the loads which they might be exposed to during the life cycle of the well. The scenarios in which the maximum loads are expected are called worst case scenarios. When it comes to burst failure, the worst case scenarios are often defined as

- Gas filled wellbore, or
- Predefined kick tolerance requirements

Kick tolerance is defined as the maximal influx size which can be circulated out of the wellbore without fracturing at the shoe. The maximum pressure induced at the casing shoe may be calculated analytically by estimating an influx density or determined by simulations. This again has to be compared with the fracture pressure at the casing shoe, obtained by the fracture pressure prognosis. Generally, the calculated maximum pressures are more conservative than the simulated. Modern Well Design[5] offers a kick tolerance guideline for floating drilling units. It suggests a kick tolerance of 1-8 m^3. This is based on the accuracy of the surface volume measurements in the active fluid system wellsite.

Using the gas filled wellbore scenario as a design criterion, the well is said to have full well integrity. Both the casing string and the open hole section can withstand the pressures exerted by a gas filled well. From a well control point of view, this is highly beneficial. However, this concept may result in a disadvantageous amount of casing sections. This is problematic with respect to time, cost and downhole and topside clearances (geometrical problem).

If the kick tolerance concept is used, the well is said to have reduced well integrity. Thus, the well can only handle a certain influx volume without losing its integrity. What is vital when applying this scenario as a design criterion, is that the weakpoint of the well is located in the open hole section of the well. This means that if a kick of higher intensity than the predefined kick tolerance is taken, the well will fracture in the open hole section, rather than bursting the casing.

Using the predefined load cases, the required load ratings of the casing sections can be calculated. This is done by introducing a design factor or a safety factor. The minimum design factors to be applied in casing design can be found in the table below.

	Burst	Collapse	Tension	Tri-axial
Minimum design factors	1,1	1,0	1,3	1,25

Table 3-1: Minimum design factors for casing design purposes[1].

The approach using minimum design factors in casing program design is often referred to as deterministic. It is required that the pressure rating of the casing fulfills the relation:

$$\frac{Casing\ Load\ Rating}{Worst\ Case\ Loading} \geq Minimum\ Design\ Factor \tag{3.1}$$

The casing load rating is supplied by the manufacturer. In general, the casing joints are made in correspondence with [7], and the ratings are tabulated in for instance [8]. For bottomhole temperatures higher than 100 ˚C[5], a down rating of the casing is necessary. This has to be done with reference to the manufacturer of the casing.

As a substitute for the deterministic approach, also probabilistic calculations may be used. In this case, the probability of failure should not exceed $10^{-3,5}$ [1]. A further description of the probabilistic approach is to be found in[4].

Generally, the production casing is set just before drilling into the reservoir zone. The production casing will have to provide full well integrity. Thus, both the casing and the open hole formation needs to withstand the pressures caused by the gas filled well scenario. Sometimes the production casing is design to match the pressure rating of the wellhead and BOP equipment.

For production and drill stem testing also a third scenario has to be considered. Leaking tubing immediately below the well head will subject the completion fluid in the annulus between the tubing and production casing (or tie-back) to the flowing pressures inside the tubing. The completion fluid will in general be more dens than the produced fluids. This will cause a collapse pressure on the tubing and a burst pressure on the non-cemented sections of the production casing.

For the intermediate casing sections, a reduced well integrity may be sufficient. Thus, if the worst case scenario should occur, the formation will fracture rather than the intermediate casing. This will cause an underground blow-out, but this may in some cases be regarded acceptable. For these sections the concept of kick tolerance is introduced.

The conductor and the surface casing have very limited well control applications. Their main function is to provide a proper fundament for the wellhead, BOP and the subsequent casing sections. Still, it is assumed that the surface casing should be subject to integrity calculations.

Casing setting depth is limited by formation pressure and fracture pressure, and the planned mud weight schedule. The setting depth of each string is determined by starting at the bottom of the well and moving upwards. In this way, the amount of casing sections can be reduced to a minimum. Every casing seat should be located in a competent and impermeable formation. This should be done in order to provide structural strength and to avoid fluid migration in the vicinity of the casing seat.

3.1.3. Well design example

This can be the results of a preliminary casing and mud weight program. At this point, calculations on well integrity have not yet been performed. Neither, will they be, as this section merely intends to serve as an example. The premises for this preliminary plan will be briefly outlined in the following.

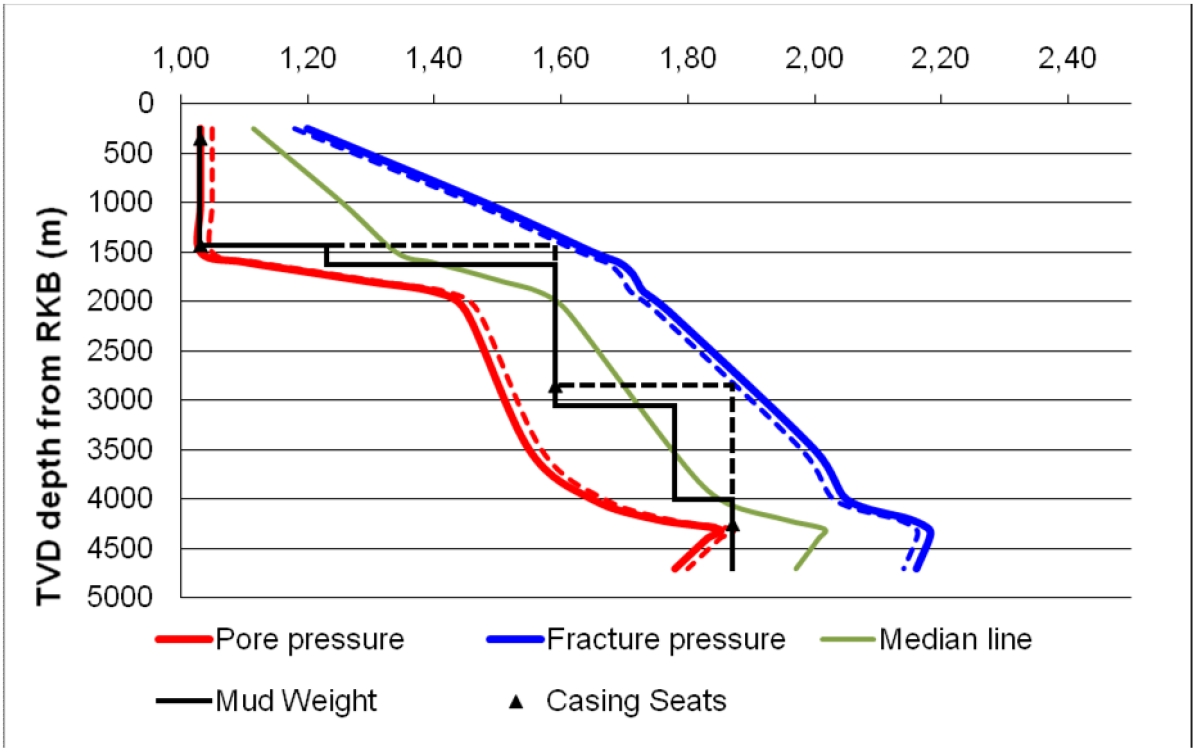

Figure 3-2: Preliminary mud weight schedule and casing program. The scale on the abscissa is in specific gravity and the pressures are measured in mud weight equivalents. The red and blue lines represent the formation pressure and the

fracture pressure with dotted safety margins. The solid black line is the mud weight schedule, while the dotted black line is the maximum hydrostatic pressure exerted at the open hole section.

The dotted lines in the vicinity of the fracture pressure and the pore pressure are safety margins. In this case they are set to 0,02 SG. The black dotted line is the maximum hydrostatic pressure exerted by the drilling fluid on the open hole sections. The scale on the abscissa is specific gravity, and the pressures are measured in equivalent mud weight.

It can be seen that a sand zone is situated below a stringer of coal at around 1000 m RKB (Figure 3-1). The coal may function as a sealing structure for the sand zone. Therefore, shallow gas may be expected. Depending on seismic and data from offset wells, it should therefore be evaluated to drill a pilot hole prior to drilling the top hole. If shallow gas is present, further drilling at this location should be re-evaluated according to a shallow gas contingency plan.

For drilling the top hole, sea water and high viscosity pills are used. The conductor is set 100 m below seabed. The seat of the surface casing is situated at 1425 m RKB. This is at the bottom of a competent shale formation (Figure 3-1). After setting and cementing the surface casing, the BOP and riser is run, and returns are taken back to the rig.

For the intermediate section the mud is weighed up twice. The first 200 m of the intermediate section is drilled using a mud weight of 1,23 SG. At 1625 m RKB the mud is weighed up to 1,59 SG. This is done with reference to the median line principle. It is possible to place the intermediate casing shoe as deep as 3500 m RKB with respect to the suggested mud weight. This will however cause the mud weight to approach the formation pressure, which could again cause borehole problems. Therefore it was decided to place the casing shoe at 2850 m RKB. This is the shallowest setting depth possible while still remaining in overbalance in the reservoir section.

The first 200 m of the production section is drilled with the same mud weight as the final interval of the intermediate section. Then the mud is weighed up to 1,78 SG. 250 m before the seat of the production casing, the mud is again weighed up to 1,87 SG. The production casing is set at 4250 m RKB in a competent chert formation (Figure 3-1).

Drilling into the reservoir, the mud weight is kept constant at 1,87 SG. This is in slight contradiction with the median line principle. However, it is believed that it is important to use a low density fluid as a drill-in fluid in order not to cause formation damage in the reservoir. This is of particular importance if a drill stem test is to be conducted, or if the well will be used for production purposes.

The simulations of section 9.2 will to some extent be based on the outlined program described above.

3.2. Preventive operational procedures

“Loss of primary well control is usually due to:

- Failure to keep the hole full.
- Swabbing.
- Insufficient drilling fluid density.
- Lost circulation.”[2]

From spudding until the well is permanently plugged and abandoned, the objective of the preventive well control procedures is to avoid these situations to occur. Thereby, a well control situation may be prevented.

Where nothing else is stated, the procedures presented in these sections are as outlined by a major drilling contractor[3].

3.2.1. Tripping

Tripping refers to pulling a string out of hole or running a string in hole. The majority of all kicks are taken while tripping out[3]. Therefore it is important to have good procedures in order to prevent this from occurring.

Failure to keep the hole full

Failure to keep the hole full is a problem associated with tripping out of hole. As pipe is pulled from the hole, the volume previously occupied by the pipe will have to be replaced with mud. This is achieved by continuously circulating on the trip tank. The trip tank has to be refilled as the fluid level in the tank drops. A trip sheet is applied in order to verify that the hole is taking the correct amount of mud, and to identify any overall losses or gains in the total active fluid system.

The pipe should preferably be pulled dry, in order to improve volume control. This is achieved by pumping a slug of high density mud. Should this for any reason be impossible, a mud bucket could be applied.

"If the hole does not take the correct volume of mud, or if the Driller has any doubt, the pipe must be run immediately and cautiously back to bottom and bottoms-up circulated."[3]

When tripping in hole the drillstring is filled with mud at regular intervals. It is important that a failure in the float valve and subsequent u-tubing of mud into the drillstring, should not cause the hydrostatic pressure exerted bottomhole to fall short of the formation pressure. Calculations should be performed, when deciding upon the intervals between filling the drillstring.

Swabbing

Swabbing is a problem associated with tripping out. For small clearances between the BHA and the borehole walls a piston like effect can be produced. The actual pressure loss due to swabbing depends on the pulling speed, the properties of the formation and the drilling fluid and on the geometrical clearances present downhole. The effect can be intensified due to bit-balling and pack-off, a thick filter cake or extensive heave. If the swabbing causes the well to go underbalance, the result can be trip gas or a swabbed kick.

The trip margin should be calculated before pulling out of hole. It is calculated as the difference between the mud weight and the equivalent mud weight corresponding to the formation pressure. The trip margin is an expression for the static overbalance in the well.

The trip velocity should be limited. Permissible pulling speeds can be determined by computer simulations. If the simulation software is not available wellsite or at low trip margins it should be evaluated to perform a short trip. The short trip is executed at the determined pulling speed. Typically 5-10 stands are pulled, before running back to bottom, flow checking and circulating bottoms up. The measured percentage of gas in the returns will show if the determined pulling speed is suitable.

If there is a risk of swabbing a kick, pumping out of the hole should be considered[3]. This will continuously replace the volumes previously occupied by the drillstring with mud. In addition, this will expose the well to a frictional pressure gradient, which assists in maintaining overbalance towards the formation.

Lost circulation

As pipe is run in hole a pressure surge may develop in front of the BHA. This effect is similar to swabbing, and can cause mud loss to the formation or even fracturing.

As for pulling out of hole, tripping velocities should be limited. This is of particular importance in the open hole sections. Permissible running speeds can be obtained by computer simulations.

It should be evaluated to break circulation before entering the open hole section. This can function as a means for reducing the pressure surges.

"Any time a trip is interrupted the hand tight installation of a safety valve is required."[3]

3.2.2. Drilling

Although it is established that the most kicks occur during tripping, a reasonable amount of kicks are taken during drilling.

Failure to keep the hole full

During drilling there is a constant circulation of drilling fluid. This generally ensures that the well is kept full at all times. However, the volumes in the active pits should be continuously monitored. A change in the active surface volume could indicate either a flowing well or lost circulation.

Swabbing

Swabbing is generally not an issue during drilling. This is due to the fact that the bit and BHA is situated at the very bottom of the well, with very limited axial movement. However, if a drilling stand is used, swabbing may occur when pulling the drilling stand for a connection. It is assumed that as long as the drilling stand is pulled with the mud pumps running, the risk of swabbing a kick will be insignificant.

Insufficient drilling fluid density

The mud should be treated and conditioned in order to have the density given by the drilling program. Density and other mud properties should be measured both in and out of the hole regularly. The mud conditioning equipment should be maintained and adjusted to work optimal under the conditions encountered.

Excessive drilling rates should be avoided in the presence of background gas and water bearing formations. This is important as cut mud will have a reduced density. The gas fraction is to be continuously monitored by mud logging engineers.

When drilling with a marginal overbalance, it is important to be aware of the drop in downhole pressures as the pumps are shut down for connection. A well could be in slight overbalance while circulating, but as soon as the pumps are shut down the well might go in underbalance. If a subsequent gas influx is taken, this is called connection gas, and will reduce the hydrostatic pressure of the fluid column.

Lost circulation

Circulation loss may be caused by leaks to permeable formations or natural fissures in the open hole section. It can also be caused by inducing formation fractures due to a high overbalance. In general, small seepage losses are to be expected until the mud has built a filter cake on the borehole walls.

It is important to be aware of the friction loss in the annulus and riser. The downhole pressures are higher during circulation than at static conditions. It is of particular importance to take care when breaking circulation. Drilling fluids are often non-Newtonian, and static mud may require a relatively high yield pressure in order to break the gel. It is therefore good practice to start rotating the drillstring before breaking circulation. This way, the gel will be broken in a gentler manner.

3.3. Procedures for well control preparedness

In order to being able to conduct the proper calculations prior to a kill procedure, information about the fracture pressure and dynamic pressure loss in the circulating system has to be known. This is regularly measured wellsite in form of leak-off tests and SCRs. A brief presentation of these procedures is included in the following sections.

3.3.1. Leak-off test

Leak-off tests are used to measure the fracture pressure of the leak-off pressure of the formation. A leak-off test is generally conducted after drilling out a casing shoe and a few meters of new formation. Additional tests can also be conducted further down in the open hole section, if formations expected to have a lower fracture gradient are encountered. The obtained leak-off values are used as estimations of the fracture pressures of the open hole section. If a measured leak-off value is lower than suggested by the fracture pressure prognosis, this will affect the kick tolerance of the section to be drilled.

The obtained leak-off pressure is used for calculating maximum allowable annular surface pressure (MAASP), which has its application in the initial phase of circulating out a kick.

3.3.2. Slow circulating rate

The dynamic pressure loss in the wellbore system is measured well site on a regular basis. These measurements are done while circulating with a constant and slow circulation rate (SCR). The rate of circulation is corresponding to a small range of possible predetermined kill rates (2-3 are recommended by [2]). Typical pump output rates are 20-50 spm, corresponding to the short side of 400-1000 lpm. The drillpipe pressure is recorded during normal circulation, and during circulation through the chokeline.

The SCR is measured at regular depth intervals. It is also measured after changing out BHA or bit nozzles, at altered mud properties (density, viscosity), after major repairs or modifications on the high pressure circulation system, etc.

The SCR measurements are used extensively in the calculation preceding a well kill.

4. Kick detection

It is vital to monitor the well continuously in order to be able to act efficiently upon taking a kick. The response time after a kick is taken, determines the size of the influx, and thereby the severity of the well control situation.

4.1. Kick indicators

There exists a variety of parameters which may indicate a kick. A selection of these is presented in the following sections.

"Establish baseline reading and continually monitor for any variation in trends for gas, mud, cuttings and drilling parameters."[3]

4.1.1. Increase in return rate and surface volumes

The most direct indicators of a kick are an increase in returns relative to the pump rate and subsequently, a gain in the surface active fluid system. This is caused by influx fluids displacing the drilling fluids downhole. It is important to have sensitive volume gauges for measuring the active surface volume.

"Consider fingerprinting the flowback trend having shut off the pumps for a connection. Establish a baseline and closely monitor for any variation in this trend during subsequent connections."[3]

4.1.2. Increase in drillability

When drilling into an abnormally pressured formation, the overbalance (chip hold down pressure[9]) will be reduced. This may result in an increase in penetration rate. If the increase is significant (100% or more over 5 ft drilled formation[3]) this is called a drilling break. However, the penetration rate is additionally a function of a range of other variable drilling parameters. Therefore the concept of drillability is introduced. The drillability is a more or less empirical function of the relevant drilling parameters and intends to give a qualitative value of the formation pressure and drilling resistance. Thus, the drillability is independent of the drilling parameters.

The d-exponent

$$d = \frac{\log \frac{ROP}{N}}{\log \frac{WOB}{D}} \qquad (4.1)[10]$$

Where d = drillability, d-exponent

ROP =Rate of penetration

WOB =Weight on bit

N =Rotational velocity (typically RPM)

D =Bit diameter

An increase in drillability is not necessarily due to drilling into a potentially kicking formation. Similar effects would also be present when simply drilling into a softer formation. However, all drilling breaks must be flow checked[3].

4.1.3. Other drilling parameters

When drilling into an abnormally pressured zone an increase in torque is expected. This is due to the chip hold down effect. When the dynamic bottomhole pressure approaches the formation pressure, the cuttings in front of the drill bit will be pushed away. This may further cause a high concentration of cuttings around the BHA, which will in turn increase the torque.

Upon taking a kick, a decrease in drillpipe pressure might occur. As the lighter kick fluids enter the annulus, the u-tube effect will cause lower pressures throughout the internal length of the drillstring.

4.1.4. Drilling fluid properties

The drilling fluid properties will change according to its composition (gas/water cut). The drilling fluids will generally contain a concentration of formation fluids. This comes from diffusion from the drilled formation and the cuttings. If the dynamic bottomhole pressure approaches the formation pressure, there will be an increase in net diffusion. This will give a decrease in density and a change in viscosity. The change in viscosity depends on the chemical properties of the mud emulsion/invert emulsion and its compatibility with the formation fluid. This is not seen before the mud is circulated to surface, and it is in that sense a delayed indicator.

4.1.5. Cuttings geometry

The cuttings geometry might change when encountering an abnormally pressured formation. This is due to the chip hold down effect, and will result in larger and more angular cuttings. This is also a delayed indicator, as a bottoms-up circulation is necessary in order to observe the cuttings geometry topside.

4.1.6. Increase in background gas

When drilling in a gas bearing formation, the return mud will generally have a small and relatively stable gas concentration. This is called background gas, and is due to diffusion from the cuttings and the formation. If the dynamic bottomhole pressure approaches the formation pressure, there will be an increase in background gas. Spikes in the background gas might also be observed after connections. This is called connection gas, and is caused by a further decrease in bottomhole pressure when the pumps are shut off.

4.1.7. Increase in temperature

Shale often functions as a seal for high pressured formations. The thermal conductivity of shale is relatively low. Hence, heat will accumulate in the formation below the shale. When drilling into an abnormally pressured formation, an increase in drilling fluid temperature may be seen topside. This effect can function as a delayed kick indicator.

4.1.8. Downhole measurements

The bottomhole assemblies of today are composed from various sophisticated tools for logging and measuring formation and borehole data while drilling. A change in the rock and fluid properties of the formation would easily be detected. However, the MWD/LWD tools are only functional in the lateral direction. Their position behind the bit will cause a delay of several meters.

4.2. Flow check

"A flow check must be conducted any time the driller has doubt about the stability of the well."[3]

If any kick indications should occur, the well will be flow checked. This is done by shutting down the mud pumps and lining the returns through the trip tank. From the trip tank, mud is pumped back through a fill up line into the top of the riser. If the well is stable, the mud level in the trip tank will remain constant. Increase in trip tank volume while flow checking will further indicate a flowing well. A typical flow check lasts for 10-15 minutes.

The reasons for lining up the mud flow through the trip tank, is that the accuracy of the volume measurements are higher than for the mud pits. This is due to a smaller cross sectional area of the trip tank, so that a small increase in volume will result in a relatively high increase in liquid height in the trip tank.

There are several effects to be aware of when flow checking. A gain in the trip tank immediately after commencing a flow check is not uncommon, even if the well is not flowing. These gains can be as large as 100-200 bbls or 16-32 m^3 [5], and can easily be misinterpreted as a kick. The flow trends while flow checking should therefore be monitored and compared in order to distinguish an actual kick from the false indications. However, "if there is any indication of flow consider shutting in the well immediately rather than taking the additional time to conduct a flow check"[3].

This type of wellbore backflow is called ballooning. Ballooning is actually caused by a range of different effects:

- Expansion of the mud due to downhole heat conduction from the formation will cause an influx indicator.
- A reduction in pressure gradient throughout the well when the mud pumps are shut off will cause a slight pressure expansion of the mud. The same mechanism might also cause a fluid exchange with the formation, where both intruded mud and formation fluid will enter the wellbore. If the formation fluid is light, this will further cause a delayed increase in the background gas reading, similar to connection gas.
- It is also a general belief that the borehole walls are elastic, and that a reduction in downhole pressure gradient will cause a wellbore contraction. This will yield a further gain in the trip tank. Simulations have shown that this effect contributes 5-14%of the net gain caused by pressure effects[5].

5. Influx containment

After taking a kick, the influx should be shut-in as soon as possible. This is managed by closing the BOP preventers and the valves on the kill- and chokelines. The situation after shutting in the well is normally:

- Drillstring hung off at pipe ram
- Annular preventer closed
- Failsafe valve on kill line closed
- Failsafe valve on chokeline open
- Choke valve closed

After the well is stabilized, the shut-in pressures can be read. SICP is read below the choke valve and SIDPP is read at the standpipe manifold. Both SICP and SIDP are important parameters when it comes to the design of a kill program.

API RP 59[2] differentiates between hard and soft shut-in.

5.1. Hard shut-in

During normal drilling operations the BOP preventers are open and the failsafe closed. All valves on the chokeline are open and lined up towards the poor boy separator with exception of the remote choke valve and the valve immediately upstream or downstream of the choke. If a kick is taken, the shut-in procedures are as follows[2, 3]:

- Pull bit off bottom
- Space out
- Shut down mud pumps
- Stop drillstring rotation
- Close annular preventer and open the chokeline failsafe valves
- Close pipe ram below tool joint, and hang off drillstring
- Inform toolpusher and operator representative
- Determine SICP and SIDPP

5.2. Soft shut-in

If soft shut-in is the desired containment procedure, the failsafe valve on the chokeline is closed during normal operations, while the choke valve is open. The other chokeline valves are open and lined up to the poor boy degasser. The valves on the kill line are all closed and the BOP preventers are open. If a kick is taken, the shut-in procedure is as follows:

- Pull bit off bottom
- Space out
- Shut down mud pumps
- Stop drillstring rotation
- Close annular preventer and open the chokeline failsafe valves
- Open failsafe valve on chokeline
- Close choke gradually

- Close pipe ram below tool joint, and hang off drillstring
- Inform toolpusher and operator representative
- Determine SICP and SIDPP

This procedure is partially based on the information found in [2].

6. Removal of influx fluid from the wellbore

If a kick is taken and the well is shut in, an appropriate kill procedure is to be initiated. Killing a well refers to removal of influx fluids from the wellbore, and re-establishment of the mud column as the primary barrier. NORSOK[11] lists four possible kill methods:

- Driller's Method
- Wait & Weight
- Volumetric Method
- Bullheading

The first two methods are widely used, while the two latter are only used in special situations. An introduction to the four kill methods will be presented in the subsequent sections.

When killing a well by conventional methods, kill sheets are applied. The kill sheets ease the calculation and design of a well kill operation, and should be systematically updated[1]. Examples of standard kill sheets are included in the appendix.

6.1. Driller's method

Driller's method is a simple method for circulating out a kick. The method is applicable if the bit is on bottom. If not, stripping to bottom will be necessary. The kill procedure is completed in two rounds of circulation. The kick is circulated out in the first round of circulation. This is done using the old drilling fluid. In the second round of circulation, the well is displaced to kill mud, and the primary well barrier is re-established. During the whole process, it is important to keep the dynamic bottomhole pressure constant and slightly higher than the formation pressure. This is to avoid further influx of formation fluids. The pressure at the weakpoint should also be lower than the fracture pressure, in order to avoid an underground blowout.

The kick is circulated out in the first round of circulation, using the old mud. The mud pump is gradually brought up to a predetermined slow rate. This is done while adjusting the choke valve. On subsea wells a constant BHP may be achieved by keeping the kill line pressure constant, while bringing the pump up to speed (annular pressure loss is assumed negligible)[2]. When the pump is running at kill rate, the drillpipe pressure will be held constant at the initial circulating pressure (ICP) throughout the first round of circulation. This is achieved by applying and adjusting the backpressure on the choke valve. As the drillstring is assumed to contain homogeneous mud of known density, the bottomhole pressure will be constant as long as the drillpipe pressure kept constant.

The ICP is defined as:

$$ICP = SIDPP + \Delta P_{SCR,Riser}$$

The equation is defined and deduced in section 7.

If the first round of circulation is a success, the influx will be completely removed from the wellbore. This can be checked by shutting down the pump and closing in the well synchronously, while still keeping constant bottomhole pressure. Thus, the drillpipe pressure will have to be reduced by the dynamic pressure loss measured through the riser. If the entire influx is removed, the static pressures on both the drill pipe side and the casing side should be stable and equal.

The second round of circulation is performed using drilling fluid at kill mud density. This is done in order to re-establish primary well control. The kill mud weight is calculated in the kill sheet, and is set to balance the formation pressure with a slight overbalance (safety margin). The pump is brought gradually up to kill rate at constant kill line pressure by adjusting the choke backpressure. Casing pressure is kept constant until the kill mud reaches the bit. While the kill mud is pumped up the annulus, drillpipe pressure should be kept constant at final circulating pressure (FCP). After the entire well is displaced to kill mud, the shut-in pressures should be reduced to the atmospheric pressure.

$$FCP = \frac{\Delta P_{SCR,Riser}}{\rho Old} \rho_{New}$$

The equation is defined and deduced in section 7.

Driller's method is perhaps the most used method for circulating out a kick. The method has several advantages. Upon shutting in on a kick, the circulation may commence immediately, without weighing up to kill mud. This is important if the influx fluid is compressible gas in water based mud, as gas migration may cause high pressures in the wellbore. Driller's method is also quite easy for the choke operator. The choke can be adjusted to maintain constant drillpipe pressure until the kick is out of the system.

In section 9 a couple of calculation examples on driller's method are included. In section 10 simulations on driller's method are conducted. The results of calculations and simulations will be further discussed and compared in section 11.

6.2. Wait & weight

The wait & weight method is very similar to driller's method. Wait & weight also uses circulation as a means for removing the influx and restoring the primary well barrier. And as for driller's method, a constant bottomhole pressure is key. The difference is that circulation with kill mud starts immediately. This means that the kick is removed and the well displaced to kill mud in one single round of circulation.

The pump is brought slowly up to kill rate while adjusting the choke, so that the kill line pressure is kept constant. At kill rate, the drillpipe pressure should be approximately equal to the calculated initial circulating pressure (ICP). If not, the reason should be investigated. As circulation proceeds, the drillpipe pressure should be reduced linearly as calculated in the kill sheet. When the whole drillstring is displaced to kill mud, the drillpipe pressure has reached the calculated final circulating pressure (FCP). For the rest of the circulation, the drillpipe pressure should remain constant at final circulating pressure.

6.3. Static volumetric method

The static volumetric method can be used if circulation through the drillstring for some reason is impossible. It also finds its application in combination with the above mentioned kill methods. In particular when gas migration is causing excessive pressure build up before the desired kill method is initiated.

The intention of the method is to keep the bottomhole pressure constant (including a safety margin) while the kick migrates up the annulus. This is achieved by stepwise bleeding off mud through the chokeline, while controlling choke backpressure. With drillstring communication (possibility to measure drillpipe pressure) volumetric method is conducted with ease. As mud is being bled off, the choke backpressure is adjusted with reference to the drillpipe pressure. Mud should be bled off until the drillpipe pressure reaches the prerecorded shut-in pressure added a safety margin (typically 100 psi[2]). This ensures that the bottomhole pressure remains within a predetermined interval, and no further influx will occur.

With loss of drillstring communication, use of the static volumetric method becomes more complicated. This will not be presented here.

6.4. Bullheading

Bullheading is a method where the influx is pumped back into the formation without returns to surface, using a constant pump rate. During the pumping the injection pressure should be low enough not to fracture the formation at the weakpoint. Exceeding the fracture pressure may provoke an underground blowout, instead of killing the well.

Bullheading is used when H_2S is expected to be present amongst the influx fluids, or when the margin towards the fracture pressure is to low for a conventional kill to be performed (driller's method or wait & weight). The method can also be used when the drillstring is out of hole, as kill mud can be pumped through the kill- and chokelines. Bullheading is most successful when the open hole section is relatively short[2].

7. An analytical model

In order to derive the traditional well control formulas, a series of simplifying assumptions has to be made. This set of assumptions to derive a simple analytical model. This model finds its application in most practical well control operations at wellsite.

7.1. Assumptions

- Conservation of mass
- Constant pressure gradient in the drilling fluid (non-compressible)
- Gas influx acts according to Boyle's law
- Influx propagates as a single bubble
- No temperature gradient
- Negligible frictional pressure loss in annulus and riser
- Chokeline friction and drillstring friction directly proportional to the fluid density
- No phase transitions between influx and drilling fluid
- Constant wellbore volume (No fluid exchange with the formation, inelastic formation)
- Simplified wellbore geometry

This will be further elaborated in the sections to come.

7.1.1. Conservation of mass

Conservation of mass is valid for the entire system. For any timestep or displacement in position, the increase or decrease in accumulated mass in a control volume, is equal to the mass which has flowed into the control volume subtracted the mass which has flowed out.

$$\Delta m_{In} - \Delta m_{Out} = \Delta m_{Acc} \tag{7.1}$$

The well is treated as a constant volume (inelastic wellbore and casing) with an inlet at the drillstring side and outlet at the annulus side. This volume may function as a control volume. It is assumed that no fluid is lost to the formation. With exception of a kick situation, the inflow rate from the formation is also assumed to be zero at all times. The latter assumption is generally valid, due to a hydrostatic overbalance in the wellbore.

7.1.2. Fluid properties

In general, the density of the drilling fluid is a function of temperature and pressure. However, the drilling fluid is approximated to be incompressible. This means all changes in density due to temperature and pressure are neglected. An implication of this assumption is that the speed of sound in the liquid phase in infinite. Any changes in pressure in one point in the liquid column, is instantaneously measured throughout the entire volume of liquid. Since the density is assumed independent of pressure, the mass conservation also implies conservation of liquid volume.

The influx gas is treated as a single bubble propagating with no-slip or constant slip through the drilling fluid. No phase transitions are assumed between the liquid phase and the gas phase. This assumption is quite accurate using water based drilling fluids. However, for oil based mud, methane and other light hydrocarbon gases may go in complete solution with the drilling fluid. As the dissolved gas is circulated to surface, the pressure is gradually reduced. When the pressure crosses the bubble point, the dissolved gas may suddenly boil out of solution.

In general gas behaves according to the real gas law.

$$PV = nZRT \qquad (7.2)[12]$$

Where P = Absolute pressure in the gas

V = Gas volume

T =Absolute temperature in the gas

Z = Compressibility factor of gas

n = Number of gas molecules in the gas volume

R =Gas constant, 8.31 $J \cdot K^{-1} \cdot mol^{-1}$

The compressibility factor is depending on the type of gas, and the temperature and pressure. For ideal gas or at atmospheric pressure and temperature the factor equals one. The temperature gradient in the well will depend on the dynamic conditions in the well. At static or steady state conditions the temperature gradient in the wellbore fluids will reach equilibrium with the temperature gradient in the formation (neglecting convection). However, this equilibrium will be disturbed by changing the rate of circulation. Both compressibility and temperature can be modeled by more or less empirical approximations.

In most of the traditional well control formulas the temperature dependency of the ideal gas law is neglected. Further, the compressibility factor z, is assumed to equal one. Thus, the gas is assumed to behave according to Boyle's Law.

$$PV = constant \qquad (7.3)$$

Where P = Absolute pressure in the gas

V = Gas volume

7.1.3. Pressure balance

The pressure balance during dynamic conditions can be expressed as

$$P_{BH} = P_{Csg} + \Delta P_{HS} + \Delta P_{Fric,ann} + \Delta P_{Fric,CL/Riser} \quad (7.4a)$$

$$= P_{DP} + \Delta P_{HS} - \Delta P_{Fric,DS} - \Delta P_{Bit} \quad (7.4b)$$

Where P_{BH} = Bottomhole pressure

P_{Csg} = Choke pressure

ΔP_{HS} = Hydrostatic pressure exerted by the fluids

$\Delta P_{Fric,Ann}$ = Frictional pressure loss in the annulus

$\Delta P_{Fric,CL/Riser}$ = Frictional pressure loss in the chokeline or riser

$\Delta P_{Fric,DS}$ = Frictional pressure loss in the drillstring

ΔP_{Bit} = Pressure loss across the bit

The first equation expresses the pressures on the annulus side, and the second on the drillstring side. At static conditions, the frictional pressure loss and the pressure loss across the bit will equal to zero, and the equations will be reduced to the following

$$P_{BH} = P_{Csg} + \Delta P_{HS} \quad (7.5a)$$

$$= P_{DP} + \Delta P_{HS} \quad (7.5b)$$

This result is of particular importance, and will be applied extensively in the sections to come.

7.1.4. Drillpipe and casing pressure

The drillpipe- and the casing pressures are measured at drill floor level. At static conditions, with no shut-in pressures, these will be equal to the atmospheric pressure. During pumping, the drillpipe pressure will in general reflect the flow resistance in the wellbore system, as the hydrostatic pressure in the drillstring and annulus are close to equal. In a kill situation, the circulation will take place through the chokeline. In this case, the casing pressure may be manipulated by choking the flow at the choke manifold.

7.1.5. Hydrostatic pressure

The hydrostatic pressure is the pressure exerted by the weight of a static fluid column. A standard form for expressing this is

$$\Delta P_{HS} = \rho g h \qquad (7.6)[12]$$

Where ΔP_{HS} = Difference in hydrostatic pressure between two points of interest

ρ = The fluid density between the two points of interest

g = The acceleration of gravity

h = The vertical distance between the two points of interest

This might seem straight forward. However, in reality, the fluid density is a function of the temperature and the pressure. The pressure is again depending on time and position. Due to fluid compressibility, the hydrostatic pressure gradient will increase at increasing pressures and vice versa. In the derivation of the traditional well control formulas, these effects are neglected. Thus, the liquid compressibility is set to zero. For conventional drilling the mud weight is set to provide a slight overbalance to the formation pressure.

7.1.6. Friction

Fluid friction works in the opposite direction of the flow. It is actually the resistance of flow between infinitesimal layers of fluid moving at different velocities. Fluid friction for flow in a pipe with circular cross section can, in general, be expressed as (Ref Drilling Engineering)

$$\Delta P_{Fric} = 2f \cdot \rho \frac{v^2}{d} \Delta S \qquad (7.7)\ [5]$$

Where f =Friction factor

v = Fluid velocity

d = Inner diameter of the pipe

ΔS = The distance along the flowpath between the two points of interest

The other symbols are defined in the previous sections.

The friction factor may be found as various functions of the Reynolds number, depending on the flow regime. The Reynolds number is defined as

$$\mathrm{Re} = \frac{\rho v d}{\mu} \qquad (7.8)[12]$$

Where μ = Fluid viscosity

For low Re, typically less than 3000 using SI units, the flow is considered laminar. For higher Re, the flow is turbulent. Laminar flow typically occurs in the annulus and riser. It can be shown that the friction factor for laminar flow equals

$$f = \frac{16}{Re} \qquad (7.9)[12]$$

The flow inside the drillstring and through the chokeline is normally turbulent. For turbulent flow, only empirical correlations for the friction factor exist, usually proportional to the Reynolds number to a small negative power. In the analytical model, this dependency is neglected, so that

$$\Delta P_{Fric,Turb} \propto \rho \cdot v^2 \qquad (7.10)$$

The dynamic pressure loss (SCR) in the wellbore system is measured well site on a regular basis. The drillpipe pressure is recorded during normal circulation, and during circulation through the chokeline. By setting the drillstring side and the annulus side of the pressure balance equal to one another, the bottomhole pressure cancel out. Further, assuming no compressibility, the hydrostatic terms cancel one another. Solving the pressure balance with respect to the difference between drillpipe pressure and casing pressure yields

$$P_{DP} - P_{Csg} = \Delta P_{Fric,DS} + \Delta P_{Bit} + \Delta P_{Fric,Ann} + \Delta P_{Fric,CL/Riser} = \Delta P_{SCR} \qquad (7.11)$$

Where ΔP_{SCR} = Dynamic pressure loss at kill rate

The frictional pressure terms in the annulus and riser are normally small compared to the other terms. Often, these pressure losses are neglected completely. Assuming a riser friction loss of zero makes it possible to calculate the frictional pressure loss in the chokeline. Simply by subtracting the dynamic pressure loss through the riser from the dynamic pressure loss through the chokeline, one will obtain

$$\Delta P_{Fric,CL} = \Delta P_{SCR,CL} - \Delta P_{SCR,Riser} \qquad (7.12)$$

These results will be made further use of in the sections to come.

7.1.7. Pressure drop across bit and choke valve

The following derivation is made with reference to[5]. The pressure drop across the bit and choke can be modeled as an abrupt reduction in cross section, assuming incompressible and inviscid flow along a streamline. Under these conditions Bernoulli's theorem is valid. The theorem states that

$$\frac{P}{\rho} + gz + \frac{v^2}{2} = constant \qquad (7.13)[12]$$

Where z = Vertical position

The pressure drop across the cross sectional reduction is obtained by further assuming the kinetic energy before the flow obstruction to be negligible. The vertical displacement is assumed to be zero. By replacing the fluid velocity at the point of obstruction with the volumetric flow rate divided by the cross section one obtains

$$\Delta P_{Bit/choke} = \frac{\rho}{2} \cdot \left(\frac{Q}{AC}\right)^2 \qquad (7.14)[5]$$

Where Q = Volumetric flow rate

A = Total flow area through the bit nozzles or the choke opening

C = Discharge coefficient

The discharge coefficient is added in order to match the theoretical equation with experimental results. The value of the coefficient depends on the design of the choke valve or the bit nozzles. A typical value for the bit is 0,95 (dimensionless).

7.2. Derivation of some of the traditional well control formulas

The above mentioned relations and assumptions, result in a simple analytical model. This model may be used in the deduction of some of the traditional well control formulas. The validity of some of the assumptions, and the errors produced by the following well control formulas, will be investigated in the discussions sections.

Upon taking a kick and shutting in the well the following data are known or can be measured.

- SIDPP and SICP
- Pit gain
- Dynamic pressure loss at kill rate
- LOT data

- Wellbore geometry and drill floor elevation
- Drilling fluid density at standard conditions

The derived formulas will have to be functions of these parameters.

7.2.1. Standard kill formulas

In order to obtain a value for the formation pressure upon taking a kick, it is assumed that the bottomhole pressure exactly equals the pressure of the formation. By using equation (7.5b) and (7.6) with an assumption of incompressible mud in the entire drillstring, one obtains

$$P_F = SIDPP + \rho_{Old} \cdot gh \qquad (7.15)[8]$$

Where P_F =Formation pressure

$SIDPP$ = Drillpipe pressure at shut-in

ρ_{Old} = Density of current drilling fluid at standard conditions

h = True vertical well depth

The kill mud is designed to exactly balance the formation pressure, so that the drillpipe pressure is reduced to the atmospheric pressure when the kill mud reaches the bit. Thus,

$$P_F = \rho_{New} \cdot gh \qquad (7.16)$$

Where ρ_{New} = Kill mud density at standard conditions

Or, by making use of the right hand sides of equations (7.15) and (7.16), and solving for the kill mud density

$$\rho_{New} = \rho_{Old} + \frac{SIDPP}{gh} \qquad (7.17)[8]$$

Assuming no liquid compressibility and conservation of mass, the pit gain at shut in will be equal to the volume of influx present bottomhole. A knowledge of the geometry of the lower wellbore and drillstring, makes it possible to calculate the vertical height of the influx. This also relies on the assumption that the gas remains as a single bubble.

$$h_{Kick,0} = \frac{V_{Pit\ gain}}{A} \cdot \cos(\theta) \qquad (7.18)[13]$$

Where $h_{Kick,0}$ = Vertical height of influx at shut-in

$V_{Pit\ gain}$ = Pit gain volume

A = Annular capacity, bottomhole

θ = Wellbore inclination, bottomhole

Knowing the vertical height of the influx, the influx density may be calculated. By equating the right hand sides of (7.5a) and (7.5b) and substituting the hydrostatic terms, one obtains

$$SIDPP + \rho_{Old} \cdot gh = SICP + \rho_{Old} \cdot g(h - h_{Kick,0}) + \rho_{Kick,0} \cdot gh_{Kick},0$$

Solving with respect to influx density yields

$$\rho_{Kick,0} = \frac{(SIDPP - SICP)}{g\,h_{Kick,0}} + \rho_{Old} \qquad (7.19)[13]$$

Where $\rho_{Kick,0}$ = Average influx density at shut-in

$SICP$ = Casing pressure at shut-in

The first term of equation (7.19) is always negative (SICP>SIDPP), and the kick density will as expected, be lower than the density of the mud.

When circulating out a kick, most methods require a constant bottomhole pressure slightly over the formation pressure. The formation pressure is given by equation (7.15). By equating the right hand side of equation (7.15) with the right hand side of (7.4b) which applies for dynamic conditions, one gets the expression

$$P_{DP} + \Delta P_{HS} - \Delta P_{Fric,DS} - \Delta P_{Bit} = SIDPP + \rho_{Old} \cdot gh \qquad (7.20)$$

Furthermore, the hydrostatic components on the right hand side and the left hand side cancel. By further solving for the dynamic drillpipe pressure yields

$$P_{DP} = SIDPP + \Delta P_{Fric,DS} + \Delta P_{Bit} \quad (7.21)$$

Here, the drillpipe pressure corresponds to the initial circulation pressure ICP, of a kill procedure. By assuming negligible pressure loss in the annulus and the riser, the loss terms in the above equation may be replaced with the dynamic pressure loss (SCR) measured through the riser. This yield

$$ICP = SIDPP + \Delta P_{SCR,Riser} \quad (7.22)[8]$$

After displacing the mud in the annulus to kill mud, the new drillpipe pressure is called final circulating pressure, FCP. The left hand side of equation (7.20) still has its validity. The right hand side, which reflects the formation pressure, may be substituted with the hydrostatic pressure exerted by the kill mud, equation (7.16). So that

$$P_{DP} + \Delta P_{HS} - \Delta P_{Fric,DS} - \Delta P_{Bit} = \rho_{New} \cdot gh \quad (7.23)$$

The hydrostatic terms in this equation are equal, and cancel. The loss terms are however greater than those measured at the SCR, due to the increase in liquid density. The flow regime in the drillstring is in most cases turbulent. That means the relation (7.10) is valid, and the friction loss is proportional to the density of the drilling fluid. According to equation (7.14), the same proportionality is valid for the pressure loss across the bit. Solving for drillpipe pressure yields the equation

$$P_{DP} = \frac{\Delta P_{Fric,DS} + \Delta P_{Bit}}{\rho Old} \rho_{New} \quad (7.24)$$

The drillpipe pressure corresponds to the final circulating pressure, FCP. By assuming negligible pressure loss in the annulus and riser, the loss terms may be substituted with the dynamic pressure loss (SCR) through the riser. This yields the equation

$$FCP = \frac{\Delta P_{SCR,Riser}}{\rho Old} \rho_{New} \quad (7.25)[8]$$

7.3. Calculation examples

In the following sections some sample calculations are performed. The calculations are based on the formulas deduced in the previous sections and formulas found in the standard kill sheets (appendix). The shut-in data and the dynamic pressure losses are all obtained from the simulations in section 10.

In the discussion part results from the following calculations will be further compared with results obtained in the computer simulations.

	DP	DC	DC x OH	DP x OH	DP x CSG	CL	Riser x DP
Capacity, [l/m]	8,00	8,00	39,4	63,3	67,8	4,56	165

Table 7-1: Volumetric capacities of the various sections. The values are set in order to be directly comparable with the values used in the simulations in section 9.2. The values are valid for both the vertical and the horizontal well.

7.3.1. Vertical well

In this section some basic kill calculations will be performed for a vertical example well. A schematic of the well is posted in Figure 7-1.

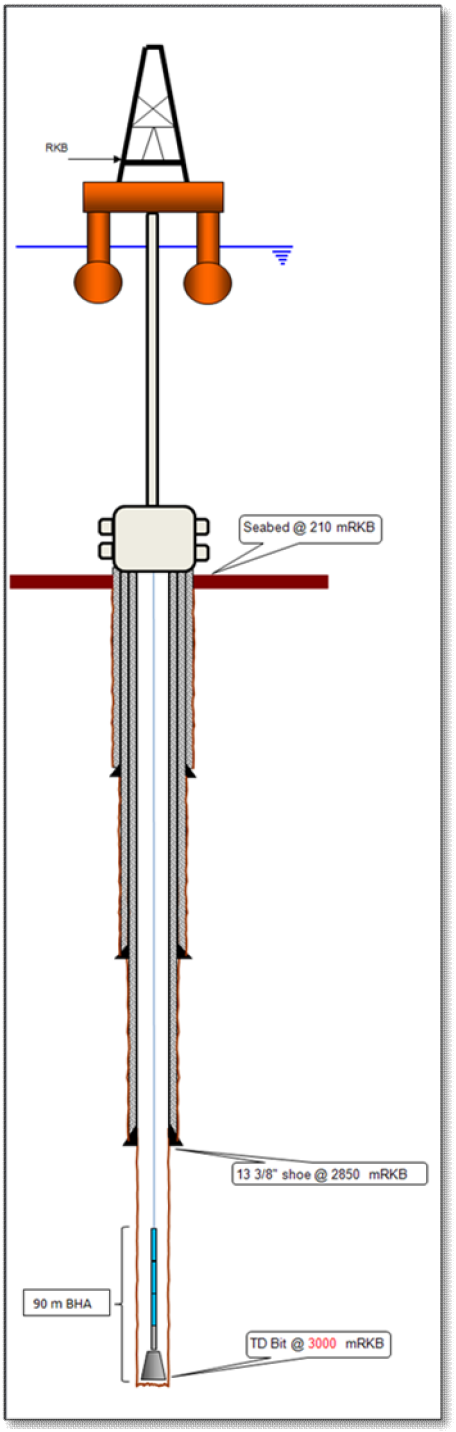

Figure 7-1: Schematic of a vertical well (not to scale).

Well depth	3000 m RKB
Sea depth	210 m RKB
Casing seat	2850 m RKB
BHA length	90 m
Mud weight	1,5 SG
Kill rate	1000 lpm
Dynamic pressure loss at kill rate	53 bar
Dynamic pressure loss through chokeline	64 bar
SIDPP	27 barg
SICP	32 barg
Pit gain	4330 l

Table 7-2: Initial data for the vertical well. Dynamic pressure loss and kick data is obtained from the simulations in section 9.2.

Volumetric calculations

First some basic volumetric calculations are considered. The volumetric calculations are based on the intuitive formula,

$$Volume, [l] = Length, [m] \cdot Volumetric\ capacity, [l/m]$$

where the volumetric capacities are given in Table 7-1. The volumes are rounded to the nearest whole liter.

Drill pipe: 2910 m · 8 l/m =23 280 l

Drill collar: 90 m · 8 l/m =720 l

Drill string volume: 24 000 l

Drill collar x Open hole: 90 m · 39,4 l/m = 3 546 l

Drill pipe x Open hole: 60 m · 63,3 l/m = 3798 l

Open hole volume: 7 344 l

Drill pipe x Casing:2 640 m · 67,8 l/m =178 992 l

Chokeline: 210 m · 4,56 l/m = 958 l

Total annulus and chokeline volume: 187 294 l

Total well system volume: 211 294 l

Knowing the volumes of the well and the pump rate, it is possible to obtain a time schedule for the well control operation. For instance, the time for a circulation bottoms-up is calculated as the annulus and chokeline volume divided by the pump rate.

$$187\,294\ l\ /\ 1000\ lpm\ =\ 187\ min$$

Kick calculations

The height of the kick is determined by equation (7.18). Here it is evident that the pit gain is larger than the volume surrounding the BHA. Thus, both the annular capacities of drill collar x open hole and drill pipe x open hole have to be applied.

$$h_{Kick} = \frac{V_{Pit\ gain}}{A} \cdot \cos(\theta) = 102\ \text{m}$$

In order to know the nature of the influx, the influx density is calculated by equation (7.19).

$$\rho_{Kick,0} = \frac{(SIDPP - SICP)}{g\,h_{Kick}} + \rho_{Old} = 1{,}0\ \text{SG}$$

This is high for a gas kick, but low for a water kick. An initial assumption may be that the influx consists of oil. However, the actual influx is gas, as described in section 9.2.1. The importance of always assuming the influx to be gas until proven otherwise is underlined.

Further, the formation pressure can be calculated by use of equation (7.15).

$$P_F = SIDPP + \rho_{Old} \cdot gh = 469\ \text{barg}$$

The kill mud weight is evaluated by equation (7.16). The kill mud weight is always rounded up to the nearest point (0,01 SG) according to field practice.

$$\rho_{New} = \rho_{Old} + \frac{SIDPP}{gh} = 1{,}60 \text{ SG}$$

The initial circulating pressure, ICP, is calculated by use of equation (7.22). This pressure is always rounded up to the nearest integer barg according to field practice.

$$ICP = SIDPP + \Delta P_{SCR,Riser} = 80 \text{ barg}$$

The final circulating pressure, FCP, is calculated by means of equation (7.25). According to field practice, the final circulating pressure should always be rounded up to the nearest whole bar.

$$FCP = \frac{\Delta P_{SCR,Riser}}{\rho_{Old}} \rho_{New} = 57 \text{ barg}$$

The chokeline friction is calculated by equation (7.12).

$$\Delta P_{Fric,CL} = \Delta P_{SCR,CL} - \Delta P_{SCR,Riser} = 11 \text{ bar}$$

7.3.2. Horizontal well

In the subsequent pages some example calculations will be performed on a horizontal well. A schematic of the well is posted in Figure 7-2. The example will not be as thorough as for the vertical well previously presented. Only a selection of the kill calculations will be presented, in particular the calculations which may be compared with the simulations of section 9.2.2. For the deviated case, a range of complicated equations arise when calculating the drillpipe pressure as the original mud is displaced to kill mud in the drillstring. These calculations will be omitted. The formulas can be found on the deviated kill sheet in the appendix.

The initial data upon which the calculations will be based, may be found is Table 7-3. The volumetric capacities may be found in Table 7-1, but will not be used extensively in the calculations to follow.

Well depth	3008 m TVD
“	3840 m MD
Sea depth	210 m RKB
KOP	2580 m TVD/MD
EOB	3240 m MD
“	3008 m TVD
Bottomhole inclination	90°
Casing seat	3680 m MD
“	3008 m TVD
BHA length	90 m
Mud weight	1,5 SG
Kill rate	1000 lpm
Dynamic pressure loss at kill rate	65 bar
Dynamic pressure loss through chokeline	76 bar
SIDPP	25 barg
SICP	27 barg
Pit gain	3460 l

Table 7-3: Initial data for the horizontal well. Dynamic pressure loss and kick data is obtained from the simulations in section 9.2.2.

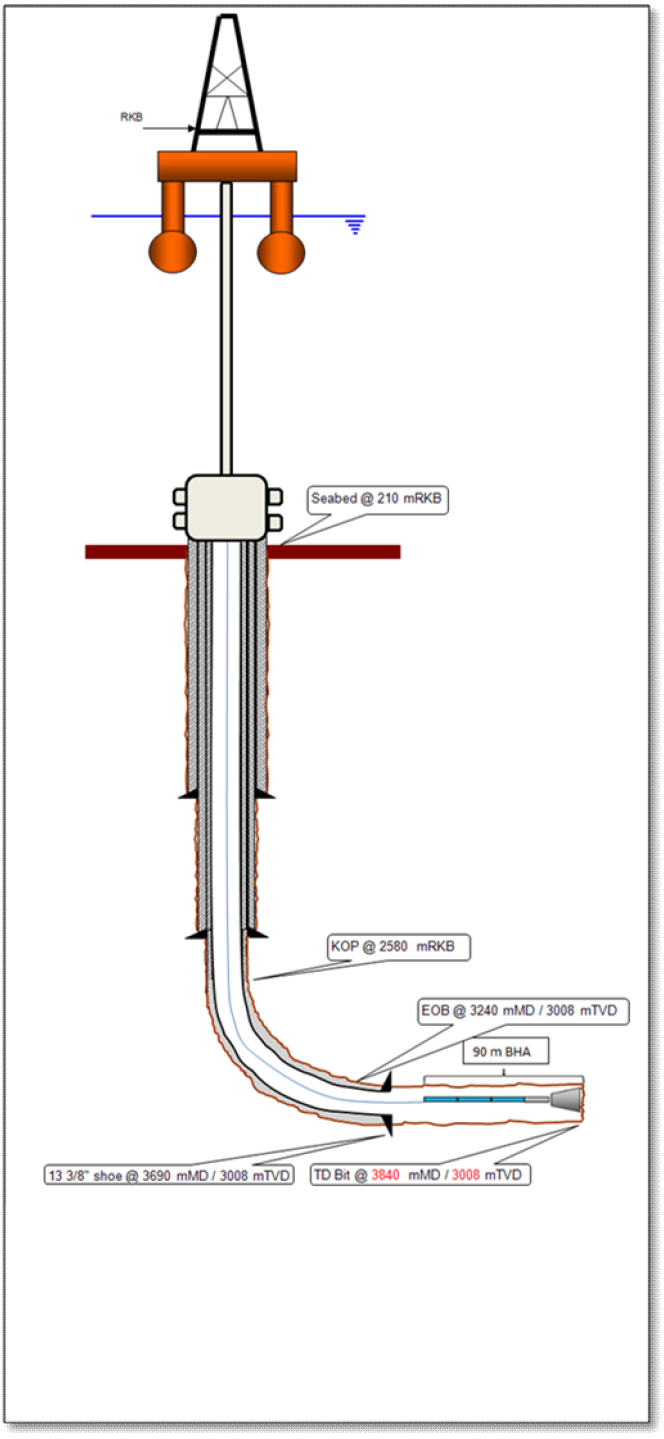

Figure 7-2: Schematic of a horizontal well (not to scale).

Volumetric calculations

The volumetric calculations will be omitted, as they resemble the calculations in the previous section. It is important to notice that for the evaluation of volumes, the measured depth has to be applied. One result will however be mentioned. The total annulus and chokeline volume is calculated to 244 246 l. At a pump rate of 1000 lpm, this corresponds to 244 min.

Kick calculations

The influx height may normally be calculated by use of equation (7.18). However, when the well is horizontal, this approach makes no sense. The vertical height of the kick is limited to the diameter of the open hole section. The open hole has a diameter of 12 ¼ inches which corresponds to 0,311 m.

By means of equation (7.19) the influx density is attempted to be calculated.

$$\rho_{Kick,0} = \frac{(SIDPP - SICP)}{g\,h_{Kick,o}} + \rho_{Old} = \text{-64,0 SG}$$

It is evident that the result is unrealistic. All approaches for estimating the density of the gas is abandoned. Equation (7.15) is used in order to calculate the formation pressure.

$$P_F = SIDPP + \rho_{Old} \cdot gh = \text{468 barg}$$

By means of equation (7.16) the necessary kill mud weight is estimated.

$$\rho_{New} = \rho_{Old} + \frac{SIDPP}{gh} = \text{1,59 SG}$$

The initial circulating pressure, ICP, is calculated by use of equation (7.22).

$$ICP = SIDPP + \Delta P_{SCR,Riser} = \text{ 90 barg}$$

In order to calculate the final circulating pressure, FCP, equation (7.25) is utilized.

$$FCP = \frac{\Delta P_{SCR,Riser}}{\rho_{Old}} \rho_{New} = \text{69 barg}$$

Equation (7.12) is used in order to estimate the chokeline friction.

$$\Delta P_{Fric,CL} = \Delta P_{SCR,CL} - \Delta P_{SCR,Riser} = \text{11 bar}$$

8. A numerical model

In order to perform well control simulations, a numerical model was adopted. In the following sections a brief introduction to the model is given. Further, some modifications are done with the goal of making the model more suitable and realistic with respect to well control situations. Finally, a presentation of the well control simulations is given. Simulations were conducted on both a vertical well and a horizontal well.

8.1. Introduction to the numerical model

The numerical model utilized in this thesis is the drift flux model. The drift flux type models are fundamentally based on a set of three equations. Two of which are relations describing the conservation of mass for the respective phases. The last equation describes the conservation of momentum for the combined fluids. In addition, a coupling between the liquid and gas velocities is necessary. Hence, a slip relation is introduced. The most reasonable results using the drift flux model are obtained when modeling flow regimes such as dispersed bubble or slug flow[14].

In order to solve the drift flux model a numerical scheme is required. The numerical scheme used in this thesis is in the family of explicit AUSM schemes (advection upwind splitting method). This particular family of discrete numerical schemes was initially developed by Liou and Steffen[15]. The AUSM scheme may be utilized to simulate two-phase flow (liquid and gas) in an isotherm environment. The scheme has been proven to competently model transport of mass as well as pressure pulse propagation in one dimension.

What separates the AUSM schemes from the other numerical schemes is the improved flux splitting scheme derived in [15]. The new flux splitting scheme attempts to combine the advantageous properties of similar flux splitting methods (FVS/FDS). Further improvements to the flux splitting scheme was proposed by Wada and Liou[16]. This was done for one-phase flow by introducing a convex combination to the velocity splitting function. The altered flux-splitting scheme eliminated the numerical dissipation caused in steady contact discontinuities. Evje and Fjelde[17] followed in the paths of Wada and Liou, and extended their scheme to applications in a two-phase system. The resulting model is called AUSMV, and is the scheme utilized in this thesis.

In the following sections the framework of the numerical scheme is outlined. The particular scheme presented in [18] was the starting point of the Matlab code applied in the well control simulations. It is essentially the same scheme as presented in [17], however the possibility of change in cross sectional area is introduced. Both [17, 18] are valuable references for a more detailed description of the AUSMV scheme. Extensions and modifications to the Matlab code for well control purposes are presented in section 10.3.

8.1.1. Conservation equations

The conservation equations are the fundament of the drift flux model. There are two equations describing the conservation of mass for the respective phases. A third equation describes the conservation of momentum. Assuming no mass exchange between the phases, this yields the following set of equations,

$$\partial_t \begin{pmatrix} A\alpha_l\rho_l \\ A\alpha_g\rho_g \\ A\alpha_l\rho_l v_l + A\alpha_g\rho_g v_g \end{pmatrix} + \partial_x \begin{pmatrix} A\alpha_l\rho_l v_l \\ A\alpha_g\rho_g v_g \\ A\alpha_l\rho_l v_l^2 + A\alpha_g\rho_g v_g^2 + AP \end{pmatrix} = \begin{pmatrix} 0 \\ 0 \\ -Aq \end{pmatrix} \quad (8.1)$$

Where $A =$ Cross sectional area.

$\rho =$ Mass density

$v =$ Phase velocity

$P =$ Absolute pressure

$q =$ Source term, sum of the pressure gradients caused by gravity and friction

The indices l and g represents liquid and fluid. The symbols ∂_t and ∂_x corresponds to the derivatives in time and position respectively. The symbol α denotes the volumetric fluid fractions, with the sum of which equal to unity. Thus, the following relation applies.

$$\alpha_l + \alpha_g = 1 \quad (8.2)$$

These relations are common for all two-phase models derived with basis in the drift flux model.

8.1.2. Mixture properties

The volume fractions are further used in describing average properties of the two-phase combination. The equations describe velocity, density and viscosity, and are all on the same form. The equations are given by,

$$v_{mix} = v_l\alpha_l + v_g\alpha_g \quad (8.3)$$

$$\rho_{mix} = \rho_l\alpha_l + \rho_g\alpha_g \quad (8.4)$$

$$\mu_{mix} = \mu_l\alpha_l + \mu_g\alpha_g \quad (8.5)$$

The viscosities for the one-phase fluids are set to constant values. Liquid viscosity is set to 5 e-2 Pa·s and gas viscosity set to 5 e-6 Pa·s. The other parameters are all depending on the dynamic system properties.

Additionally, an approximation to the sonic velocity of the combined phases is given by,

$$\omega^2 = \frac{P}{\alpha_g \rho_l (1 - K\alpha_g)} \tag{8.6}$$

Where ω = Approximated sonic velocity

K =Flow dependent parameter (from slip relation, see next section).

In the approximated sonic velocity the K is set to unity. This was done as this was seen to have little influence on the values obtained for the sonic velocities[18].

8.1.3. Slip relation

The slip relation is given by,

$$v_g = K v_{mix} + S \tag{8.7}$$

Where K = Concentration profile parameter, set to a constant value of 1,2 (dimensionless)

S = Drift velocity, set to a constant value of 0,5 m/s

The slip relation is responsible for gas migration and distribution throughout the system. In systems with a static liquid component, the gas phase will migrate with a velocity just over S. Therefore, S is often referred to as the drift velocity.

8.1.4. Fluid densities

The fluid densities are due to compressibility, functions of pressure. The liquid density function is modeled by the relation,

$$\rho_l = \rho_{l,STC} + \frac{P - P_{STC}}{c_l^2} \tag{8.8}$$

Where $\rho_{l,STC}$ = Liquid density at atmospheric conditions, initially set to 1000 kg/m^3

$P - P_{STC}$ = Gauge pressure

c_l = Sonic velocity in one-phase liquid, set to 1000 m/s

The gas density function is modeled by the relation,

$$\rho_g = \frac{P}{c_g^2} \tag{8.9}$$

Where c_g = Sonic velocity in one-phase gas, set to 316 m/s

8.1.5. The source term

The source term q, on the right hand side of equation (8.1) contains the hydrostatic gravity gradient and the frictional gradient. The gravity gradient is given by,

$$\left(\frac{dP}{dx}\right)_{Grav} = g \cdot \rho_{mix} \cos(\theta), \tag{8.10}$$

Where g = Acceleration of gravity, 9,81 m/s^2

The friction model initially implemented is valid for laminar flow of a Newtonian fluid in a tube of circular circumference (section 9.1.6). The friction is given by,

$$\left(\frac{dP}{dx}\right)_{Fric} = 2f \cdot \rho_{mix} \frac{v_{mix}^2}{d_o} \tag{8.11}$$

Where d_o =Outer diameter (typically open hole diameter or inner diameter of casing)

f =Friction factor, generally set to 16/Re for laminar flow

The resemblance with equation (7.7) in the analytical model is obvious. However, also a slightly new definition of the Reynolds number is introduced:

$$Re_{Ini} = \frac{\rho_{mix} v_{mix} d_o}{\mu_{mix}} \tag{8.12}$$

Combining the two previous expressions yields the implemented friction model

$$\left(\frac{dP}{dx}\right)_{Fric,Ini} = \frac{32 v_{mix} \mu_{mix}}{{d_o}^2} \tag{8.13}$$

The sum of the gravitational and frictional pressure gradients makes up the source term, q.

8.1.6. Flux splitting

The flux is associated with position. Thus, it is represented by the second column vector of equation (8.1). The column vector is divided into convective terms and pressure terms. This yields the expression,

$$F = F_C + F_P = \begin{pmatrix} A\alpha_l \rho_l v_l \\ A\alpha_g \rho_g v_g \\ A\alpha_l \rho_l v_l^2 + A\alpha_g \rho_g v_g^2 \end{pmatrix} + \begin{pmatrix} 0 \\ 0 \\ AP \end{pmatrix} \tag{8.14}$$

The convective flux is further divided into its liquid and gas components.

$$F_C = F_{C,l} + F_{C,g} = A\alpha_l \rho_l v_l \begin{pmatrix} 1 \\ 0 \\ v_l \end{pmatrix} + A\alpha_g \rho_g v_g \begin{pmatrix} 0 \\ 1 \\ v_g \end{pmatrix} \tag{8.15}$$

The fluxes across the segment interfaces are determined by a weighted average of values calculated at the segment midpoints immediately above and below the interface. The weighting is conducted as a function of the phase velocities, approximate sonic velocity and a χ-factor. The χ-factor is introduced in order to remove the numerical dissipation at steady contact discontinuities, and separates the AUSMV scheme from the other AUSM schemes. The value of the χ-factor needs to meet the requirement,

$$\chi_R \alpha_R - \chi_L \alpha_L = 0 \tag{8.16}$$

Here, the indices L and R refer to the segment midpoint immediately below and above the interface. In the proposed scheme the χ-factor values were chosen to be $\chi_R = \alpha_L$ and $\chi_L = \alpha_R$.

Although the principles of flux splitting are relatively comprehensible, the associated equations and the determination of the actual fluxes are quite complex, and it is recommended to read [17, 19] for a more thorough description.

8.1.7. Discretization

The time is divided into small timesteps, Δt. Spatial discretization is conducted in axial direction, where the length of each segment is denoted Δx. The value of these steps is time and space are required to meet the CFL-condition,

$$\frac{\Delta x}{\Delta t} \leq \max(|\lambda_1|, |\lambda_2|, |\lambda_3|) \tag{8.17}$$

For subsonic flow λ_1, λ_2 and λ_3 corresponds to the velocity of the pressure pulses travelling in positive and negative direction and the fluid velocity.

The set of conservation equations (8.1) can be expressed as,

$$\partial_t(\boldsymbol{Q}) + \partial_x F(\boldsymbol{Q}) = G(\boldsymbol{Q}) \tag{8.18}$$

Introducing the discretization in time and space, and solving for **Q** at time (n+1) Δt at segment number I yields the expression,

$$\boldsymbol{Q}_i^{n+1} = \boldsymbol{Q}_i^n - \frac{\Delta t}{\Delta x}\left(F_{i-1/2}^n(\boldsymbol{Q}_{i-1}^n, \boldsymbol{Q}_i^n) - F_{i+1/2}^n(\boldsymbol{Q}_i^n, \boldsymbol{Q}_{i+1}^n)\right) + \Delta t \cdot G(\boldsymbol{Q}_i^n) \tag{8.19}$$

Here $F_{i\pm1/2}^n$ are the fluxes at upper and lower segment interface of segment i.

This particular equation is together with the flux-splitting equations, the core of the Matlab code. These equations are evaluated at every timestep as progress in time is made. This way, the new conserved variables ($\mathbf{Q}^{n+1}$) may be calculated from the old ($\mathbf{Q}^n$).

8.1.8. Calculation of primitive variables

The primitive variables in the new timestep are unknown. There are a total of seven primitive variables which needs to be calculated:

- Volume fractions of the respective phases
- Density of the respective phases
- Velocity of the respective phases
- Pressure

For evaluation of seven variables, a set of seven independent equations is required. The three first equations are found by using the definition of **Q** obtained by comparing equations (8.1) and (8.16).

$$\boldsymbol{Q} = \begin{pmatrix} A\alpha_l\rho_l \\ A\alpha_g\rho_g \\ A\alpha_l\rho_l v_l + A\alpha_g\rho_g v_g \end{pmatrix} \quad (8.20)$$

In this context, **Q** is the calculated conserved variable. In addition to the above expression, equations (8.2), (8.7), (8.8) and (8.9) are utilized, in order to evaluate the seven variables.

In the solution strategy implemented in the Matlab code, the pressure is the first variable to be evaluated. The reason for this is that the pressure can be calculated directly from the conserved variables from the mass conservation. The calculation is done using a second order equation, obtained by combining the above mentioned equations. Knowing the pressure, the density of the respective phases can easily be calculated. This is done using the pressure dependent density relations (8.8) and (8.9). This is followed by calculation of the volume fractions and the velocities.

8.1.9. Simplifications

It is important to realize that the proposed numerical scheme does not describe the real nature of a two-phase system with total accuracy, nor is it expected to. The concept of finite discretization and numerical modeling in itself induces inaccuracy. Additionally, a few simplifications must be mentioned.

- Isotherm system.
- No mass exchange between the two phases.

However, this numerical scheme is assumed to be a substantially better approximation to reality than the analytical model proposed in section 7.

8.1.10. Remarks

In the following, a few remarks on the particular numerical scheme and Matlab code are included. They are not of importance for the totality of this thesis, but should be noted for future simulations with the implemented Matlab code.

Flow related variables which can be altered during a simulation

Not all variables can be changed during a simulation run. There are primarily three variables which can be continuously controlled:

- Liquid mass rate at the inlet (pump rate)
- Gas mass rate at the inlet (influx rate)
- Pressure at the outlet (choke pressure)

It is recommended to utilize a steady ramp up/down (typically 10 s) if these variables are to be changed. Rapid changes may induce excessive pressure pulses or water hammering.

Additionally, the outlet can be changed from open/closed (shut-in) or vice versa at any time during the simulations.

Initialization of pressure and density

For a vertical well, the pressures and densities are initialized at standard conditions, and with gravity set equal to zero. During the first 100 seconds of every simulation, the gravity is linearly increased from 0 to 9,81 m/s^2. This gives reasonable static pressures and mass distribution throughout the wellbore.

For illustrational purposes, it may be compared to “hoisting” the well from horizontal to vertical.

On the implementation of cross-sectional changes

For the model to function properly, any changes in cross-section have to occur at the segment midpoints[18]. This is related to the calculation of the mass fluxes.

For illustrational purposes one-phase simulations were done on a horizontal pipe of length 3000 m. The diameter of the left 1500 m is 0,1 m, while the diameter of the right 1500 m is 0,2 m. A constant liquid mass rate of 10 kg/s was used (from left to right). The first simulation was done with the change in cross section located at a segment interface (50 segments). The following simulation was done with the change in cross section at the segment midpoint (25 segments).

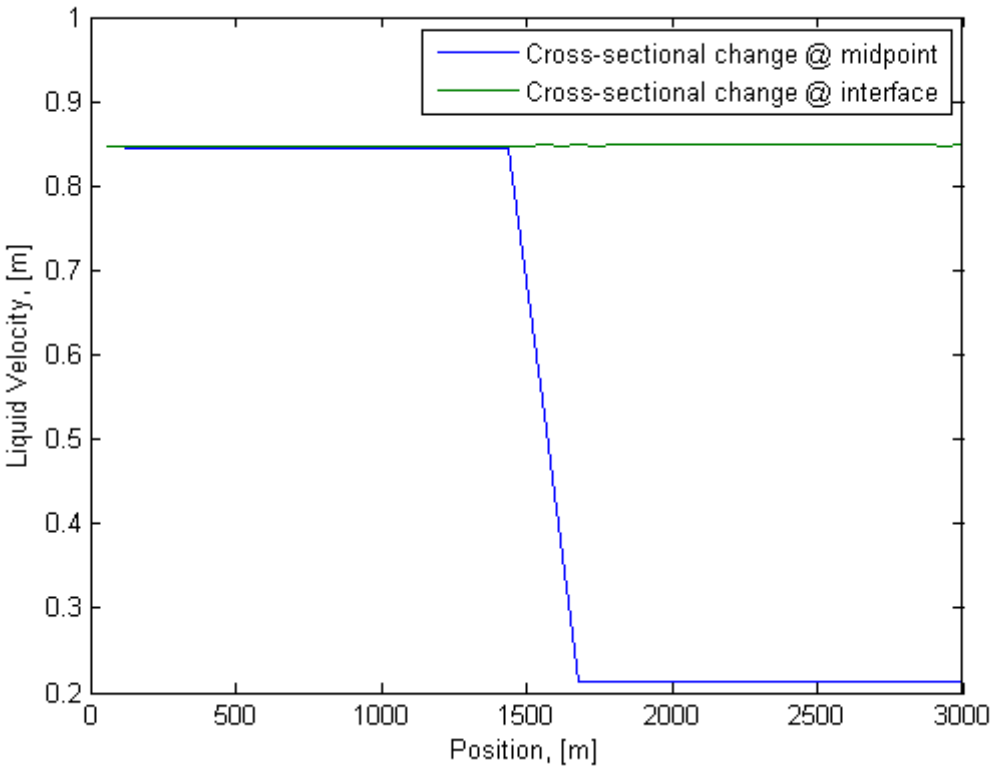

Figure 8-1: Liquid velocities with cross-sectional change in the segment midpoint versus in the segment interface. This illustrates the importance of implementing changes in the cross section in the segment midpoints.

The plot shows the steady state velocity profile in the pipe (time 1000 s). The scale on the abscissa corresponds to position relative to the inlet at far left.

For incompressible flow, the liquid velocity in a segment should be inverse proportional to the cross-sectional area of the segment. As seen in the plot, this is clearly not the case when the cross-sectional change occurs in the segment interface.

Velocity profiles

The gravitational term in the equation for momentum conservation seems to cause a slight defect in the velocity profile of the system. At non-horizontal situations, the velocity in the various segments of the well is underestimated. This is most noticeable when the flow rate is set to zero or close to zero. Then, the average velocity in the system becomes negative. Thus, the flow direction is downwards. In reality, the average velocity should be zero. The error seems to diminish, as the number of segments increase.

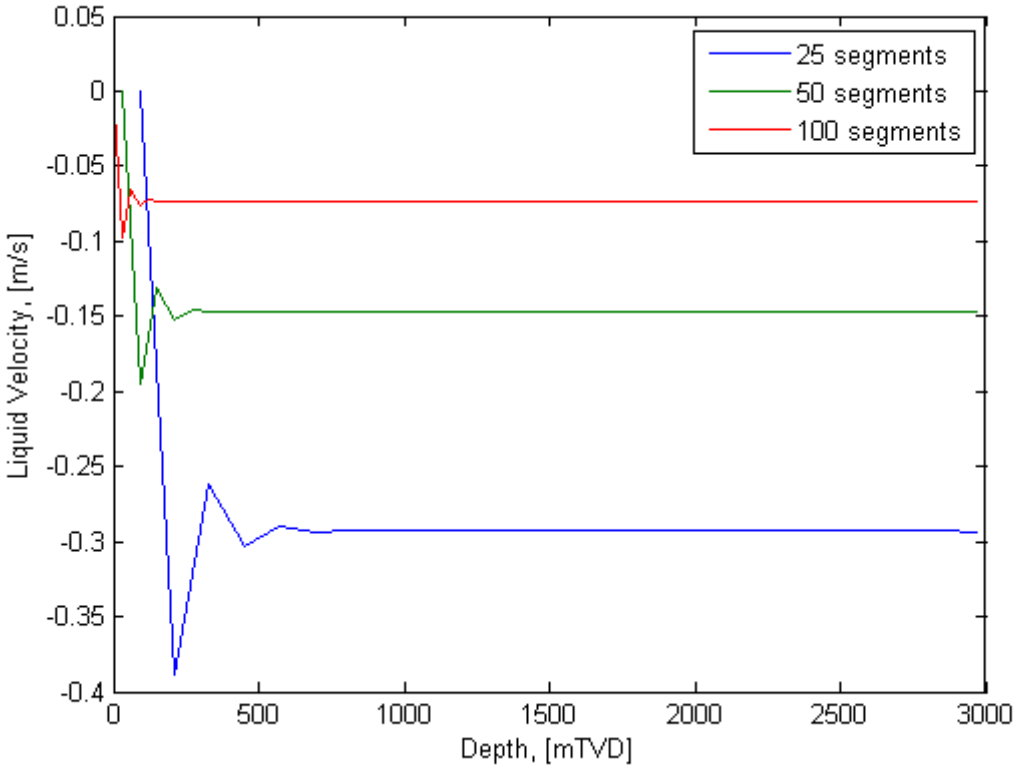

Figure 8-2: A numerical error causes the fluid velocity profiles to be consistently underestimated. The plot is produced at zero flow rate with increasing discretization. It can be noticed that the fluid velocities approach zero when increasing the number of segments.

It is assumed that this effect might be due to numerical dissipation, but the mechanisms behind this should be further investigated.

8.2. Development of a crude kick simulator

The model described in section 8.1 is the starting point in developing a Matlab code for simulations on well control. The main objectives are to make the model more suitable for simulations, and to make the model more realistic. In order to do this a series of extensions and modifications has to be implemented:

- A more realistic friction model.
- Changing the liquid component of the system from water to drilling fluid (altering the liquid density).
- A backpressure regulator, in order to circulate kicks at constant bottomhole pressure.
- A more accurate reading of bottomhole and casing pressures.
- A drillstring function, which makes it possible to read drillpipe pressure.
- A chokeline and riser for simulation on subsea wells.
- A pit gain reading.
- Opening up for wellbore deviation.
- A Darcy relation for influx where influx size and mass rate depends on downhole pressure differential. This is important for drilled kicks or connection kicks.
- Additionally, a choke model was implemented in the model, but it has not been used in the simulations. The choke model depicts the backpressure as a function of fluid density, flow rate and choke opening.

In the following sections, the implementation of these modifications is described.

8.2.1. Standard test case

A standard test case is introduced in order to verify and compare the modifications done in the Matlab code. The test case is mainly used in sections 8.2.2-3 where nothing else is stated. The subsequent modifications are verified by the simulations conducted in sections 8.3 and 8.4. Elements of the test case will also be referred to in later sections.

Test well

The simulations to follow are mainly conducted on a common test well of 3000 m. The well is vertical well with surface BOP. In order to simplify, the borehole has a constant diameter of 12 ¼ in from top to bottom. The well is drilled with 5 inch drillstring and a 180 m 8 ½ inch BHA. The well is divided into 25 segments of 120 m.

Test influx

A swabbed gas kick of 1867 kg is taken in the test well. The majority of the influx (1600 kg) is taken during a time period 130-190 s at a constant mass rate of 26,67 kg/s. In addition, there is a 10 s linear ramp up/down in both ends of the time interval.

At hydrostatic bottomhole pressure exerted by 1,0 SG mud, the kick mass will occupy on the high side of 6 m^3. With 1,5 SG mud it will occupy just over 4 m^3.

Time line

The well is turned to vertical in the first 100 s. The test influx is taken in period 120-200s. Shut-in occurs at time 260 s, with a 240 s build up of downhole pressures. The kill is initiated at time 500 s at a kill rate of 1000 lpm.

8.2.2. Friction model

The initial friction model (briefly described in sections 8.1.5) displays excessive oscillation. Additionally, it does not take into account that the flow in a wellbore is annular, nor does it allow for turbulent flow to occur. Two different solutions were proposed and will be tested and compared. The results of the test will result in three alternatives:

- Keeping initial model (model #1).
- Extending initial model to apply for annular flow (model #2).
- Introducing new model for annular flow, which also takes turbulent flow into account (model #3).

Model #1

As described in the previous paragraph, there are a number of problems associated with the initial friction model. The friction model displays excessive oscillations. This is assumed to be due to an unrealistically low frictional gradient. If the friction is increased the oscillations are expected to be damped more rapidly. The friction model utilizes the diameter of the open hole/casing, i.e. the outer diameter of the annulus. This does not take into account that the flow is annular, and will underestimate the friction. The model is based on laminar flow, although turbulent flow is known to occur in a wellbore. This will further underestimate the friction.

Model #2

The second model is based on descriptions in [4]. It will make use of equation similar to those of section 8.1.5. However, the concept of annular thickness is introduced as an alternative to the outer diameter used in equation (8.13). This will increase the friction, and is also more realistic than the initial model. This yields the general expression for the frictional gradient.

$$\left(\frac{dP}{dx}\right)_{Fric,Ann} = 2f \cdot \rho_{mix} \frac{v_{mix}^2}{d_o - d_i} \tag{8.21}$$

The friction factor is still calculated as for laminar flow, and is set to 16/Re. However, the diameter in the general definition of the Reynolds number is exchanged with the annular thickness. Thus,

$$Re_{Ann} = \frac{\rho_{mix} v_{mix} (d_o - d_i)}{\mu_{mix}} \tag{8.22}$$

Combining equations (8.21) and (8.22) yields the expression,

$$\left(\frac{dP}{dx}\right)_{Fric,Ann} = \frac{32 v_{mix} \mu_{mix}}{(d_o - d_i)^2} \tag{8.23}$$

This expression is implemented directly in the source term of the Matlab code.

Model #3

Model #3 was suggested in [20], and utilizes annular thickness. Hence, equations (8.21) and (8.22) are valid. The model is also valid for turbulent flow, thus relies on two expressions for the friction factor. For laminar flow the friction factor is calculated as,

$$f = 24/Re_{Ann} \tag{8.24}$$

For turbulent flow, the friction factor is calculated as

$$f = 0{,}052 \cdot Re_{Ann}^{-0{,}19} \tag{8.25}$$

The model uses Re=2000 as the upper limit for laminar flow. Lower limit for turbulent flow is set at Re = 3000. In the transition between laminar and turbulent flow linear interpolation is applied in order to obtain a smooth transition.

This model is implemented in the Matlab code as a function which calculates the frictional gradient in steps. Therefore, the explicit expressions for the frictional gradient will not be presented here.

Model testing and results

The testing is performed on the standard test case defined in section 8.2.1. During the circulation, the outlet pressure is kept at a constant level equal to SICP.

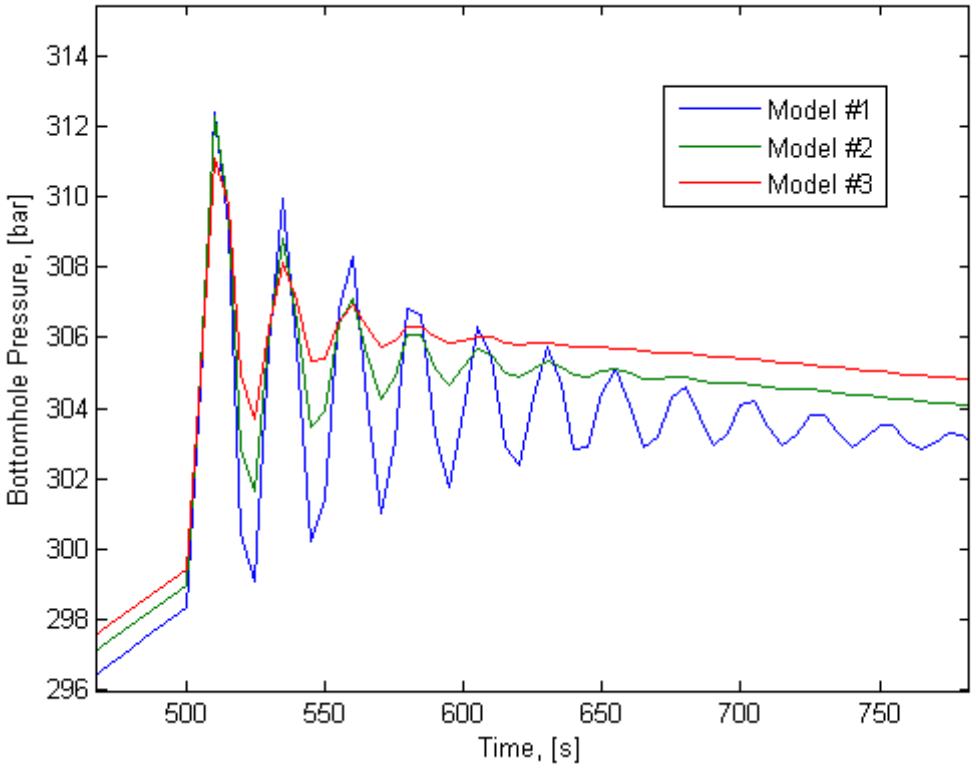

Figure 8-3: Response in bottomhole pressure as circulation is initiated in the standard kill test case. The plot shows the response for the different friction models.

The resulting plot is shown in figure 8-3. The oscillations are produced as circulation commences. It can be observed that the initial model produces excessive oscillations. It also underestimates the friction compared to the other models. The third model dampens the oscillations rapidly. The amplitude of the oscillations is practically zero after four periods. It also seems to produce a higher steady state bottomhole pressure. The properties of model #2 are close to a cross between the properties of the other two models. It shows a fairly efficient damping. The steady state bottomhole pressure is from the plot expected to settle at close to the average of the other models.

It was decided to permanently implement model #3 to the Matlab code, as this was interpreted to have the most desirable properties.

8.2.3. Density

The liquid density was initially set to 1 SG. Usually the tophole of a well is drilled with sea water and high viscosity pills. In that respect a liquid density of 1 SG is appropriate. However, the lower sections are drilled with weighted mud. Therefore the density of the liquid component of the system had to be increased. A mud weight of 1,5 SG was selected. This is a common mud weight when drilling the deeper sections of a well.

In the Matlab code this is implemented with ease, and tested under the same conditions as for the friction models. The new mud weight is simply set by changing the mud weight at standard conditions.

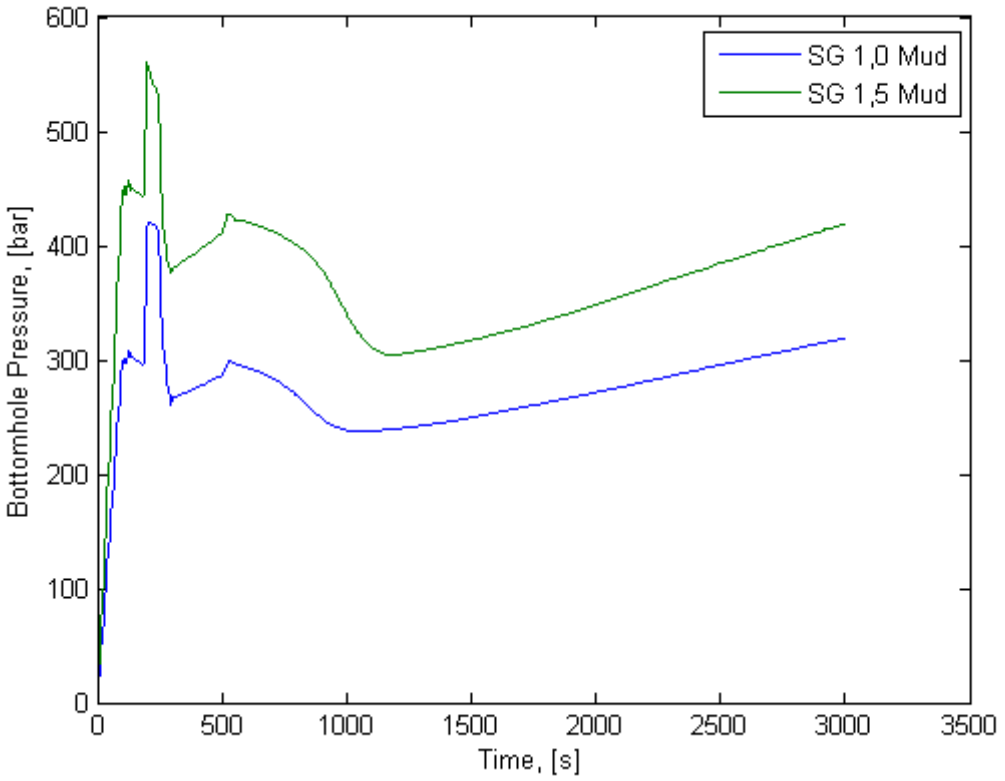

Figure 8-4: Bottomhole pressure for liquid densities 1,0 SG and 1,5 SG. The plot is produced in accordance with the standard kill test case with choke pressure equal to SICP during the circulation.

Figure 8-4 is produced according to the standard test case, with outlet pressure set equal to the shut-in casing pressure. It can be seen from the figure that the implementation was a success. As seen, there is an approximate 50% increase in BHP, when increasing the mud weight by 50 points. This was expected, since a 50 % increase in mud weight, should lead to a 50 % increase in the hydrostatic pressure.

The difference in slope should also be noticed. This is interpreted to be due to a change in frictional gradient as a function of the increase in density.

8.2.4. Implementation of an outlet pressure regulator

Most kill methods are performed using constant bottomhole pressure. In a well control situation this is obtained by manually operating a choke valve at the outlet. However, in the current numerical scheme it is not possible to simply set the bottomhole pressure to a constant value. This is due to the fact that the scheme incorporates pressure pulses. It would therefore be highly beneficial to implement an automatic regulator, which would be able to control the bottomhole pressure by applying a variable outlet pressure. Ideally, the outlet pressure should be a function of the choke opening in the choke model introduced in section 8.2.11, as this would be most realistic. However, it was decided to utilize the outlet pressure directly.

Control Theory

This section is written with reference to [21]. Through regulation of an output variable, a related process variable is attempted to be kept at a desired predetermined value. This value is called the

setpoint. In this case, the output variable will be the outlet pressure (choke pressure). The variable to remain constant will be the bottomhole pressure.

A general PID-regulator (proportional, integral, derivative) continuously gives the output variable as the sum of three main terms.

- The proportional term.
- The integral term.
- The derivative term.

The proportional term contributes to the output variable with a value proportional to the deviation (error, denoted e) between the setpoint and the actual process variable at any given time. The proportionality factor is called the proportional gain and denoted K_p. In this context the setpoint will be the bottomhole pressure measured at shut-in, the process variable will be the measured bottomhole pressure.

The integral term is meant to assure that the errors accumulated in time will approach zero. This is achieved by adding a contribution to the output variable, equal to the time integral of the error multiplied by a factor. The factor is called the integral gain, and is equal to the proportional gain divided by the integral time (K_p/T_i).

The derivative term intends to compensate for sudden changes in the process variable. The derivative term contributes to the output variable with a value proportional to the time derivative of the error. The proportionality factor is called the derivative gain, and can be further decomposed to the proportional gain multiplied with the integral time ($K_p T_d$).

An optional parameter called the nominal output (u_o) may be added to the PID-regulator. This is set at a value in the same range in which the output variable is expected to vary.

The proportional gain, integral time, derivative time and the nominal output must all be tuned in order to achieve optimal regulation. This is achieved using Ziegler-Nichols' closed circuit method, described in the appendix. The tunable parameters have to be adjusted for every change in process dynamics (kick size, well depth, fluid properties etc.).

The PID-regulator is generally given by the expression,

$$u = u_0 + K_p e + (K_p/T_i) \cdot \int_{\tau=t_0}^{t} e \, d\tau + K_p T_d \cdot \frac{de}{dt} \qquad (8.26)$$

Where u = Output variable, in this case outlet pressure

u_0 = Nominal output, in this case set to SICP

e = Error, the difference between the setpoint and the process variable

t = Time

K_p = Proportional gain

T_i = Integral time

T_d = Derivative time

Equation (8.26) is based on a continuous scale, both in time and space. However, in the numerical scheme, time and space are discrete. Thus, equation (8.26) has to be converted to discrete form. The integral term is therefore implemented as a sum, and the derivative as a difference. The formula then takes the form

$$u(t) = u_0 + K_p e(t) + (K_p/T_i) \cdot \sum_{\tau=t_0}^{t} (e(\tau) \cdot T_s) + K_p T_d \cdot \frac{e(t)-e(t-1)}{T_s} \quad (8.27)$$

The regulator may also take an equivalent form, by subtracting u(t-1) from u(t), so that

$$u(t) = u(t-1) + K_p[e(t) - e(t-1)] + \left(\frac{Kp}{T_i}\right) e(t) \cdot T_s + K_p T_d \frac{e(t)-2e(t-1)+e(t-2)}{T_s} \quad (8.28)$$

Where T_s = Sample time, the period in time between every adjustment in the output variable. Set to dt where nothing else is stated.

Equations (8.27) and (8.28) are both implemented in the Matlab code, and yields equivalent results.

If satisfactory regulation is not achieved after tuning the parameters according to Ziegler-Nichols routine, it is suggested to scale the regulator parameters by multiplying them with a common factor. This is done as a means for adjusting the rate of convergence or the stability of a regulator. That is, Kp, 1/Ti and Td may be adjusted by a factor c, so that

$$u = u_0 + c \cdot K_p e + c^2 \cdot (K_p/T_i) \cdot \int_{\tau=t_0}^{t} e \, d\tau + c^2 \cdot K_p T_d \cdot \frac{de}{dt} \quad (8.29)$$

In order to increase the convergence rate of the regulator, c is set to a value greater than 1. In order to improve the stability, c is set less than 1. However, c should not be set to a negative value, as this will make the proportional term counteract the convergence of the bottomhole pressure. By setting c=1, the regulator parameters remains unchanged. Setting c=0 will simply reduce the regulator output to the nominal output u_o.

Complications

The design of a choke regulator is a challenge, due to the complexity of the wellbore system. There is a time lag between any pressure regulation on top and the following response in bottomhole pressure. This time delay is not only dependent on the measured well depth, but also on the volume fractions and variable properties of the respective fluids.

Another complicating factor is that the bottomhole response of a choke pressure adjustment is variable throughout a round of circulation of a kick. This is due to gas expansion, which leads to increasing volume fractions of gas in the wellbore. The gas acts as an accumulator which partially absorbs any choke pressure adjustment.

Rapid manipulation of the choke pressure will induce oscillating pressure pulses in the wellbore system. This may result in over-compensating the output pressure.

Regulator tuning

The implemented PID-regulator is tuned using Ziegler-Nichols' closed circuit method, described in the appendix. Initially, three approaches were considered for the purpose of tuning the regulator:

- Tuning the regulator with respect to an increase in pump rate in a liquid filled well.
- Tuning the regulator with respect to an increase in pump rate in a well partially filled with gas.
- Tuning the regulator with respect to a well control situation.

In all cases the test well introduced in section 8.2.1 is considered. The outlet regulator commences from time 500 s.

In the first two cases an increase in bottomhole pressure was induced by going from static conditions to a 5000 lpm pump rate. The volume rate is applied from time 500 s, and yields an increase in bottomhole pressure of just more than 1 %. The nominal output pressure is set to 1 bara, and the set pressure was set to 438,8 bara (approximately 1 bar below the hydrostatic pressure). The first approach is conducted in a well completely filled with drilling fluid. For the second approach, the well was initialized (before turned to vertical) with a 0,1 volume fraction of gas. For the third approach, the full test case outlined in section 10.2.1 was conducted.

By an application of Ziegler-Nichols routine, the critical values K_{pk} and T_p were found, and from these the tuned parameters were obtained. The results are presented in the table below.

Approach #	Regulator	K_p	T_i, [s]	T_d, [s]
1	PID	0,6	3,0	0,75
"	PI	0,45	5,0	0
2	PI	0,405	6,67	0
3	PI	0,135	12	0

Table 8-1: Tuned regulator parameters for the various approaches.

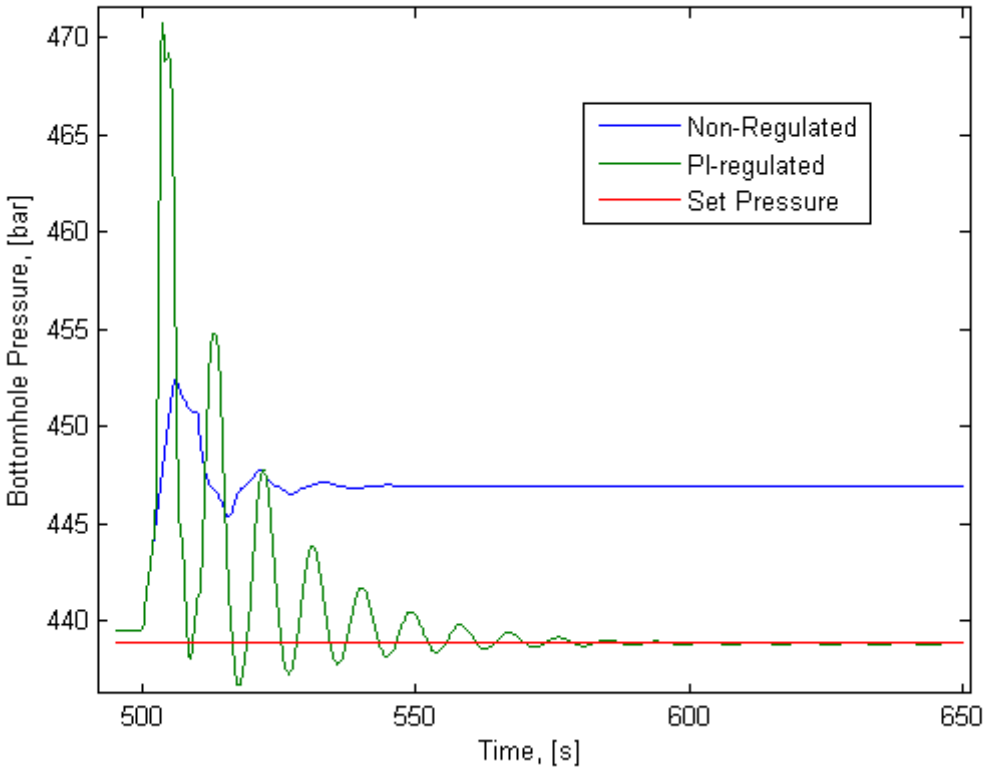

Figure 8-5: PI-regulator tuned with respect to approach #1 compared with non-regulated bottomhole pressure. Pressure response as pump rate is raised from 0 to 5000 lpm at time 500 s.

The figure above is produced with basis in the first approach. It displays the PI-regulator with the parameters as stated in the table. It is observed that the PI-regulated bottomhole pressure successfully converges towards the setpoint. Another observation is that the regulator operates with negative outlet pressures. This was later altered, and an upper and lower limit for the outlet pressure was introduced. The lower limit is the atmospheric pressure, 1 bar. The upper limit is set to 1035 bar, which corresponds to a choke valve pressure rating of 15000 psi. This is a typical value used on high pressure equipment.

The PID-regulation was not included in the figure due to instability and excessive oscillations. The high amplitudes were not only caused by pressure pulses, but also regulator instability. It was assumed that some of the instability was caused by the derivative term of the regulator. In the further work it was decided to completely abandon the PID-regulation, and focus on PI-regulation.

The plot produced from the second approach will not be presented here, as it is resembles Figure 8-5. The figure obtained from the third approach will be presented in the next section, where it also will be compared with the two previous approaches.

Regulator testing

Further, the tuned regulators obtained from the different approaches were tested and compared in a test case. However, a mistake was made, and the actual test case deviates slightly from the case defined in section 10.2.1. The main difference from the defined test case is that the bottomhole pressure is read from the bottom of segment one instead of in the midpoint (see section 10.2.5), while the regulator operates with respect to the segment midpoint. Additionally, the length of the

BHA is set to 300 m, as opposed to 180 m for the defined test case. This deviation from the standard test case is not expected to cause a degradation of the qualitative results of the test. Quantitatively however, this will affect the downhole pressures throughout the simulation runs.

The nominal output pressure was set equal to the shut-in casing pressure. For the setpressure, a value equal to the shut-in bottomhole pressure was utilized.

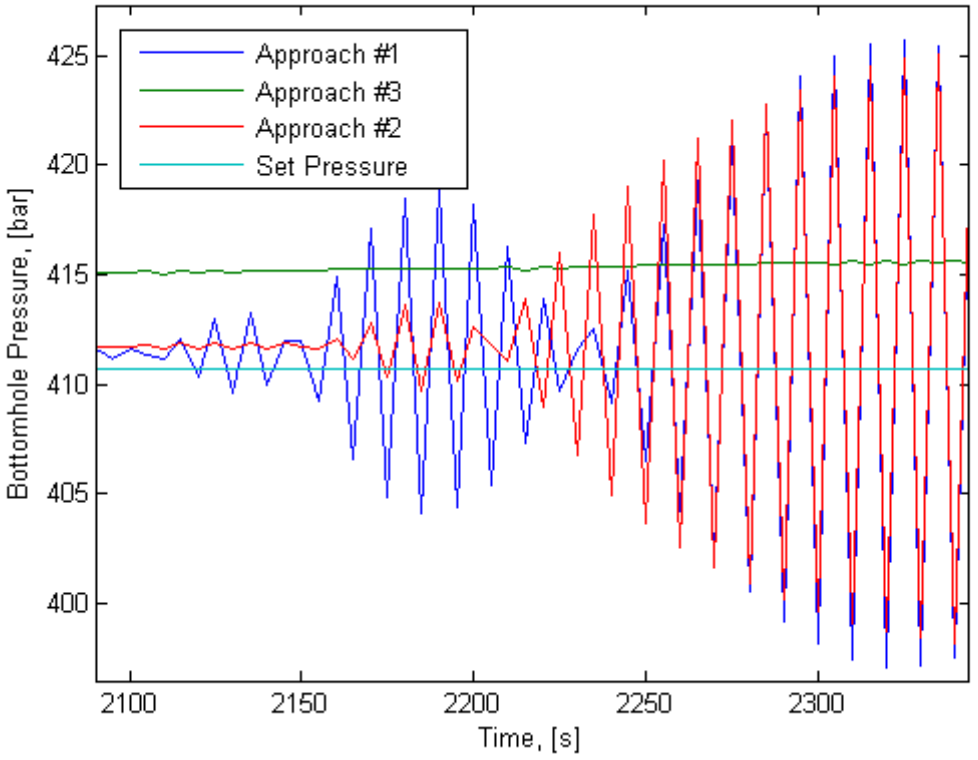

Figure 8-6: Testing of the PI-regulators tuned with respect to the various approaches. The regulators are tested in a well control situation slightly deviating from the standard test case.

The results of the testing may be seen in the figure above. All regulators functioned satisfactory in the time before 2100 s. However, it can be seen that the regulators tuned with respect to the first two cases displayed substantial instability from time 2100 s. After analysis of the gas/liquid fraction profiles, it was discovered that this coincides with the time in which the gas approaches the surface. The massive gas expansion close to surface, challenges the dynamic properties of the regulator. This means that the tuning of the regulator parameters is not optimal, with respect to a situation with large amounts of gas present.

The root mean square of the error was calculated for the different approaches. For the respective approaches the values were found to be 9,76 bar, 9,19 bar and 4,81 bar (approach #1, approach #2 and approach #3 respectively). As might be expected and as seen in the figure above, the regulator tuned directly with respect to the kill situation displayed the best performance. The performance is however not satisfactory. Thus, it was decided to scale the parameters found from the third approach, in accordance with equation (8.29).

Scaling the regulator parameters

Using the tuned parameters found by approach #3 (K_p=0,135; T_i=10), a range of different scaling factors were tested. This was done in order to investigate the effect with respect to stability and rate of convergence. The ultimate objective is to make the regulator perform with a high rate of convergence while still maintaining satisfactory stability. The scaled regulators were tested according to the standard test case defined in section

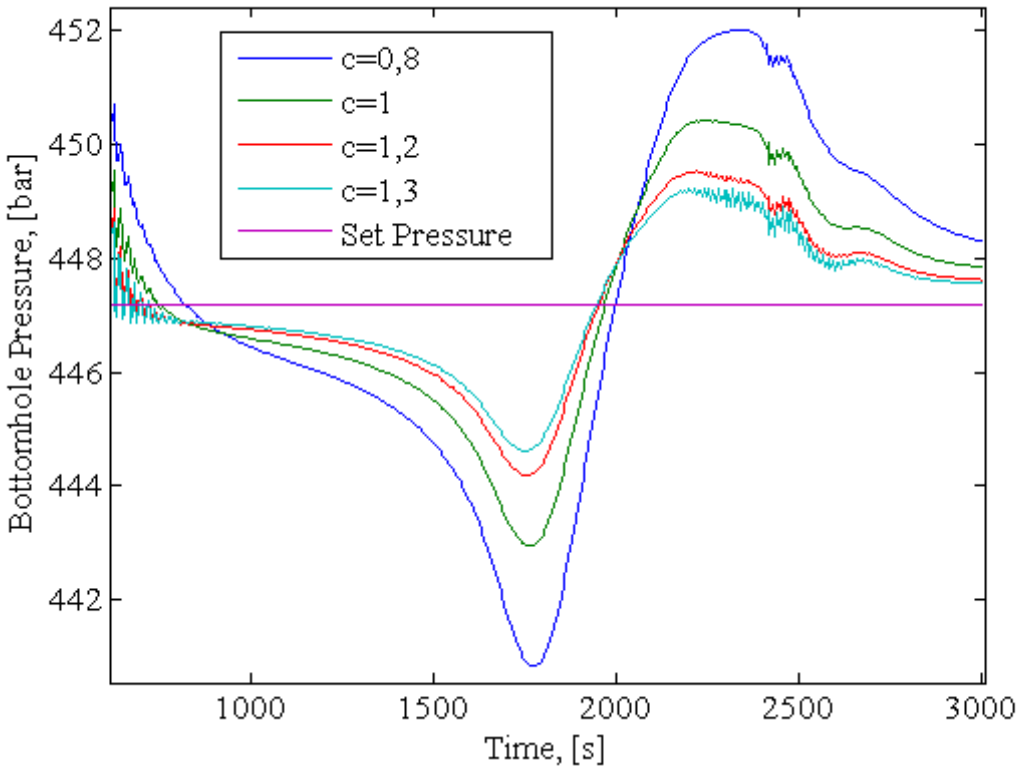

8.2.1

Figure 8-7: Regulator parameters from approach #3 scaled with a range of different scaling factors c. The performance of the scaled regulators is tested according to the defined standard kill test case from section 8.2.1.

As can be seen in the figure, the scaling of the parameters by a factor c, affects the variable pressures as previously claimed. Increasing c, yields a higher rate of convergence on the expense of loosing stability and vice versa. Simulations were also run for scaling parameters higher than 1,3. These are however not included in figure 8-7, as heavy oscillations occurred.

c	**0,8**	**1,0**	**1,2**	**1,3**	**1,4**	**1,6**
RMS, [bar]	3,29	2,38	1,88	1,72	1,98	3,15

Table 8-2: Root mean square of the error (e), for the various scaling parameters in Figure 8-7.

In Table 8-2 the root mean square of the error for the different scaling factors are to be found. Looking at the table, the lowest RMS value is found for c=1,3. Hence, this may be looked upon as the best scaling factor. However, considering Figure 8-7, sustained oscillations occur around time 2250 s with the particular scaling factor. The damping of the initial oscillations is also poor. Thus, a value of 1,3 were in this case assessed as to be too high. The most convergent regulator, while still maintaining sufficient stability is found for c=1,2.

Even though the scaled regulator performed decent, the maximum bottomhole pressure after the initial oscillations are damped is 449,5 bar, the minimum pressure is 444,2 bar. This means the

interval in which the error e varies is reduced from 7,4 to 5,3 bar with respect to c=1. This is however still not satisfactory regulation. In traditional control theory, the next step in improving the regulation is gain scheduling. This approach will not be attempted in this thesis, as it is expected to be a fairly time consuming process. However, a novel approach was discovered, which displayed better properties. This will be introduced in a subsequent section.

Altering the sample time

In the previous regulators the outlet pressure was altered in every timestep (T_s=dt). It was decided to investigate if increasing the sample time would improve the properties. The regulator parameters are tuned for every different sampletime. The tuned parameters are found in Table 8-3.

Ts, [s]	Kp	Ti, [s]	c
dt	0,135	10	1,2
3dt	0,135	10,83	1,2
1	0,09	11,67	1,2
3	0,09	12,5	1,2

Table 8-3: Optimally tuned regulator parameters.

Figure 8-8 is produced by using the optimized parameters for the various sample times. The testing is conducted on the defined standard kick case (section 8.2.1).

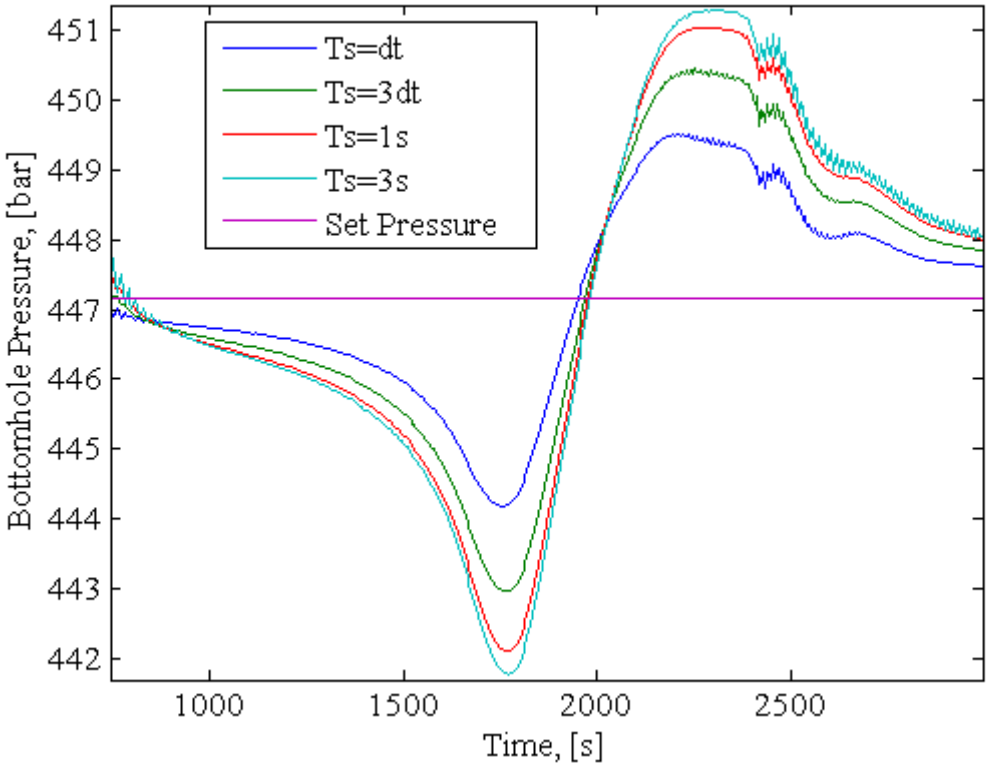

Figure 8-8: PI-regulation with increasing sample time. Testing conducted on the defined standard kick case.

As might be expected, the rate of convergence decreases at increasing sample time. The best regulation is accomplished with sample time set to dt. In the further work, sample time will consistently be set equal to dt.

Testing regulator sensitivity

It was decided to test the regulator response for a range of scenarios with various system dynamics. An initial assumption is that the regulator will have problems with high outlet volume rates of the respective fluids. Three sets of tests were conducted:

- Variable kick size.
- Variable well depth.
- Variable kill rate.

The testing is conducted on the defined standard test case where nothing else is mentioned. However, the bottomhole pressure is read at the very bottom of the well, as opposed to in the midpoint of the lower segment. This definition of bottomhole pressure will be introduced in a subsequent section. Qualitatively, this should not have any influence on the obtained results. The sensitivity testing will be executed using the best set of regulator parameters previously found (K_p=0,135; T_i=10; T_d=0; T_s=dt; c=1,2).

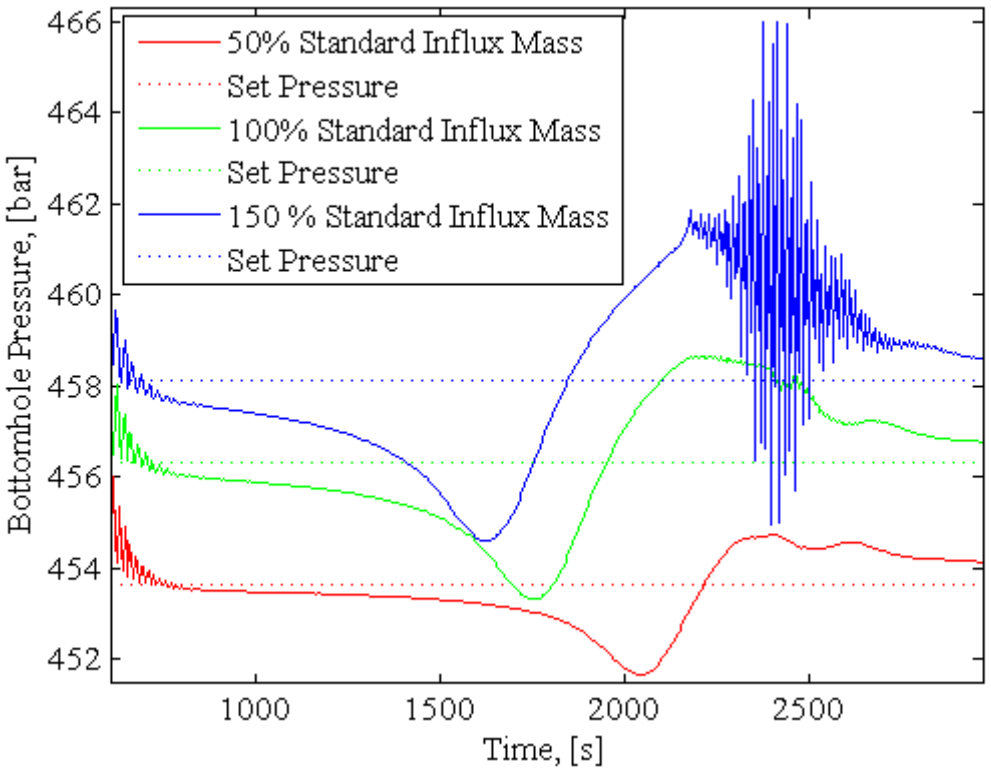

Figure 8-9: Testing regulator sensitivity with respect to influx mass. Standard influx mass equals 1867 kg, which yields a volume of approximately 4 m^3 at the prevailing bottomhole conditions.

In Figure 8-9 the regulator sensitivity is tested with respect to influx mass. An increase in bottomhole pressure as a function of influx mass is observed. The regulation has the highest rate of convergence for the smallest kick size. At the smallest kick size the regulator also displays the best properties when it comes to stability. At increasing influx size the regulation becoming worse. In the case with

the highest influx mass, regulator instability occurs as gas reaches the surface. This agrees with the initial assumption.

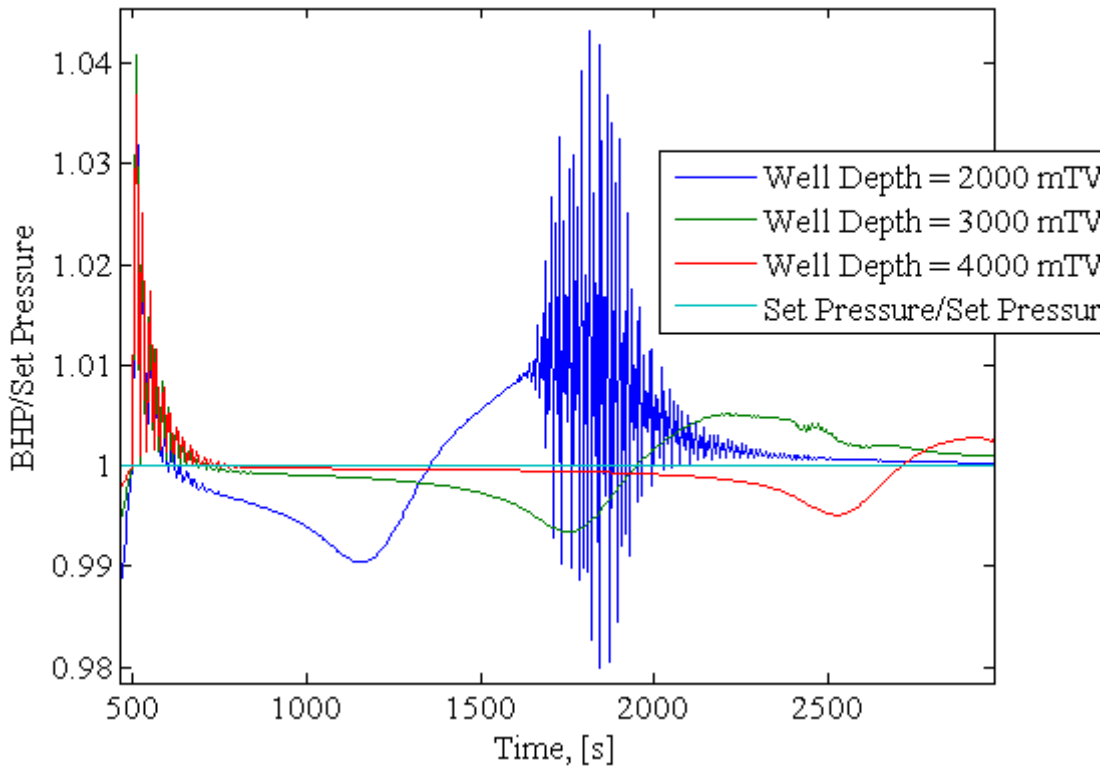

Figure 8-10: Testing regulator sensitivity with respect to well depth. The vertical geometry of the standard test well has been elongated and contracted. The bottomhole pressure has been normalized by dividing with the set pressure. This is done to get the testing results in the same frame of reference.

Figure 8-10 is the result of a set of tests for finding the sensitivity of the tuned regulator with respect to well depth. In order to present the bottomhole pressures in the same frame of reference, they have been divided with the respective set pressures.

The properties with respect to rate of convergence and stability are best for the deeper wells. For the 2000 m well, excessive oscillations occur as gas reaches the surface. As the influx mass is the same in all three simulations, this is interpreted as an effect of gas distribution. In the shallow well, the gas will reach surface before it has been properly distributed. In the deeper wells the distribution profile of the gas will be more elongated due to migration and gas slippage. Thus, the volumetric rates of gas will be lower as it reaches surface. This supports the initial assumption.

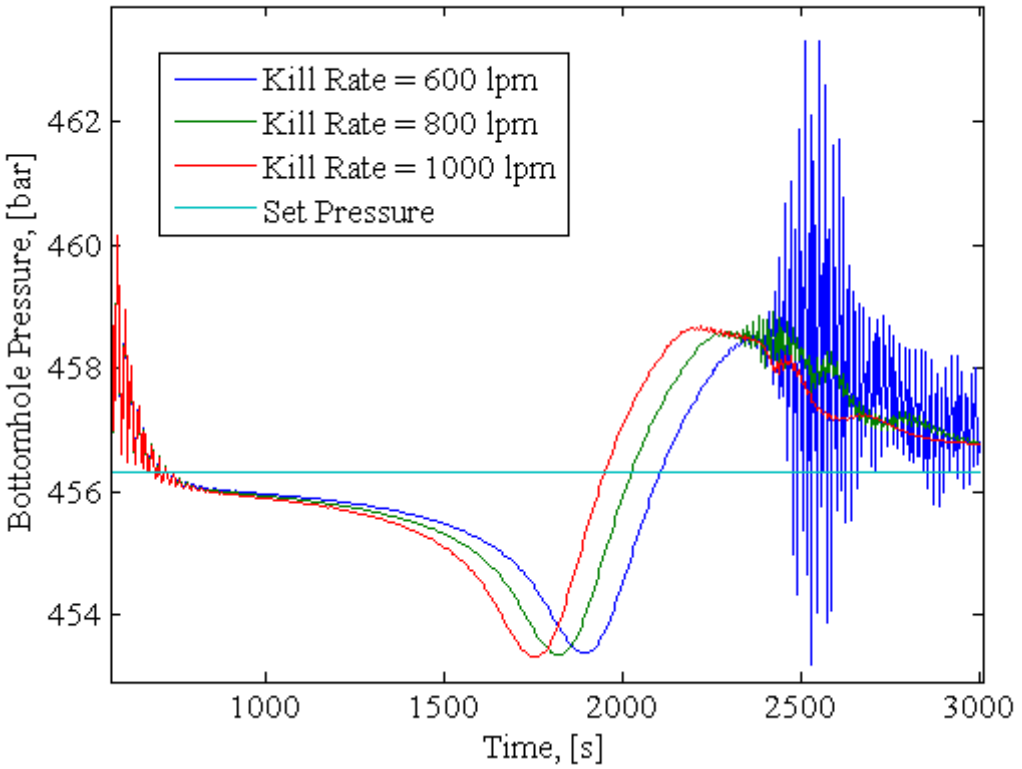

Figure 8-11: Testing regulator sensitivity with respect to kill rate.

In Figure 8-11 the results from the sensitivity tests with respect to varying pump rate are shown. Unexpectedly, the stability decreases at lower volume rates out. This is in contradiction with the initial assumption, and should be further investigated.

A novel approach

According to classical control theory, the next step in improving the regulation convergence and stability is gain scheduling. However, a new approach is suggested. The constant nominal output in the PID regulator is replaced with a variable reflecting the changes in dynamic properties, as the gas bubble rises in the annulus. By simply replacing the nominal output, with the output value at time t-1, impressive regulation was accomplished. This yields the relation,

$$u(t) = u(t-1) + K_p e(t) + (K_p/T_i)\cdot\sum_{\tau=t_0}^{t}[e(\tau)\cdot T_s] + K_p T_d \cdot \frac{e(t)-e(t-1)}{T_s} \quad (8.30)$$

The reasons for the success of this approach and its further implications, are not fully understood, and should be investigated.

The regulator was tuned by the same routine as done in previous sections. Satisfactory stability may be achieved by reducing the proportional gain by three orders of magnitude, compared to the typical

proportional gains used in the previous sections. At sample time dt, critical proportional gain is found to be 0,0011. The critical period is 19 s. The tuned regulator parameters are therefore set to K_p=4,95 · 10^{-4} and T_i=15,83 s according to Ziegler-Nichols. The optimal scaling factor c was found to be 1,1.

The new regulator was compared with the tuned regulator obtained from the classical approach. The standard test case was run using bottomhole pressure measurement in the midpoint of the lowermost segment.

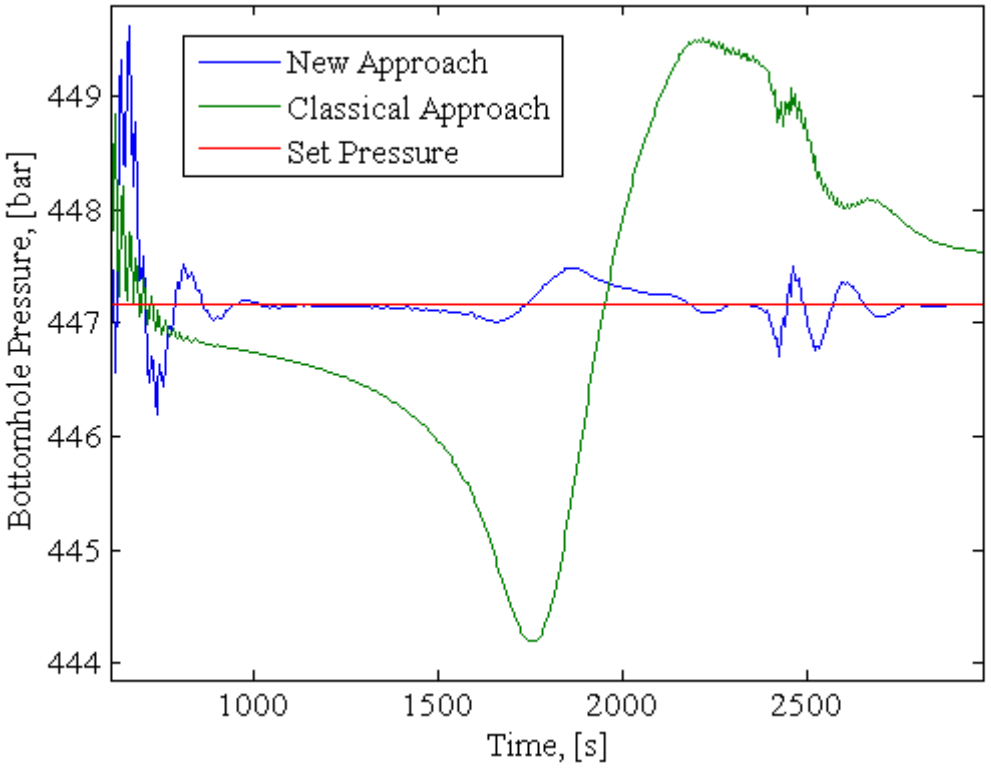

Figure 8-12: Tuned new approach tested against tuned classical approach. The testing was conducted on the standard test kick situation.

Using the new approach and after the initial oscillations are damped, the bottomhole pressure varies in an interval of 0,8 bar around the setpressure, whereas the corresponding interval of the classical approach is 5,3 bar. The respective root mean square of the error is 1,36 bar and 1,88 bar. This is a significant improvement. It seems that the new approach handles the dynamic nature of the kick situation in a better manner. Similar results could possibly also be achieved using classical control theory and gain scheduling. However, the new approach is less time consuming, while yet produces satisfactory regulation. Hence, the new approach will be used in the kick simulations to follow.

8.2.5. Accurate pressure readings

The bottomhole pressure initially read in the model is actually a pressure reading at the midpoint of the bottom segment. For a 3000 m well divided into 25 segments, this corresponds to a pressure reading 60 m off bottom. A more accurate pressure reading was desired. This was obtained by linear interpolation.

$$P_{BH} = P_1 + \frac{P_1 - P_2}{2}$$

Where P_{BH} = True Bottomhole Pressure

P_1 = Pressure at midpoint of segment 1

P_2 = Pressure at midpoint of segment 2

This equation neglects any difference in pressure gradient in the 1 1/2 bottom segments. Thus, it is assumed that the volume fractions, fluid velocities and densities are equal in the segments. These assumptions might produce a slight error. However, the error will diminish if the segment length is allowed to approach zero.

The same correction was made for the choke pressure.

8.2.6. Implementation of drillstring

The most important topside pressure when it comes to well control situations is the drillpipe pressure. The pressure is applied the kill sheet, and is also the parameter used in order to control the bottomhole pressure during the kill circulation. The drillpipe pressure is measured at drill floor level, at the standpipe manifold. It would be useful to have a drillpipe pressure reading implemented in the Matlab code.

A rather simple drillpipe pressure function was implemented. It is directly deduced from the bottomhole pressure, and does not take into account the time delay in the pressure response, nor the acceleration terms found in the AUSM model. The implemented drillpipe pressure is a function of a constant hydrostatic head of the mud column contained in the drillstring, and the friction loss due to mud flow. Further, a pressure loss across the drill bit was added. The entire drillstring was modeled as one segment, and constant capacity of the drillstring was assumed to be 8 l/m. This corresponds to an inner diameter of 0,10 m. The concept of the function may be stated as,

$$P_{DP} = P_{BH} - \Delta P_{HS} + \Delta P_{Fric,DS} + \Delta P_{Bit} \qquad (8.31)$$

Where the denotation is as described in section 7.1.3.

Hydrostatic pressure

The hydrostatic pressure in the drillstring is awkward to model. Simply setting the mud weight in the drillstring to 1,5 SG will cause a to high drillpipe pressure, as the mud on the annulus side is compressible. The average mud weight on the annulus side is higher than 1,5 SG. The selected solution is to make use of the bottomhole pressure measured after the well is turned to vertical. Immediately after the well is turned to vertical, the bottomhole pressure will exhibit exponentially damped oscillations, converging towards a value of hydrostatic pressure. An attempt was made to find the correct value of hydrostatic pressure, by averaging the oscillations over time. This would make the model flexible with respect to changes in density or well depth. However, this proved

difficult, as the hydrostatic bottomhole pressure was slightly overestimated. Other attempts were made to weight the average in various ways, so that the values produced with the lowest amplitudes was emphasized. It was also attempted to average the maximum and minimum values of the oscillations, and the values at the inflection points. None of these strategies were successful. Finally, a simulation was run to 1000 s, using no downhole inlet rates, nor any manipulation of choke pressure. The bottomhole pressure was converged to a constant value of 448 bar. This value was set constant in the drillpipe model. However, in reality the average density is a function of the pressure, so that the hydrostatic pressure would increase when subjected to pump pressure. This effect was neglected, but the resulting errors are assumed to be small, as the drilling fluid is close to incompressible.

Friction

For friction, the function implemented in section 8.2.2 was utilized. Only the input parameters are changed. The liquid density may be derived from the hydrostatic pressure. It is obtained by dividing the hydrostatic pressure by the well depth and the gravity acceleration. This yields an average density of approximately 1,52 SG. The liquid velocity is set to liquid mass flow rate divided by the average density derived from the hydrostatic pressure. This is again divided by the capacity of the drillpipe to obtain velocity. The liquid volume fraction in the drillstring is set to 1. This is realistic, as there normally is a float valve in the BHA, so that flow of gas into the drillstring is prohibited. The pressure input is set to the average between the drillpipe pressure and the bottomhole pressure. The diameter is set to correspond with the capacity of the drillpipe. The viscosity is set to 0,05 Pa*s.

Pressure drop across bit

The pressure drop across the bit was obtained as described in section 7.1.7.

The cross-sectional area of the bit nozzles is set to 0,902 square inches, with reference to the BHA presented in the appendix. In SI units this corresponds to $5{,}82 * 10^{-4}$ m^2. This is assumed to be a typical value. The discharge coefficient C, depends on the design of the nozzle, but is set to 0,95 with reference to [5].

8.2.7. Implementation of chokeline and riser

An offshore well with a subsea BOP, has a chokeline and riser which connects the BOP to the surface drilling facilities. During normal drilling operations, mud returns are taken through the riser. However, in a well kill scenario, the BOP will be closed, and the circulation will take place through a chokeline to the choke manifold. The chokeline has a small diameter, and acts itself as a choke valve due to friction loss. Typical inner diameters of the riser and chokeline are 18 ¾ inch and 3 inch.

In order to simulate well control procedures with a subsea BOP, a chokeline and riser had to be implemented. The intention was to let the wellbore branch into two different sets of segments from seabed to drill floor. The flow was to be controlled during simulations by operating a failsafe valve in conjunction with the BOP. Closed BOP and open failsafe valve would direct the flow through the chokeline, open BOP and closed failsafe would direct the flow through the riser. However, this was proven to be a quite cumbersome task, with respect to boundary conditions and fluxes at the segment boundaries. It was therefore decided to initialize the well with the desired geometry (chokeline or riser), rather than being able to manipulate the failsafe valve during simulations. Thus, there is no possibility of changing flow path between riser and chokeline during simulations, nor shutting in the well at seabed. This reduces the flexibility of the model. However, it may be assumed that the shut-in pressures below seabed should remain equal, whether the actual point of shut-in is

situated at surface or seabed. This assumption is valid as long as the effect of pressure pulses is negligible, and as long as the influx is situated below seabed.

The kill simulations to follow are run in two sequences. First a shut-in sequence with returns through riser. All data from the shut-in sequence is exported, except the conservative variables and the geometric data, and the simulations continued with failsafe open, i.e. with returns through the chokeline.

For convenience, a pressure recording at seabed was implemented. It is found by linear interpolation between the pressures read at the midpoint above and below the segment boundary corresponding with the seabed.

8.2.8. Implementation of pit gain

After a kick has been taken and the well is shut-in, the pit gain is read. This parameter is an indirect measurement of the influx size, and is used to calculate the kick height and the kick's average density. In that sense, it is an important parameter.

A pit gain monitor was implemented. The pit gain equals the time integral of the liquid volumetric flow rate at the outlet subtracted liquid volumetric flow rate into the hole. The integral is set to zero for at least the first 100 s of the simulations, as there occurs a negative outlet rate due to liquid compression when the well is hoisted to vertical.

8.2.9. Implementation of wellbore deviation

In order to be able to perform simulations on non-vertical wells, every segment was assigned an average angle (in radians). This angle is generated automatically, by setting a kick off point, an end of build and a final bottomhole inclination angle. The cosine of the various inclination angles were also introduced in the gravitational term in the conservation of momentum equation. Furthermore, slight changes had to be done in the drillstring function. The mean density of the drilling fluid in the drillpipe has to be calculated as a function of true vertical depth, rather than measured depth.

The slip-relation which was introduced in the previous sections is valid for vertical flow (inclination angle = 0). For horizontal flow, no-slip was assumed (inclination angle = π/2). For inclination angles in between, there was assumed a relation proportional to cosine of the angle of inclination. Thus,

$$v_G = [(k-1)\cos\theta + 1] \cdot v_{Mix} + s\cos\theta \tag{8.32}$$

This relation yields zero drift velocity s, at horizontal sections. This is a reasonable assumption since the drift velocity of the gas phase is a function of buoyancy. Buoyancy is directed upwards, thus the drift velocity should be directly proportional with the vertical component of the segment length.

8.2.10. Implementation of Darcy relation for influx

The previous simulations on kicks were made with gas influx rates reminiscent of swabbed kicks. The influx rate was slowly ramped up to a predefined influx rate. After the desired kick volume was

present in the lower segments of the wellbore, the influx rate was again ramped down to zero. This corresponds to pulling out pipe at slow rate, and stopping for connection.

The further simulations will be performed on drilled kicks. In order to get a realistic pressure build up, a pressure dependent influx relation has to be implemented. According to Darcy's law for pseudo-steady state[13], the influx rate is proportional to the formation pressure squared subtracted the bottomhole pressure squared. Thus

$$\dot{m} \propto {P_F}^2 - {P_{BH}}^2 \tag{8.33}$$

Where $\dot{m}$ = mass flow rate

By assuming a constant formation pressure larger than the hydrostatic pressure of the mud column, and a reference flow rate at known bottomhole pressure (here equal to the hydrostatic pressure), an influx relation may be established. This yield,

$$\dot{m} = \dot{m}_0 \cdot \frac{{P_F}^2 - {P_{BH}}^2}{{P_F}^2 - {P_{HS}}^2} \tag{8.34}$$

Where $\dot{m}_0$ =Reference flow rate (at bottomhole pressure equal to hydrostatic), set to 10 kg/s

P_{HS} =Absolute hydrostatic pressure exerted bottomhole

P_F = Formation pressure, set to 475 bara

The reference flow rate will depend on the pressure drawdown between the formation and the wellbore (kick intensity), and on the area of the wellbore/formation interface. It will also depend on the viscosity of the formation fluid and the formation properties (geometry, permeability).

The influx rate has to be gradually ramped up in order to avoid water hammering and serious pressure oscillations. The influx will cease when the well is shut in, and bottomhole pressure equals formation pressure.

8.2.11. Implementation of a choke model

In section 8.2.4, the choke back pressure has been regulated directly by setting a value for the pressure at the outlet. This is however a rather artificial concept. In reality, the back pressure is regulated by a choke valve. Therefore, a choke valve was implemented in the model. The relation defining the choke valve is equation 7.14. The pressure response in the choke valve depends on the opening in the choke, and is given in terms of a fraction, where 1,0 is fully open and 0,0 is fully

closed. However, the choke setting may never equal 0, as the outlet pressure then will approach infinity. This will require a different set of boundary conditions.

The choke valve is implemented in the Matlab code, but has not been used in the simulations to follow.

9. Simulations

In the following sections some simulations will be run, predominantly well control simulations on one vertical well and on one horizontal well. First however, a few initial simulations will be conducted.

9.1. Initial simulations

Initially a few simulations were run, partly in order to test the scheme, partly to look at some physical properties of the two-phase system. Some of these cases are vital for the analysis of the well control simulations in section 9.2. The initial simulations are kept as simple as possible, in order to investigate the particular effects. A 3000 m pipe of a uniform diameter of 0.1 m was considered. The pipe was divided into 25 segments, and the timestep was set to 0,025 s.

9.1.1. Compressibility

A 3000 m open ended vertical pipe is considered. An outlet pressure of 500 bara was applied from the very beginning. From time 500 s the pressure was ramped down in steps of 100 bar, 100 s for each step, until finally 0 bara of backpressure was applied on the top. The simulation was run until time 1200 s. Two different cases are considered.

- Static, liquid filled pipe.
- Static, gas filled pipe. Slip relation was set to no slip.

Case #1

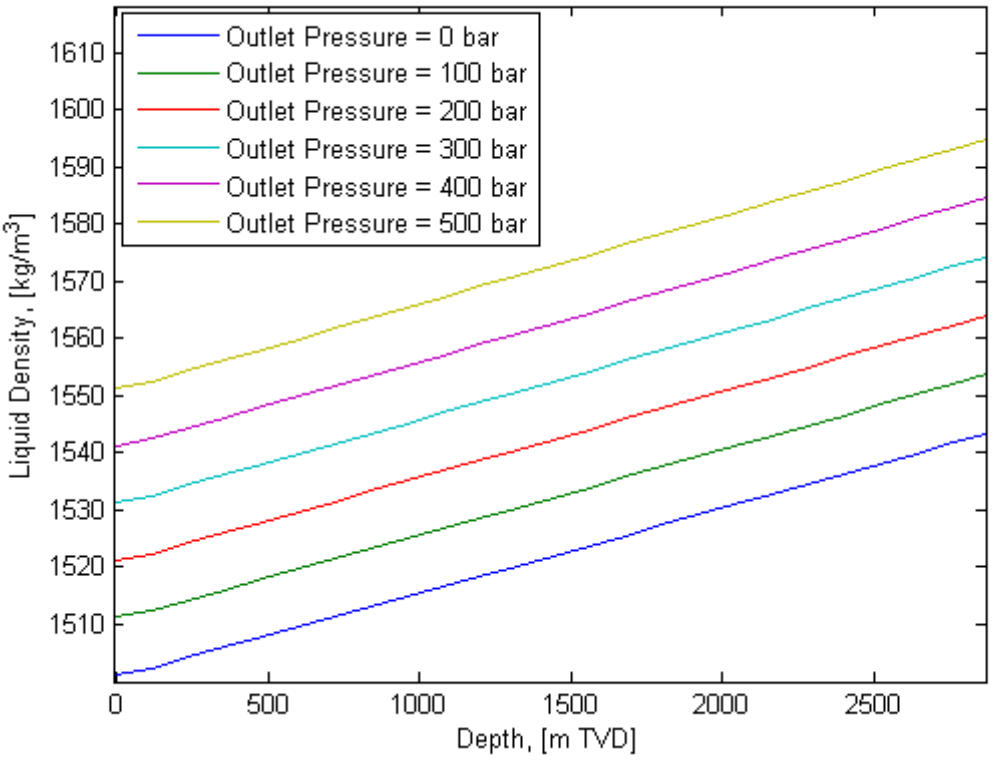

Figure 9-1: Liquid density throughout the wellbore as a function of increasing pressure. Liquid density at standard conditions is 1500 kg/m^3.

From Figure 9-1 it is evident that the density of a liquid is very dependent on the prevailing pressures. An increase in

Case #2

The attempt was a failure, as there seems to be a numerical problem.

9.1.2. Pressure pulse

A 3000 m open ended horizontal pipe is considered. Two different cases are investigated.

- Static, liquid filled pipe. Pressure pulse induced by rapid increase in outlet pressure.
- Static, partially gas filled pipe with a 0,5 volume fraction of gas (no-slip). Pressure pulse induced by rapid increase in outlet pressure.

Case #1

At time 250 s the pressure is ramped up from 1 to 11 bara in a one second interval.

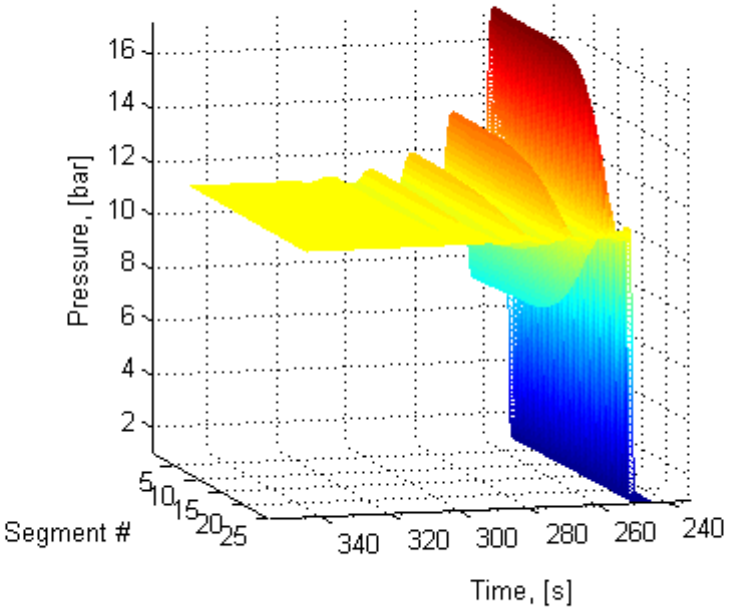

Figure 9-2: Pressure pulses produced in liquid filled pipe by a rapid increase in outlet pressure from 1 bara to 10 bara. The pipe is horizontal with an open end.

Figure 9-2 illustrates a pressure pulse in a liquid filled horizontal pipe with an open end. It is evident that the pressure pulses cause excessive oscillations in pressure. The oscillations are more violent further from the outlet. The maximum and minimum pressure at the inlet is respectively 17,0 bara and 8,7 bara (water hammering effect). The oscillations are exponentially dampened due to friction, and the inlet pressure stabilizes at 11 bara around time 340 s, 90 s after the occurrence of the pressure shock.

During further analysis of the inlet pressures, it was discovered that the first incremental pressure increase (0,001 bar) at the inlet occurs 1,9 s after the pressure shock has been applied at the outlet. The vertical displacement between the outlet and the pressure recording at the inlet is 2940 m. The sonic velocity in one phase liquid is 1000 m/s. Thus, a pressure increase should first be observed at the inlet 2,9 s after the pressure shock occurred. The reason for this is not known, and it should be investigated further.

It was found that the average oscillation period at the inlet for the four first oscillations is 11,8 s. This is close to four times the expected pressure pulse propagation time (one way). It is expected that this is due to the fact that two pressure waves are propagating in opposite direction. This may cause the period of the amplifications (both pressure waves on top of one another) to be misinterpreted as the period of oscillation.

Case #2

The same rapid increase in pressure was applied to a system containing 0,5 volume fraction of gas homogeneously distributed. No slip was assumed as the system is horizontal. Hence, the slip parameters were adjusted to k=1 and s=0.

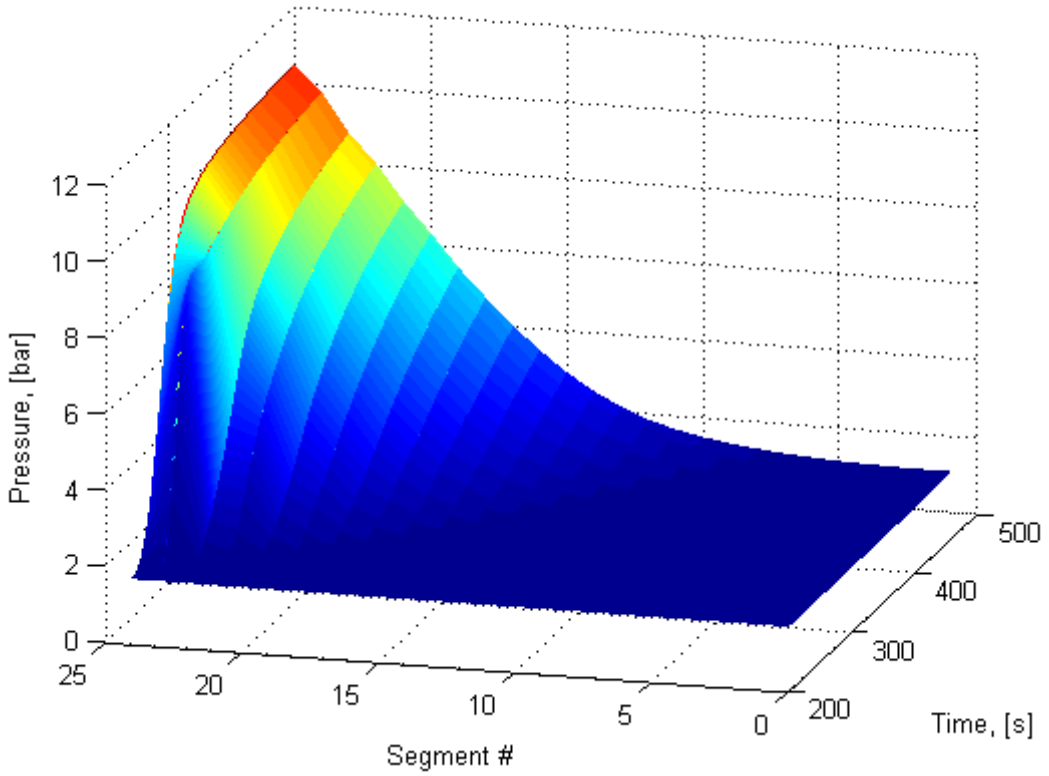

Figure 9-3: Pressure pulse produced by a rapid increase in outlet pressure from 1 bara to 11 bara. A horizontal pipe is initially filled with 0,5 volume fraction liquid and 0,5 fraction of gas. (As pressure increase the volume fraction of gas will decrease.) The pipe is open ended at the endpoint of segment 25.

Figure 9-3 displays the pressure propagation in a partially gas filled horizontal pipe. It can be observed that the pressure wave travels at a very low velocity. An initial incremental increase in pressure (0,001 bar) at the inlet is first recorded at time 390 s. This is 140 s after the pressure shock is applied at the outlet. This yields a sonic velocity of 21 m/s, and is due to a reduced sonic velocity in the two-phase mixture. One phase gas velocity is set to 316 m/s while the corresponding for gas is 1000 m/s.

The simulation was continued to 5000 s in order to establish if there would be any further oscillations. It was however found that the outlet pressure stabilized at 11 bara without any kind of oscillation. This occurred at time 1500 s.

9.2. Well control simulations

In this section, the results of the conducted well control simulations will be briefly presented. The simulations will be done in two different subsea wells, one vertical and one horizontal. These wells are the same as those introduced in the example calculations in sections 7.3.1 and 7.3.2. Four different sets of simulations will be run for each well.

- SCR
- Shut-in
- Partial kill using Driller's Method

- Worst case

The primary objective for the SCR simulations is to obtain a value for the dynamic pressure loss through the chokeline and through the riser. The values for dynamic pressure loss are found by subtracting the atmospheric pressure from the dynamic drillpipe pressure. These values are further used in the example calculations in sections 7.3.1 and 7.3.2. In this way, the example calculations and the simulated kill will be directly comparable. Additionally, the respective loss components (drillstring friction, pressure loss across bit, annular friction and friction loss in chokeline/riser) will be measured. This will give an illustration of the distribution of pressure loss with respect to the various pressure loss components. The sum of the loss components should ideally match dynamic drillpipe pressure.

The main purpose of the shut-in simulation is to provide the shut-in pressures and pit gain for the kill calculations in sections 7.3.1 and 7.3.2. Further, the shut-in sequence serves as a basis for the kill simulations and partially the worst case simulations.

The partial kill simulations are executed in order to verify the analytical model and the kill sheet, and to detect any flaws in the kill procedures. The partial kill features the first round of circulation using Driller's Method. Thus, the kick is circulated to surface using the original drilling fluid. The PI-regulation is conducted with respect to the drillpipe pressure. This is done for the purpose of realism.

Two worst case simulations will be run for each well. One reflects the conventional worst case scenario (approach #1) as defined in section 3.1.2. This will be directly comparable with the example calculations in section 7.3.1. Another scenario was considered, with a slug of gas migrating in a shut-in well (approach #2). The comparisons are to be found in section 0.

For the well control simulations, the timestep is set to 0,0125 s and the well divided into 50 segments. This is done in order to increase the accuracy of the simulations.

9.2.1. Vertical well

A 3000 m RKB vertical well was initialized. The 13 3/8 inch (ID = 32 cm) casing shoe is situated at 2850 m, and the remaining 150 m consists of 12 ¼ inch open hole. Water depth is 210 m RKB, with 18 ¾ inch riser and 3 inch chokeline. The drillstring is composed of 5 inch drillpipe and a 90 m 8 ½ inch BHA. The capacity in the drillstring is assumed to be 8 l/m, uniform throughout the entire drillstring (including BHA). This is the very same well as presented in the example calculations in section 7.3.1.

Simulated SCR

The simulations were performed with the kill rates 600, 800 and 1000 lpm, which correspond to 30, 40 and 50 spm at a pump output of 20 l/stroke. These kill rates are typical.

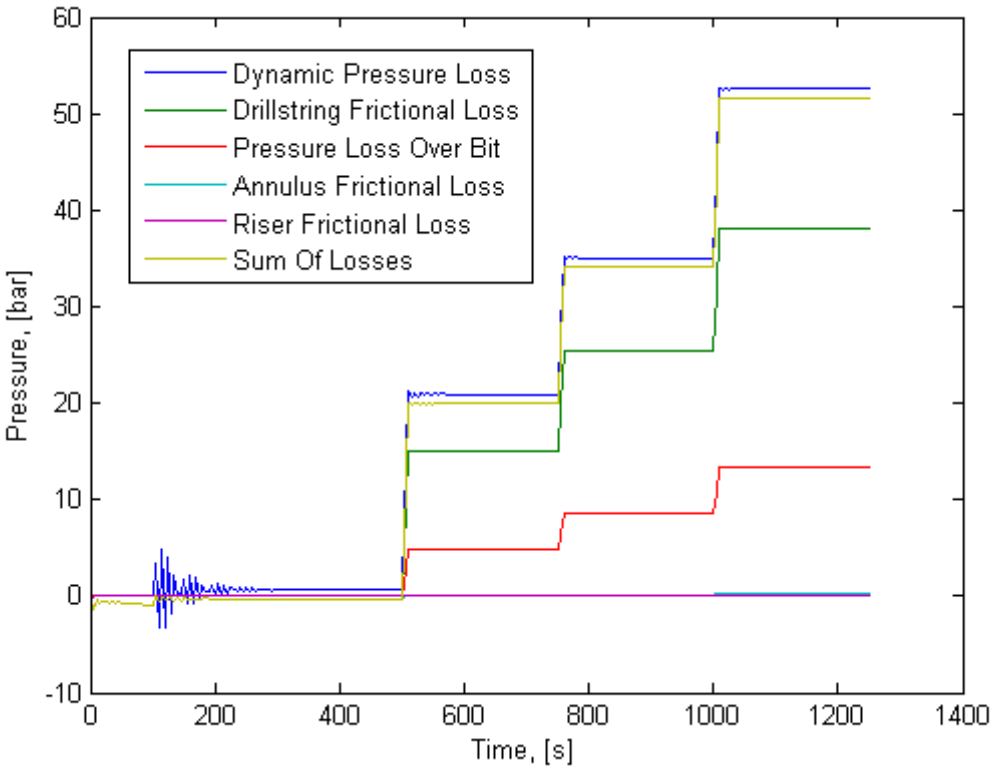

Figure 9-4: SCR through the riser in a vertical well. The dynamic pressure loss is subdivided in to its respective pressure loss components.

Figure 9-4 is obtained by a simulated SCR through the riser. The dynamic pressure loss is subdivided in to its respective components. The initial oscillations are an effect of turning the wellbore to vertical. The stepwise increase in pressure loss is due to increase in flow rate. Until time ~500 s the flow rate is zero. It is observed that the pressure loss in the annulus and riser is actually negative. This is due to the numerical problem with negative flow velocity on the annulus side at low flow rates (section 8.1.10). It can further be seen that the frictional losses in the riser and annulus are close to zero at the entire range of flow rates. This agrees with the assumptions made in the analytical model. At 1000 lpm, the frictional pressure loss in the annulus and riser contributes to the total dynamic pressure loss with less than a half percent (0,48 %). This result is not to be emphasized to any degree, due to the errors produced by the velocity profiles on the annulus side. However, it is assumed that the order of magnitude of these observations is quite reasonable.

Another observation is that the dynamic pressure loss does not exactly equal the sum of the pressure losses throughout the system. The dynamic pressure loss is actually slightly higher. This was initially interpreted as a compression effect. However, if this was the case, the effect should increase in magnitude at higher downhole pressure gradients. In Figure 9-4 the deviation between the sum of losses and the measured dynamic pressure loss is constant at all applied pump rates. If the respective curves were parallel displaced in such a way that they would display zero pressure loss at zero pump rate, it would be found that they coincide throughout the entire time interval.

The dynamic pressure loss at 1000 lpm will be applied in sections 7.3.1 and 0. The total pressure loss when circulating through the riser is measured to 52,6 bar, or using field practice rounding rules 53 bar.

A similar simulation was conducted with 1,0 SG mud. This will not be included here, as it is not regarded relevant. However, it will be analyzed and compared with the previous simulation in section 10.

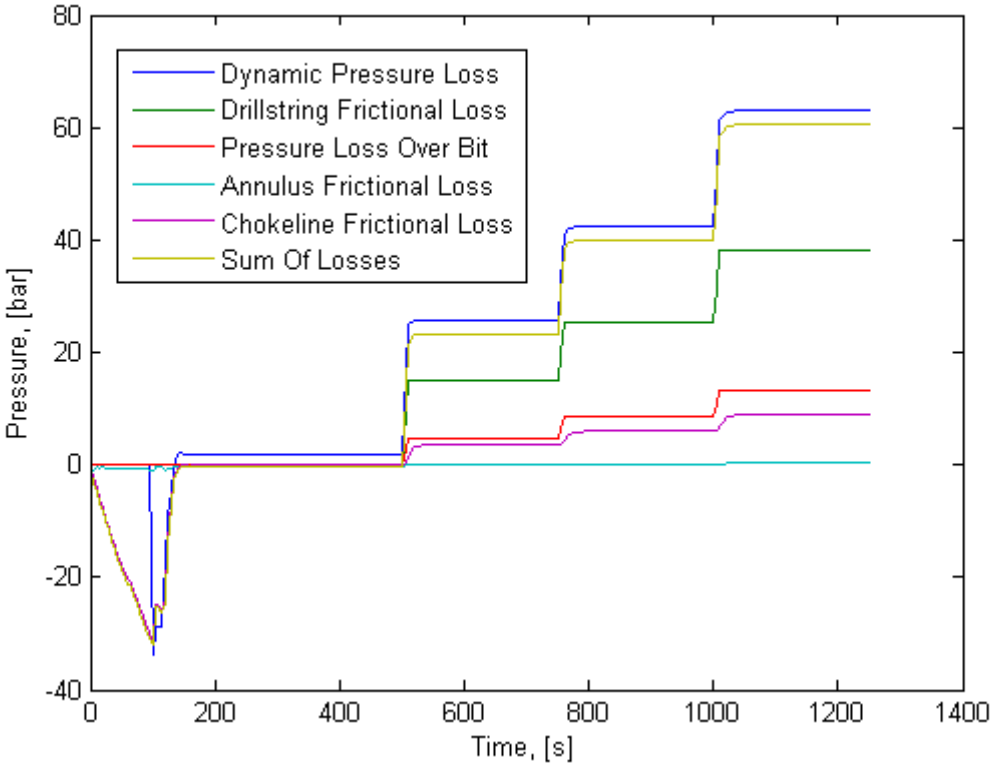

Figure 9-5: SCR through chokeline of a vertical well. The dynamic pressure loss is subdivided in to its respective pressure loss components.

Figure 9-5 is obtained by SCR through the chokeline. The dynamic pressure loss is subdivided in to its respective components. A great deal of the observations and assessments for the SCR through the riser is still valid. It is observed that Figure 9-4 and Figure 9-5 are practically identical with exception of the added chokeline friction. An additional observation is the dip in pressure loss observed in the period before time 200 s. This is interpreted to be a result of the numerical problem with underestimated fluid velocities at low fluid velocities (section 8.1.10). It is also observed that in spite of the well not being deepwater, the chokeline friction accounts for a considerable contribution to the total dynamic pressure loss.

The dynamic pressure loss when circulating through the chokeline at 1000 lpm is found to be 63,2 bar, or using field practice rounding rules 64 bar.

Shut-in

A gas kick is taken from time 200 s in a vertical well. A formation pressure of 475 bara is assumed. The reference mass rate is assumed to be 10 kg/s. The well is shut-in at time 370 s, and the influx will continue until the bottomhole pressure equals the formation pressure.

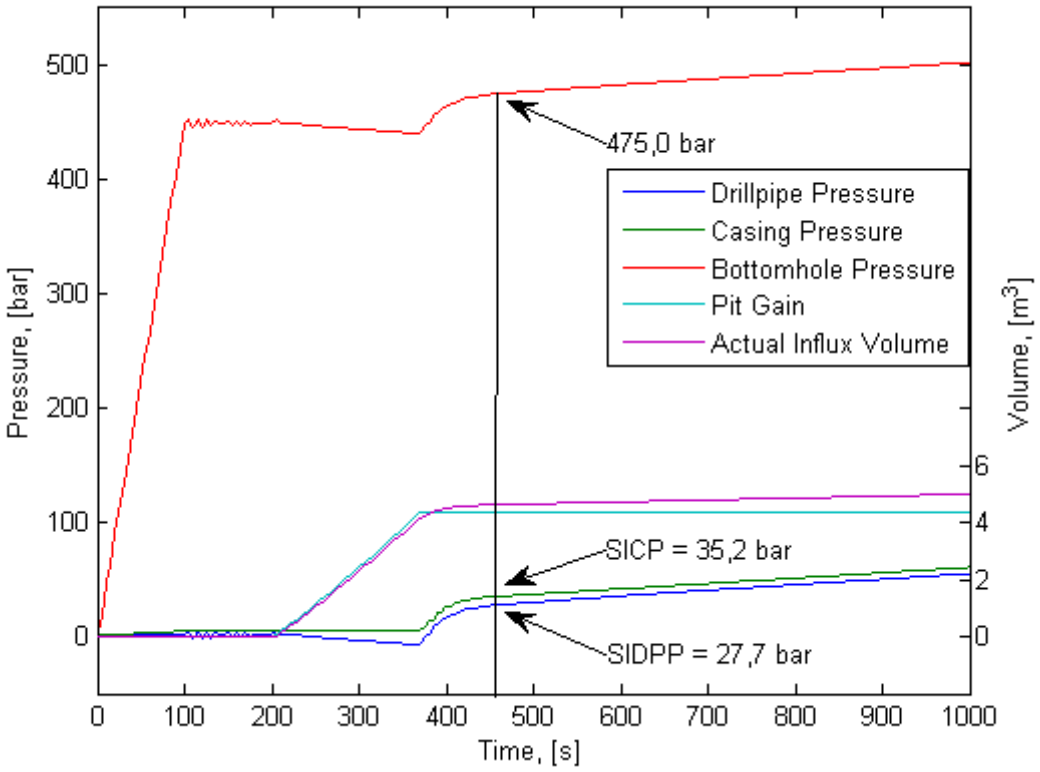

Figure 9-6: Shut-in in a vertical well. Pit gain and actual influx volume refers to the secondary ordinate axis.

Figure 9-6 is obtained by taking an influx and shutting in the well. The bottomhole pressure builds up until it surpasses the formation pressure (Darcy function, see section 8.2.10). This occurs at time 460 s. The further increases in pressures are due to gas migration.

The pit gain and the actual influx volume refer to the secondary ordinate axis. The actual influx volume is obtained by a summation of the gas volumes in the lower segments. It can be observed that the pit gain and the actual influx volume at shut-in are not equal. This is due to gas expansion and liquid compressibility. Additionally, the formation continues to flow even after the well is shut-in.

SIDPP, [bar]	SICP, [bar]	Pit gain, [m^3]	Influx volume, [m^3]	Influx mass, [kg]
27,7	32,5	4,33	4,64	2082

Table 9-1: Various values read at shut-in of a vertical well. The influx volume and influx mass are the actual downhole values obtained by summing gas volume and mass for the bottom segments.

The three first values in Table 9-1 are the top side pressure and volume values at shut-in. These are the values used in the example calculations in the analytical model (section 7.3.1). The influx volume and mass refers to actual downhole values at shut-in. They are obtained by a summation of the gas volumes and masses in the lowermost segments.

Kill circulation using driller's method

The first round of circulation using driller's method was simulated. Only the first round of circulation is possible, due to limitations in the current AUSM scheme. The system may only contain two fluids (influx and original mud).

For the choke pressure regulator, the drill pipe pressure was utilized as process variable, as opposed to bottomhole pressure. The drill pipe pressure was attempted to be held at a constant value ICP equal to 81 bara, with reference to section 7.3.1. The optimized regulator parameters were found to be (K_p=2,25e-4; T_i=13,33 s; T_d=0; T_s=dt; c=0,3).

All data from the shut-in sequence were exported, except the conservative variables and the geometric data. The simulations were continued from time 460 s with failsafe open, i.e. with returns through the chokeline. In the further simulation the Darcy influx was turned off. This was done as it proved difficult to maintain overbalance in the well during the first oscillations as the regulation was initiated.

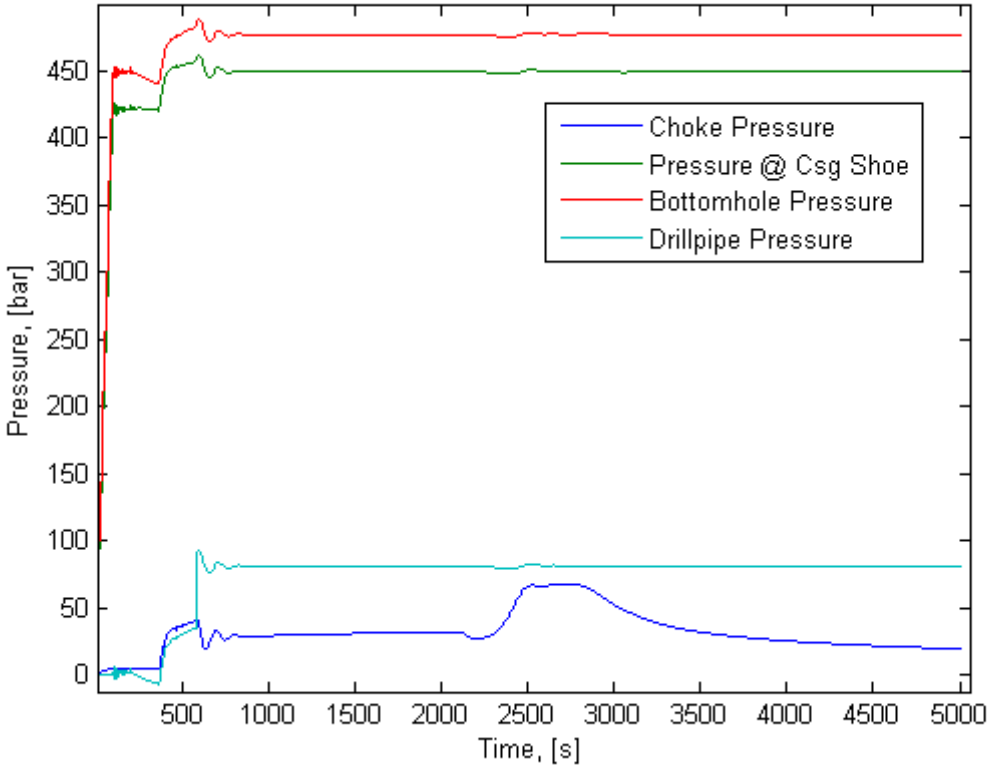

Figure 9-7: Pressure response during kill in a vertical well. The first round of circulation with Driller's Method is conducted. PI-regulation with respect to drill pipe pressure (ICP=81 bara).

Figure 9-7 displays the pressure response obtained by the kill simulation. It can be observed that the bottomhole pressure was remaining approximately constant throughout the round of circulation. There are some problems holding constant pressure as the choke regulation is initialized. At 2500-3000 s, a high backpressure is applied. This corresponds with the time at which the influx reaches the surface.

Worst case simulations

First a gas filled well scenario was considered. The simulation was run until the entire well was displaced to gas. Then the well was shut-in and the bottomhole pressure was allowed to increase until it was equal with the formation pressure. Total simulation time was 20000 s.

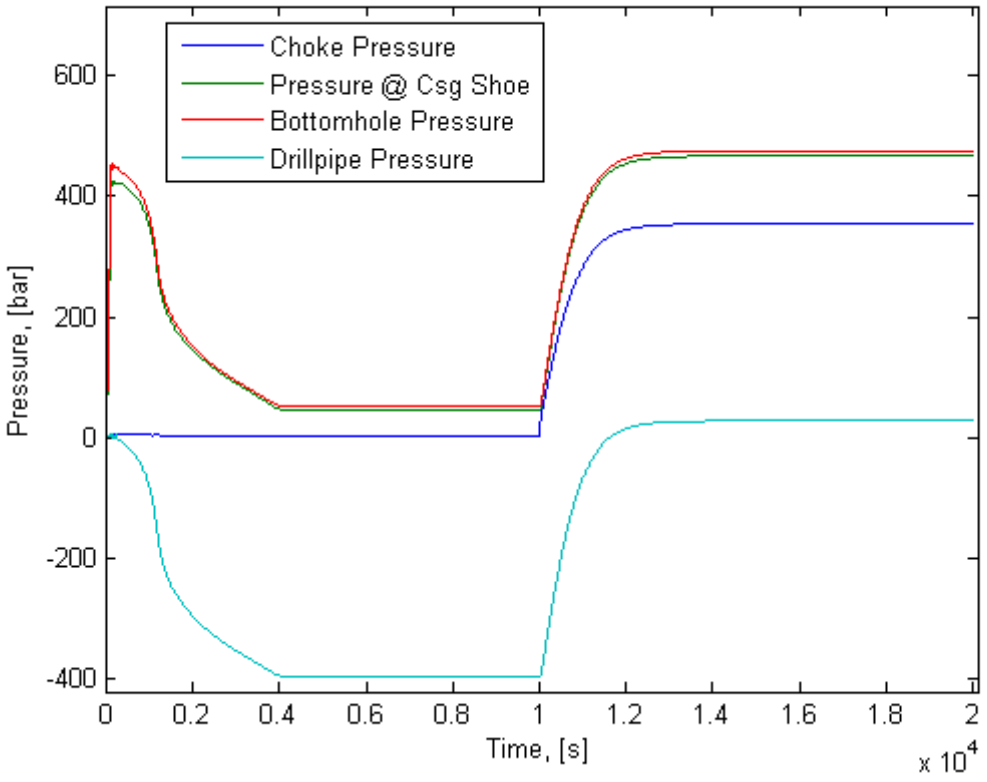

Figure 9-8: Gas filled well scenario (approach #1) in a vertical well.

In Figure 9-8, a gas filled well scenario is simulated. It can be observed from the various pressures that the well is completely filled with gas at close to 4000 s. Steady state gas migration continues until the well is shut-in at time 10000 s. A build up of pressure occurs until the bottomhole pressure equalizes the formation pressure around time 14000 s. The little separation between the bottomhole pressure and the pressure at the casing shoe is caused by a small vertical displacement between the casing shoe and bottomhole. The distance between the two points is only 150 m.

Another observation is that the drill pipe pressure has negative values due to the u-tube effect. Negative pressures are physically impossible, but the effect is caused by the drilling fluid being modeled as incompressible within the drillstring. Maximum and minimum pressures recorded at the casing shoe is 467 bara and 46,4 bara.

Secondly an alternative approach was investigated. The concept is to take a kick, shut-in and let the gas migrate to the top. The data from the shut-in sequence were exported, and the simulation continued with failsafe open (see section 8.2.7). The well is shut-in at RKB. This will cause an overestimation of the downhole pressures after gas break through. By assuming incompressible liquid, the overestimation is approximated to the high side of 2 bar (liquid density · gravity · chokeline volume/annular capacity).

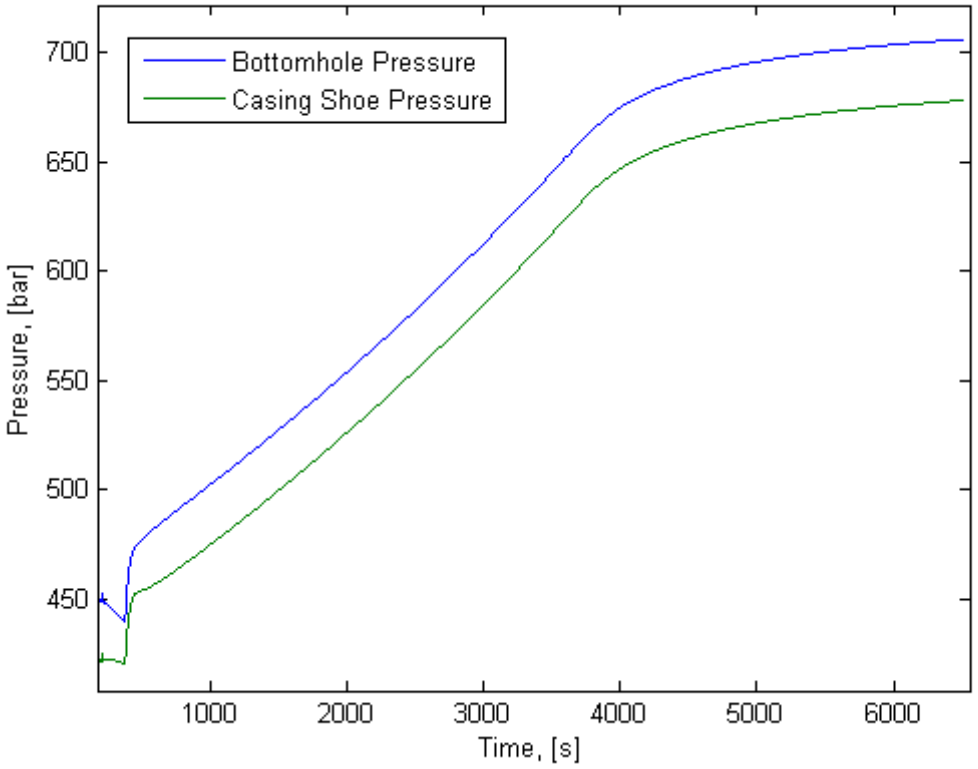

Figure 9-9: Alternative worst case scenario (approach #2). Gas migration in a shut in vertical well.

Figure 9-9 illustrates gas migration in a shut in well. At time less than ~500 s the shut-in sequence is taking place (see Figure 9-6). In the interval ~500-800 s a slightly different slope can be distinguished for the casing shoe pressure compared to the bottomhole pressure. This is due to gas contents in the annular volume below the casing shoe. From 800 to around 4000 s there is an approximately linear rise in downhole pressures. This is due to steady gas migration. Then the slope of the curves decreases. This is caused by gas break-through at surface. After 4000 s, there is still a raise in downhole pressures as gas accumulates below the choke manifold. The highest recorded pressure at the casing shoe was 678 bara. Considering that the pressure is still increasing and the estimated error of 2 bar, 678 bara seems like a generous estimate for the maximum pressure on the casing shoe.

9.2.2. Horizontal well

A horizontal well was initialized. The well is vertical to the kick off point situated at 2580 m RKB. A uniform build rate is used and from 3240 m MD and out the well is horizontal (90 deg inclination). Total well depth is 3840 m MD and 3008 m TVD. The 13 3/8 inch (ID = 32 cm) casing shoe is situated at 3690 m MD, and the remaining 150 m consists of 12 ¼ inch open hole. Water depth is 210 m RKB, with 18 ¾ inch riser and 3 inch chokeline. The drillstring is composed of 5 inch drillpipe and a 90 m 8 ½ inch BHA. The capacity in the drillstring is assumed to be 8 l/m, uniform throughout the entire drillstring (including BHA). The very same well is used in the example calculations in section 7.3.2.

For the simulations on the horizontal well the hydrostatic of the fluid column in the drillstring was not adjusted. Since the well is 8 m TVD deeper this results in an overestimation of the drillpipe pressure 1,1-1,2 bar.

Simulated SCR

As for the vertical case, the SCR in the horizontal well was conducted at 600, 800 and 1000 lpm.

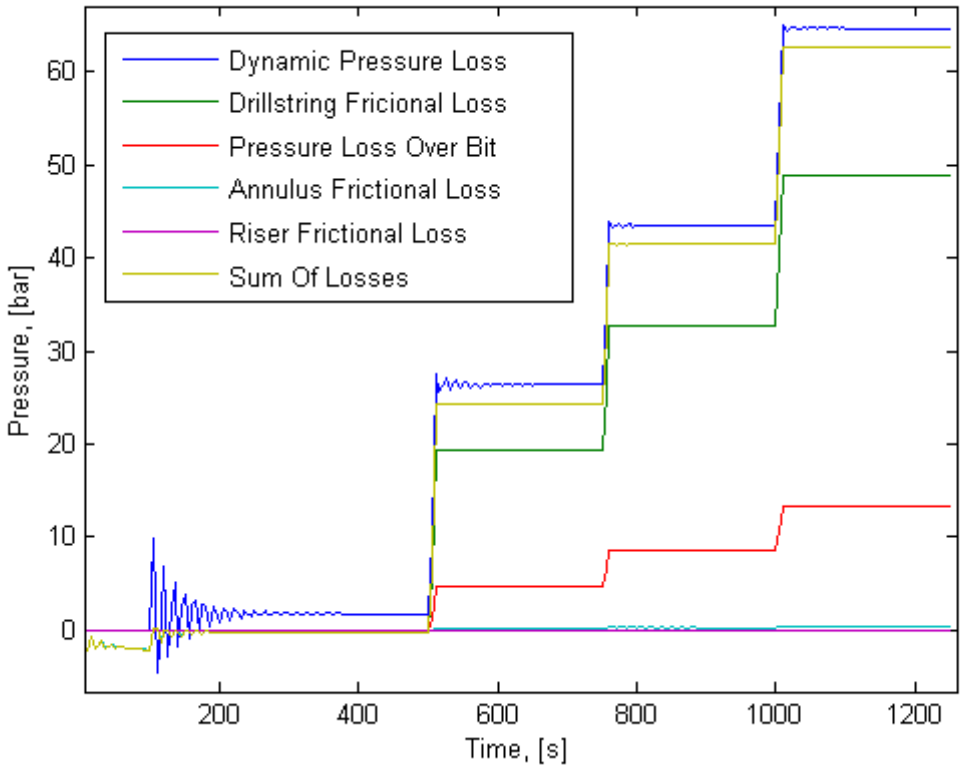

Figure 9-10: SCR through the riser in a horizontal well. The dynamic pressure loss is subdivided in to its respective pressure loss components.

Figure 9-10 illustrates the recorded dynamic pressure loss through the riser during an SCR. The dynamic pressure loss is subdivided into its respective pressure loss components. The SCR is conducted in a horizontal well.

An initial observation is that the dynamic pressure loss is higher for the horizontal well than for the vertical well. This is expected since the frictional pressure loss is depending on the measured depth. Further investigation shows that the increase in dynamic pressure loss is primarily due to increase in drillstring friction. The other components are nearly equal for the horizontal and the vertical well.

Dynamic pressure loss when circulating through the riser at 1000 lpm is measured to 64,68 bar, or using field practice rounding rules 65 bar.

An SCR was also conducted through the chokeline. The plot is not included as it was very similar to the previous plot and the plots in section 0. Compared to the previous plot, the main difference was the chokeline friction. When comparing with Figure 9-5, the primary difference is the increased frictional pressure loss in the drillstring.

The dynamic pressure loss when circulating at 1000 lpm through the chokeline is measured to 75,25 bar, or using field practice rounding rules 76 bar.

Shut-in

A gas kick is taken from time 200 s in a horizontal well. A formation pressure of 475 bara is assumed. The reference mass rate is assumed to be 10 kg/s. The well is shut-in at time 370 s, and the influx will continue until the bottomhole pressure equals the formation pressure.

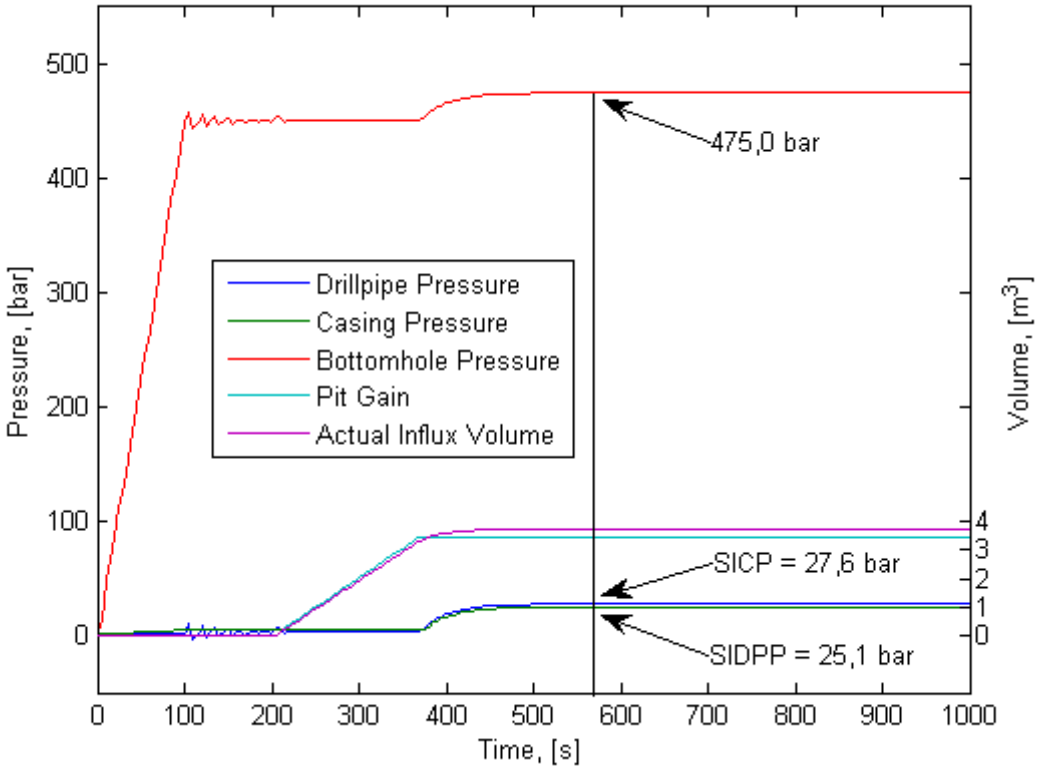

Figure 9-11: Shut-in in a horizontal well. Pit gain and actual influx volume refers to the secondary ordinate axis.

Figure 9-11 displays the shut-in sequence for a horizontal well. The influx of formation fluids continues until the well again is in overbalance. This occurs at time 570 s, and the shut-in pressures and the pit gain is read. In the time following there is no increase in downhole or topside pressures, nor any increase in actual influx volume. This is caused by the implemented slip relation and the assumption of no slip in the horizontal section of the well.

The pit gain and the actual influx volume refer to the secondary ordinate axis. The actual influx volume is obtained by a summation of the gas volumes in the lower segments. It can be observed that the pit gain and the actual influx volume at shut-in are not equal. This is due to the well keeps flowing until the bottomhole pressure matches the formation pressure.

SIDPP, [bar]	SICP, [bar]	Pit gain, [m^3]	Influx volume, [m^3]	Influx mass, [kg]
25,1	27,6	3,46	3,74	1773

Table 9-2: Various values read at shut-in in the horizontal well. The influx volume and influx mass are the actual downhole values obtained by summing gas volume and mass for the bottom segments.

The three first values in Table 9-2 are the top side pressure and volume values at shut-in. These are the values used in the example calculations in the analytical model (section 7.3.1). The influx volume and mass refers to actual downhole values at shut-in. They are obtained by a summation of the gas volumes and masses in the lowermost segments. The reason for a difference in pit gain and actual influx volume is the expansion of the influx continues after the well has been shut-in.

Kill circulation using driller's method

A kick is circulated out using Driller's Method in a horizontal well. The regulator parameters were tuned to (K_p=33,75e-4; T_i=47,5 s; T_d=0; T_s=dt; c=0,6). The regulation was done with the drillpipe pressure functioning as a process variable. Due to a mishap, the set pressure (ICP) was set to 93 bara, while the calculated value was 91 bara. It is assumed that simply subtracting 2 bar off of all downhole pressure will not cause any significant errors.

Similarly as for the vertical case the shut-in sequence was continued with the riser closed and the chokeline open.

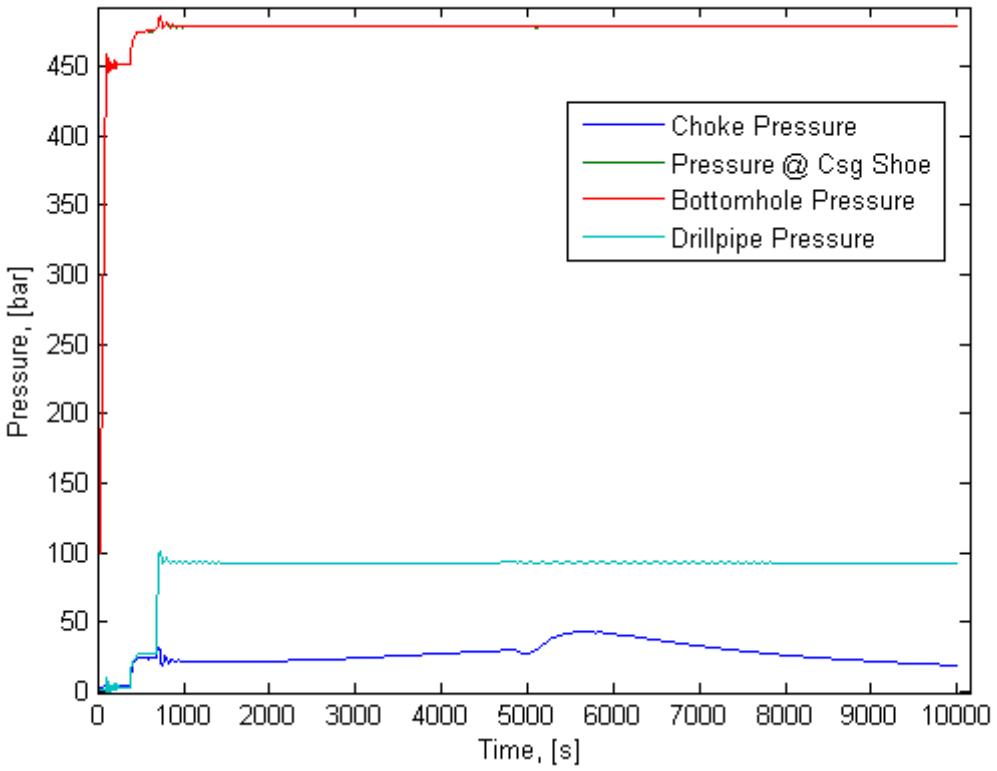

Figure 9-12: Pressure response during kill in a horizontal well. The first round of circulation with Driller's Method is conducted. PI-regulation with respect to drill pipe pressure (ICP=93 bara). The casing shoe pressure is coinciding with the bottomhole pressure due to no vertical displacement.

Figure 9-12 illustrates the pressure response in the horizontal well as a kick is circulated to surface. It can be observed that the casing shoe pressure coincides with the bottomhole pressure. This is caused by no vertical displacement between the two points. It is also evident that the time to circulate the kick to surface is remarkably longer than for the vertical case. This is partly due to an increased measured depth, partly due to low drift velocities in the deviated sections. Another

observation is the smoothness of the curves corresponding to the downhole pressures and the choke pressure. An explanation may be suggested with reference to the sensitivity testing of section 8.2.4. Due to the increase in measured depth (compared to section 0), the influx will be more distributed as it reaches the surface. This results in low volumetric rates of gas across the choke and hence, better regulation.

Worst case

There was conducted a simulation on the gas filled well scenario. However, it was decided to leave it out from the thesis as is displayed the exact same results as for the vertical case (within 1 bar). The alternative worst case scenario was not simulated, as the implemented slip relation will cause no gas migration in the horizontal section.

10. Discussion and analysis

In this section the development of the simple kick simulator will be discussed. Further, the results obtained from the well control simulations will be analyzed and compared with the calculated data from the analytical model.

10.1. On the development of a crude kick simulator

A simple kick simulator has been developed with basis in the numerical AUSMV scheme. The purpose was to realistically model well control simulations, and to compare analytical results with the simulated results obtained by use of the numerical scheme. The primary objective was to verify or expose weaknesses in the traditional well control calculations.

10.1.1. Benefits and possibilities by utilizing a numerical scheme

There are several advantages using a numerical scheme compared to the simple kill sheet. When using the proposed model, a variety of complex physical effects can be treated in a fairly realistic manner.

Pressure pulses

The AUSMV scheme can be used to handle propagating sonic waves in two-phase mixtures. In a kill sheet, pressure pulses are completely neglected. It has been shown that a rapid increase in pressure produces excessive oscillations and water-hammering in one-phase liquid. The effect is exponentially dampened by friction. In two-phase mixtures with high volume fractions of gas, the effect is not as pronounced. This is reasonable, as the water-hammering will be partially absorbed by the compressible gas. It has also been shown that the speed of sound in a two-phase mixture is lower than in one-phase liquid or gas.

The numerical schemes have applications in well control training simulators, where the time delay between an adjustment in applied backpressure or pump rate will propagate with the speed of sound of the two-phase mixture.

Frictional effects

Kill sheets and simple analytical models utilize simplifying assumptions when it comes to frictional pressure loss. In the numerical scheme, the friction can be modeled more realistically by implementation of experimental or analytical friction models. Hence, the numerical scheme can be used to test the validity of the assumptions made in the analytical model.

Gas slippage

In a kill sheet, the influx is modeled as single bubble. An influx is assumed to propagate with no slip compared to the liquid fraction, or at a constant drift velocity. However, due to gas slippage depending on gravity and flow regime the influx will be distributed. This causes the analytical models to be more conservative than the numerical schemes. Drilled kicks will be additionally distributed, as they are taken with the pumps running. Connection kicks or swabbed kicks may be more concentrated. Another effect caused by gas slippage, is that gas breakthrough at RKB level occurs ahead of time according to the calculated time to circulate bottoms up.

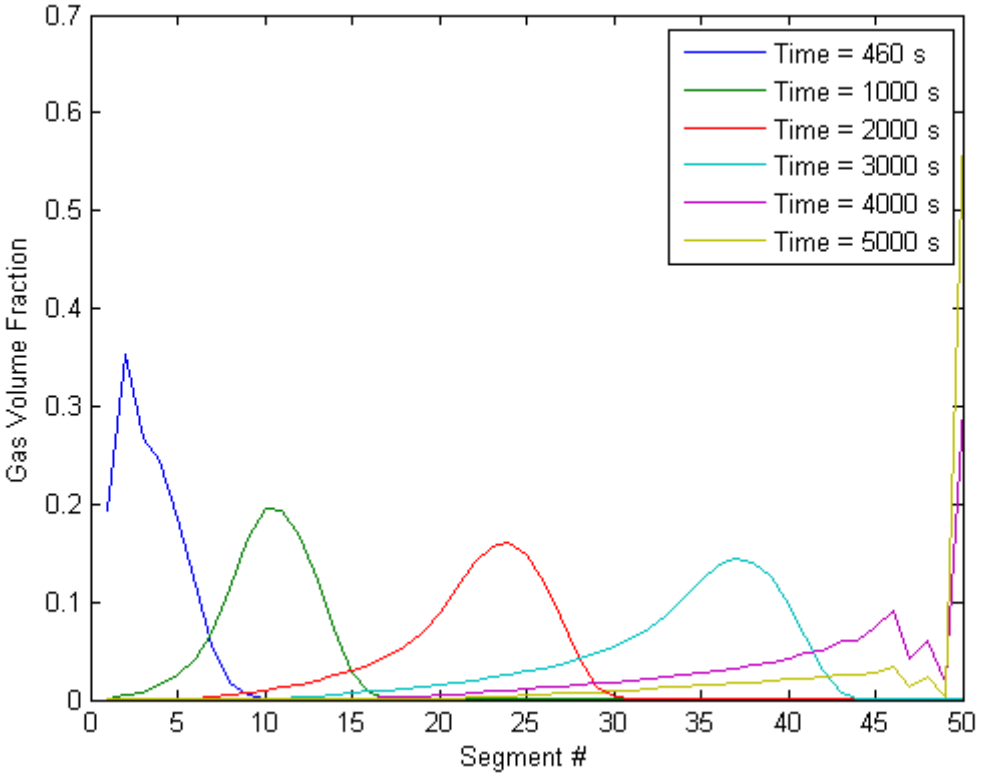

Figure 10-1: Gas distribution and migration in a shut in vertical well. Segment 1 refers to bottomhole, segment 50 to topside. The plot is produced in conjunction with Figure 9-9.

Figure 10-1 illustrates the gas distribution profiles in a shut-in wellbore at various points in time. The well is vertical, and the displacement of the gas volume is caused by gas migration. It can also be seen that the area below the distribution profiles is approximately constant. Hence, the pressure in the gas will be fairly constant at the different points in time.

Compressibility

The traditional analytical model assumes incompressible liquid. Using the numerical scheme, an increase in average static density in the order of magnitude of a couple of points compared to the density at standard conditions, was obtained for a well of 3000 m TVD. Both the liquid and gas

compressibilities are overestimated in the current numerical schemes. This is caused by unrealistically low sonic velocities in the one-phase fluids.

Under realistic conditions the compressibility effects will be counteracted by temperature effects. The current numerical scheme does not take into account temperature variations.

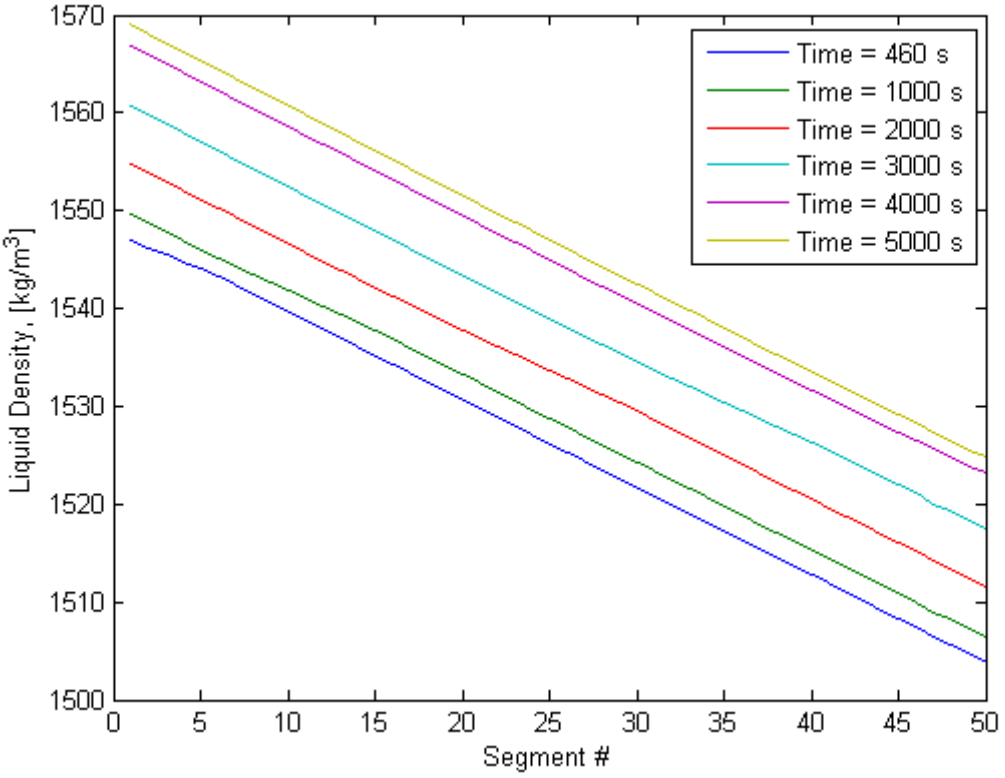

Figure 10-2: Liquid densities at different points in time in a shut in vertical well. The overall pressure is increasing as a function of time. The segments are numbered from bottomhole and upwards. The plot is produced in conjunction with Figure 9-9.

Figure 10-2 displays the compressible nature of a drilling fluid. The liquid density increases as a function of the prevailing pressure conditions in the wellbore. The plot is produced as a volume of gas migrates in a shut-in vertical well.

10.1.2. PI-regulation

When a conventional kill method is applied in order to circulate a kick out, the bottomhole pressure is held steady at a constant value in slight overbalance against the formation pressure. The AUSMV scheme does not allow for setting the bottomhole pressure constant. This is due to the acceleration terms of the drift flux model. Thus, there was a need to implement a method with the ability to keep the bottomhole pressure stable within a reasonable interval.

A simple PI-regulator was implemented. It functions by regulating the choke pressure directly without the use of a choke model. Both drillpipe pressure and bottomhole pressure was regulated successfully. However, the regulation required comprehensive tuning and adjustment in order to function satisfactory.

The sensitivity of the PI-regulator was tested with respect to changes in well dynamics. It was initially assumed that the rate of convergence and the stability of the PI-regulator would increase as an effect of a reduction in system dynamics. The assumption was supported by two sets of tests with variable well depth and influx mass. However during a third set of tests with variable kill rate, it was discovered that the stability of the regulation was reduced at reduced pump rates. This is in contradiction to the initial assumption, and should be further investigated.

A slightly new approach for PI-regulation was discovered, which displayed impressive properties and performance with respect to stable and convergent regulation. The reasons for the success are not fully understood, but it seems to capture the dynamic nature of a kill in a better manner than what is the case for the conventional approach. The new approach was used in all the conducted kill simulations.

10.1.3. Additional modifications and extensions to the numerical scheme

The PI-regulation of the bottomhole pressure was the most important and time consuming extension in order to adapt the numerical scheme to application in well control scenarios. Additionally, various minor modifications were conducted in order to increase the realism and suitability of the scheme as a simple kick simulator.

The ability to read well control parameters such as drillpipe pressure and pit gain was implemented. This was done for the ability to compare the simulated results with the kill sheet calculations. Further, a simple chokeline and riser was incorporated, for the purpose of simulations on subsea wells. Additional modifications were made in order to conduct simulations on deviated and horizontal wells.

More realistic friction models were tested and implemented, amongst others to model turbulent flow with a high degree of accuracy. The density of the liquid component in the system was changed to resemble a typical drilling fluid. In addition, a pressure dependent influx function was implemented. Hence, the shut-in sequence can be modeled more accurately. Initially, the bottomhole pressure and the choke pressure were measured in the midpoint of the bottom and top segment. For a 3000 m well with 50 segments, this cause an error in the read pressure of around 4 bar at static conditions (1,5 SG mud). This was altered by extrapolation, such that the pressures are actually measured at the end points.

A choke model was implemented, but not used in the simulations.

10.2. Interpretation of the well control simulations in light of the analytical model

Well control simulations have been conducted on a vertical and a horizontal well. The results from the simulations will be discussed and compared to corresponding values obtained from the analytical model.

10.2.1. Kick simulations using driller's method

In the vertical case the average bottomhole pressure overbalance throughout the round of circulation is 2,1 bar. The corresponding overbalance in the deviated well is 1,2 bar (subtracted the 2 bar excess ICP, see section 9.2.2). Further analysis is required in order to find the reason for the overbalance.

ICP calculation

In a kill situation, it is often assumed that the pressure losses in the annulus and riser are negligible, due to a relatively high cross sectional area and low liquid velocities. This causes the initial circulating pressure to be calculated as the sum of the dynamic pressure loss and the shut-in drillpipe pressure.

Analysis is conducted on the horizontal well as this will produce higher frictional pressure loss in the annulus. Thus, the error by assuming negligible annular friction is greater.

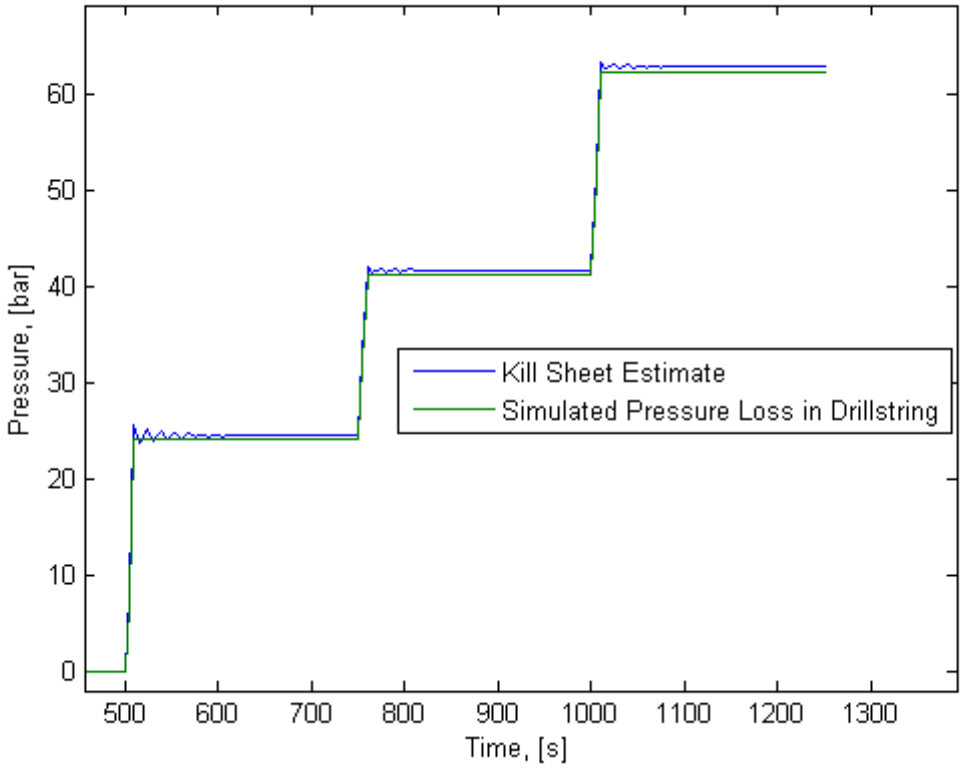

Figure 10-3: Plot obtained from the SCR for the deviated well. Due to a problem with obtaining consistent pressures, the values have been parallel displaced in such a way that the pressures losses are zero at zero flow rate. The kill sheet estimate refers to the simulated dynamic pressure loss through the riser, which is used directly when calculating the

initial circulating pressure. The simulated pressure loss in the drillstring is the sum of the pressure loss across the bit and the friction in the drillstring.

Figure 10-3 illustrates the difference between the estimated drillstring pressure loss (dynamic pressure loss through the riser) and the actual pressure loss through the drillstring (sum of the drillstring friction loss and the pressure loss across the bit). It is evident that the values coincide to a high degree. Another observation is that the difference between the estimated and the true values seems to increase at higher flow rates. The difference between the estimate and the actual loss components at kill rate (1000 lpm) is 0,5 bar (see Table 10-1 for elaboration). This may serve as a safety margin.

Flow Rate, [lpm]	Kill Sheet Estimate, [bar]	Simulated Pressure Loss in Drillstring, [bar]	Safety Margin
600	24,6	24,6	0
800	41,7	41,2	0,5
1000	62,9	62,2	0,5

Table 10-1: Values obtained from Figure 10-3. The kill sheet estimate is the corrected dynamic pressure loss through the riser. This is used directly when calculating the initial circulating pressure. The simulated pressure loss in the drillstring is the sum of drillstring friction and pressure loss across the bit. The safety margin is obtained by subtracting the simulated pressure loss in the drillstring from the kill sheet estimate. This value reflects the associated downhole overbalance produced by applying a choke pressure equal to shut-in casing pressure subtracted the kill sheet estimate of the chokeline friction (relevant in when initiating a kill circulation).

The field practice rounding rules will add an additional safety margin towards the formation pressure of 0,8 bar (dynamic pressure loss is rounded up to the nearest integer bar). This yields a total safety margin of 1,3 bar caused by the ICP. It is noticed that the safety margin produced by the ICP is 0,1 bar higher than the average bottomhole overbalance.

FCP calculation

The calculation of the final circulating pressure relies on a direct proportionality between the dynamic pressure loss measured through the riser and the liquid density (see equations (7.10) and (7.14)). In this section the proportionality will be further investigated. The final circulating pressure is however not included in the simulations, due to limitations in the numerical scheme.

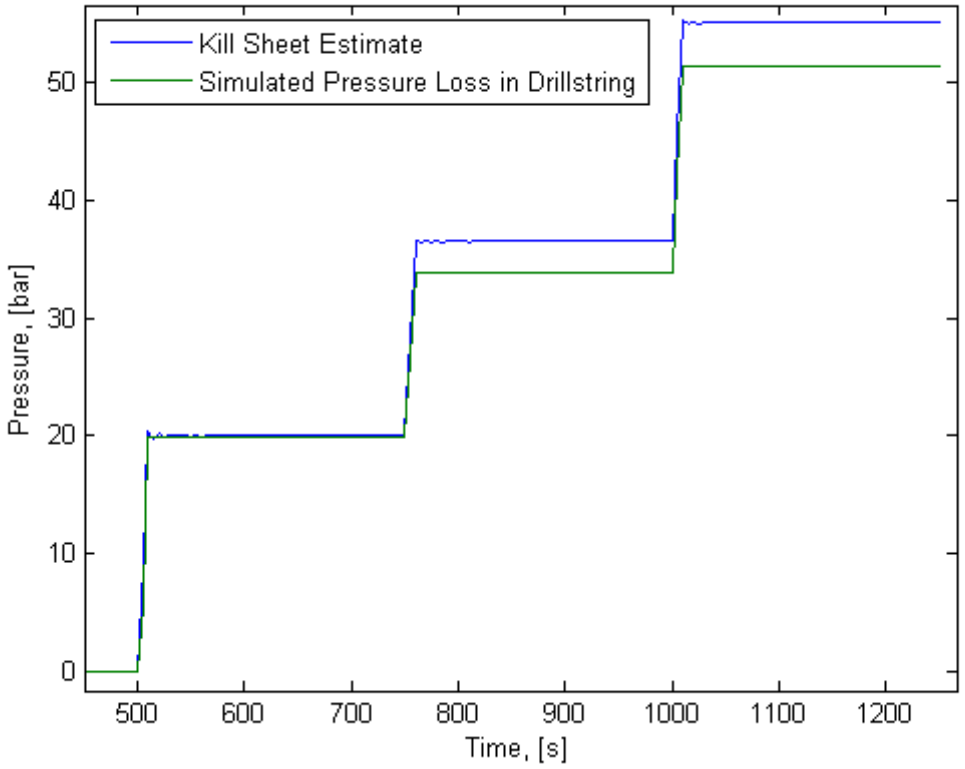

Figure 10-4: Plot obtained from the SCR for the vertical well. Due to a problem with obtaining consistent pressures, the values have been parallel displaced in such a way that the pressures losses are zero at zero flow rate. The kill sheet estimate refers to the final circulating pressure obtained by means of the density proportionality. The dynamic pressure loss produced with 1 SG mud is used as a reference when calculating the final circulating pressure with 1,5 SG mud. The simulated pressure loss in the drillstring is the sum of the pressure loss across the bit and the friction in the drillstring.

Figure 10-5 is based on the SCR simulation through the riser for the vertical well. The kill sheet estimate is calculated with basis in the dynamic pressure loss measured through the riser for 1,0 SG liquid and the density proportionality. An increase in 50 points from original mud weight to kill mud is however not realistic. It is assumed that the difference between actual (simulated) and calculated pressure will be less, if the difference in mud weight is less.

Flow Rate, [lpm]	Kill Sheet Estimate, [bar]	Simulated Pressure Loss in Drillstring, [bar]	Safety Margin
600	20,0	19,9	0,1
800	36,5	33,9	3,4
1000	55,1	51,4	4,4

Table 10-2: Values obtained from Figure 10-4. The kill sheet estimate refers to the final circulating pressure obtained by means of the density proportionality. The dynamic pressure loss produced with 1 SG mud is used as a reference when calculating the final circulating pressure with 1,5 SG mud. The simulated pressure loss in the drillstring is the sum of drillstring friction and pressure loss across the bit. The safety margin is obtained by subtracting the simulated pressure loss in the drillstring from the kill sheet estimate. This value reflects the associated downhole overbalance produced by applying a choke pressure equal to shut-in casing pressure subtracted the kill sheet estimate of the chokeline friction (relevant when initiating a kill circulation).

Table 10-2 displays the values obtained from Figure 10-4. It is observed that the safety margin produced by applying the final circulating pressure on the drillstring side increases as a function of pump rate. The field practice rounding rules provides an additional margin towards the formation pressure.

Estimation of chokeline friction

Chokeline friction is often used as a means for initiating a kill circulation. When circulation is initiated, the pump output is gradually brought to kill rate, while the choke valve is slowly opened. At kill rate it is often assumed that the choke pressure corresponding to constant bottomhole pressure, equals shut-in pressure subtracted the chokeline friction (see equation (7.12)). Chokeline friction is then calculated from the measured dynamic pressure losses as described in the equation.

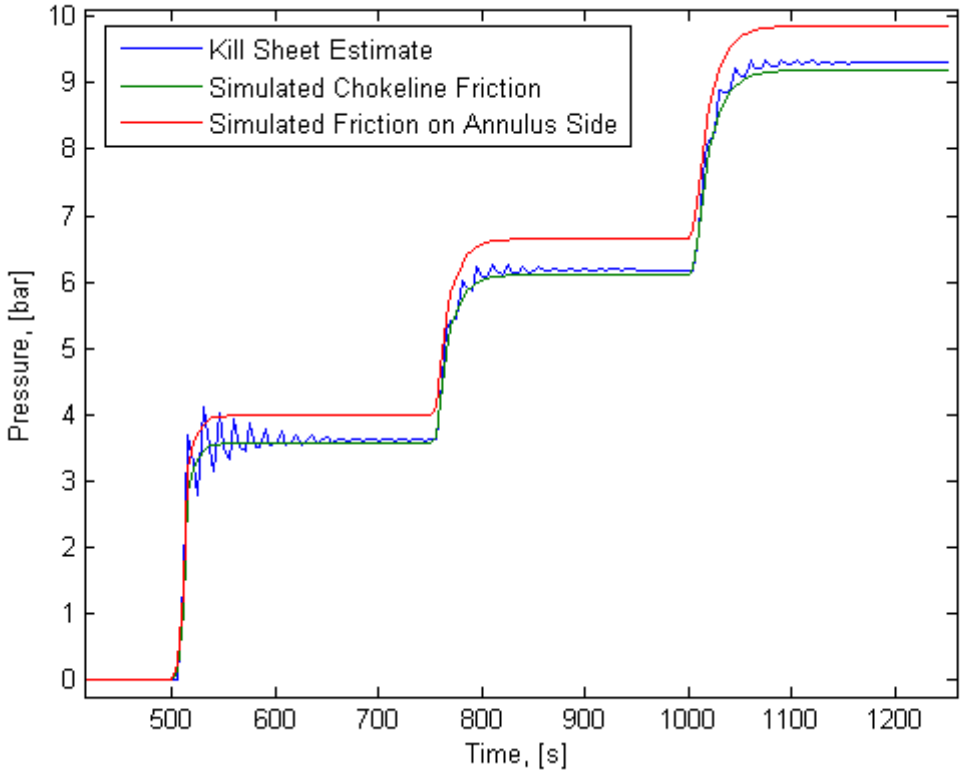

Figure 10-5: Plot obtained from the SCR for the horizontal well. Due to a problem with obtaining consistent pressures, the values have been parallel displaced in such a way that the pressures losses are zero at zero flow rate. The kill sheet estimate refers to a value for chokeline friction obtained by subtracting the simulated dynamic pressure loss through the riser from the simulated dynamic pressure loss through the chokeline. The simulated chokeline friction is the friction component obtained directly from the simulation. Simulated friction on annulus side is obtained by adding the frictional components on the annulus side (simulated annular friction added simulated chokeline friction).

Figure 10-5 is produced with basis in the SCRs conducted in the horizontal well (section 9.2.2). It is evident that the estimated chokeline friction slightly overestimates the simulated chokeline friction. However, what is interesting in context of keeping the well in overbalance, is actually the entire pressure loss on the annulus side. The estimated chokeline friction underestimates the pressure loss on the annulus side. Hence, this yields a positive safety margin bottomhole.

Flow rate, [lpm]	Kill Sheet Estimate, [bar]	Simulated Chokeline Friction, [bar]	Simulated Friction on Annulus Side, [bar]	Safety Margin, [bar]
600	3,6	3,6	4,0	0,4
800	6,2	6,1	6,6	0,4
1000	9,3	9,2	9,9	0,6

Table 10-3: Values obtained from Figure 10-5. The safety margin is obtained by subtracting the simulated friction on annulus side from the kill sheet estimate. This value reflects the associated downhole overbalance produced by applying a choke pressure equal to shut-in casing pressure subtracted the kill sheet estimate of the chokeline friction (relevant in when initiating a kill circulation).

In Table 10-3 the values from the previous figure is posted. It is observed that the safety margin at kill rate is 0,6 bar. The field practice rounding rules will decrease the safety margin. However, the relation for establishing circulation is only used as a guideline. In an actual kill situation, the drillpipe pressure will be utilized for determining the applied choke backpressure.

Estimation of influx size

The measured pit gain at surface is an estimate of the influx size. However, it is not a good estimate, as the formation will keep flowing in some time after the well is shut-in. The influx volume will also change as it propagates towards the surface, and as will the influx density. The only obtainable invariant value reflecting a kick size is its mass.

	Vertical Well		Horizontal Well	
	Kill Sheet	Simulated	Kill Sheet	Simulated
Volume, [l]	4330	4640	3460	3740
Density, [SG]	1,0	0,45	N/A	0,47
Mass, [kg]	4330	2082	N/A	1773

Table 10-4: Influx size as determined directly from shut-in simulations in sections 9.2.1 and 9.2.2, and from the kill sheet calculations in sections 7.3.1 and 7.3.2. The kill sheet volumes which are referred to, is the pit gain measured at shut-in.

In Table 10-4 values reflecting the kick size is posted. The kill sheet values are values calculated in sections 7.3.1 and 7.3.2, for the vertical well and horizontal well respectively. The volume in the kill sheet column is the measured pit gain. The simulated values are obtained directly from the shut-in sequences of sections 9.2.1 and 9.2.2.

An initial observation is that there is no kill sheet values for density or mass obtained for the horizontal well. This is due to zero vertical influx height. Hence, equation (7.19) is meaningless. Another observation is the major discrepancy between calculated values and simulated values for mass and density in the vertical well. The reasons for this are not understood, and should be investigated.

Estimation of formation pressure

In both the vertical and the horizontal well control simulations, the formation pressure was set to 475 bara. However, when calculating the formation pressure from the kick data using equation (7.15), the calculated pressure was an average of 5,5 lower than the actual 475 bara. This is interpreted as an effect of the compressible mud. Since the average density of the drilling fluid in reality is higher than the density at standard conditions, incompressible mud yields a slight underestimation of the formation pressure.

The underestimation of the formation pressure will cause a successive underestimation of the kill mud density. However, this is assumed to again be balanced by the increase in kill mud density due to compressibility.

10.2.2. Worst case scenarios for well design purposes

A gas filled well is commonly defined as a worst case scenario in well design. If the wellbore can withstand the pressures exerted by the gas filled well scenario, it is said to have full well integrity. However, from Figure 9-8 and Figure 9-9 it can be observed that a gas bubble migrating in a shut-in wellbore result in higher downhole pressures than the conventional gas filled well scenario. The maximum recorded pressure at the casing seat for the gas filled well scenario was 467 bara, while the shut-in gas migration caused an estimated casing shoe pressure of 678 bara (only estimation due to shortage of data). This underlines that even though a wellbore is said to have full well integrity, it is still of great importance that the weakpoint of a wellbore is situated in the open hole section.

11. Conclusion

A crude kick simulator has been developed with basis in the drift flux model and the explicit numerical scheme AUSMV. A range of modifications and extensions to the simple numerical scheme has been introduced.

When killing a kicking well, the bottomhole pressure is traditionally kept constant and in slight overbalance compared to the formation pressure. The intention is to avoid further influx of formation fluids. This is achieved by applying a variable choke backpressure. The choke valve is operated by rig personnel. As the AUSMV scheme does not allow for the bottomhole pressure simply to be set to a constant value, the primary accomplishment in the development of the simple kick simulator was the implementation of an automatic PI-regulator. The PI-regulator keeps the bottomhole pressure constant within reasonable limits, as an influx is circulated out from the wellbore. Extensive tuning is required each time the dynamics or the geometry of the well is altered.

The sensitivity of the regulator was tested with respect to variable system dynamics (well depth, influx size and kill rate). It was assumed that the stability and rate of convergence of the regulator would improve as a function of reduced dynamics. However, unexpected instability was experienced at low kill rates. The reasons for this are not understood, and should be further investigated.

A novel approach to the pressure regulation was discovered. The approach takes advantage of the classical equation defining the PI-regulator, and introduces an additional variable which reflects the dynamic state of the wellbore system. The approach has shown admirable results compared to the classical PI-regulator. The reasons for the success are however not fully understood, and should be investigated more extensively.

The additional modifications and extensions with respect to the numerical scheme can be summed up as follows,

- A more realistic friction model.
- Chokeline and riser for simulation on subsea wells.
- Implementation of a possibility for wellbore deviation.
- A more accurate reading of bottomhole and casing pressures.
- A drillstring function, which makes it possible to read drillpipe pressure.
- A pit gain reading.
- A Darcy relation for influx where influx size and mass rate depends on downhole pressure differential. This is important for simulations on drilled kicks or connection kicks.
- Changing the liquid component of the system from water to drilling fluid (altering the liquid density).
- Additionally, a choke model was implemented in the model, but it has not been used in the simulations. The choke model depicts the backpressure as a function of fluid density, flow rate and choke opening.

The developed kick simulator was used for well control simulations in one vertical and one horizontal well. The simulated data was compared with results from corresponding well control formulas. It was found that even though the estimates obtained from the formulas and kill sheets were not always corresponding with the simulated results, the errors produced by the formulas exclusively would function as safety margins with respect to the downhole pressure overbalance. Although the traditional well control formulas rely on a range of simplifying assumptions, they have proved to perform surprisingly well during the conducted well control simulations.

A major discrepancy was found when calculating the influx density and the influx mass from the shut-in pressures and the pit gain for the vertical well. Both of the calculated values were around twice the magnitude of the values obtained directly from the simulation. The cause of this is not known.

Simulations on well control scenarios indicated that the conventional gas filled well scenario induces less pressure at the weakpoint than a gas bubble migrating in a shut-in annulus. It is therefore important to ensure that the weakpoint of a wellbore is located in the open hole section, even if the well is said to have full well integrity.

11.1. Further work

The AUSMV scheme has potential as a kick simulator. If simulations similar to the ones presented in this thesis are to be conducted, it is recommended to model the drillstring in a better manner. By also using the AUSMV scheme within the drillstring, one could obtain more accurate simulation results. Particularly compressibility is important for trustworthy readings of drillpipe pressure. Further, it is suggested to implement an ability to shut-in the well at seabed, and to take returns through the chokeline or riser as desired. This would add flexibility to the simulations and open new possibilities for modeling for instance hard and soft shut-in. Another recommendation is to make better use of the implemented choke model.

Two issues should be resolved. The underestimation of fluid velocities at low flow rates causes inaccuracy, primarily with respect to friction loss. It has been shown that the error is reduced at finer discretization. However, it should be investigated if this malfunction could be resolved completely. The second issue is the PI-regulator. The tuning of the regulator is quite cumbersome and time consuming. A better way to maintain constant bottomhole pressure should be established. If this cannot be achieved, perhaps the biggest potential in the current scheme is as a training simulator, where the bottomhole pressure does not need to be automatically regulated.

References

1. Standard Norway, *NORSOK STANDARD D-010: Well integrity in drilling and well operations*. 2004.
2. American Petroleum, I., *Recommended practice for well control operations: upstream segment*. 2006, Washington, D.C.: API. V, 92 s.
3. Transocean, *Well Control Handbook*. 3rd ed. 2009.
4. Mitchell, R.F., *Drilling engineering*. Petroleum engineering handbook. Vol. Vol. 2. 2006, Richardson, Tex.: Society of Petroleum Engineers. viii, 763 s.
5. Aadnøy, B.S., *Modern well design*. 2010, Boca Raton: CRC Press/Balkema. X, 303 s.
6. Fjelde, K.K., *SVALEX Festningen Pt. 3 (unpublished)*. 2010: Stavanger.
7. American Petroleum, I., *Specification for casing and tubing: API Specification 5CT, Eight ed., July 1, 2005 = ISO 11960:2004, Petroleum and natural gas industries - steel pipes for use as casing and tubing for wells*. 2005, Washington, D.C.: American Petroleum Institute. 291 s.
8. Gabolde, G. and J.-P. Nguyen, *Drilling data handbook*. 2006, Paris: Editions Technip. 1 b. (flere pag.).
9. Garnier, A.J. and N.H.v. Lingen, *Phenomena Affecting Drilling Rates at Depth.* 1959.
10. Jorden, J.R. and O.J. Shirley, *Application of Drilling Performance Data to Overpressure Detection.* SPE Journal of Petroleum Technology, 1966. **18**(11).
11. Standard Norway, *NORSOK STANDARD D-001: Drilling facilities*. 1998.
12. Finnemore, E.J., J.B. Franzini, and R.L. Daugherty, *Fluid mechanics with engineering applications*. 2002, Boston: McGraw-Hill. XXV, 790 s.
13. Watson, D., T. Brittenham, and P.L. Moore, *Advanced well control*. SPE textbook series. Vol. vol. 10. 2003, Richardson, TX: Society of Petroleum Engineers. IX, 386 s.
14. Shi, H., et al., *Drift-Flux Modeling of Multiphase Flow in Wellbores*, in *SPE Annual Technical Conference and Exhibition*. 2003: Denver, Colorado.
15. Liou, M.-S. and C.J. Steffen, *A New Flux Splitting Scheme.* Journal of Computational Physics, 1993. **107**(1): p. 23-39.
16. Wada, Y. and M.-S. Liou, *An Accurate and Robust Flux Splitting Scheme for Shock and Contact Discontinuities.* SIAM J. Sci. Comput., 1997. **18**(3): p. 633-657.
17. Evje, S. and K.K. Fjelde, *Hybrid Flux-Splitting Schemes for a Two-Phase Flow Model.* Journal of Computational Physics, 2002. **175**(2): p. 674-701.

18. Fjelde, K.K., Evje, S., *The AUSMV Scheme - A Simple but Robust Model for Analyzing Two-Phase Flow (unpublished work note)*. 2010, University of Stavanger: Stavanger.
19. LeVeque, R.J., *Finite volume methods for hyperbolic problems*. 2002, Cambridge: Cambridge University Press. XIX, 558 s.
20. Lage, A.C.V.M., *Two-phase flow models and experiments for low-head and underbalanced drilling*. 2000, UiS: [Stavanger]. p. XXIV, 218 s.
21. Haugen, F., *Praktisk reguleringsteknikk*. 2003, Trondheim: Tapir akademisk forl. 278 s.

A. Appendix

A.1. Closed circuit Ziegler-Nichols routine

The routine used for tuning the choke regulators used in this thesis, is based on Ziegler-Nichols routine for closed circuits. As a means for reproducing the results obtained in this thesis, this detailed routine is presented.

	K_p	T_i	T_d
P-regulator	$0,5*K_{pk}$	Infinity	0
PI-regulator	$0,45*K_{pk}$	$T_p/1,2$	0
PID-regulator	$0,6*K_{pk}$	$T_p/2$	$T_p/8$

Table A-1: Table for calculation of tuning parameters.

1. Set T_i to 10 000 000 and T_d to 0, so that the output produced from the integral term and the derivate term of the PID-regulator is zero. Thus, the regulator is reduced to a P-regulator.
2. T_s is set equal to dt, or a positive multiple of dt, depending on the desired frequency of regulation.
3. Set K_i to a low value (0,1 has been used), and run a simulation. The simulation is either run with a rapid increase in pump rate, or with a propagating kick in the wellbore, in order to provoke instability in the system.
4. Increase the value of K_p in steps of 0,1 until sustained oscillations occur.
5. The critical proportional gain K_{pk}, is defined as the lowest value of K_p which produces sustained oscillations. It is read with one decimal. A tuned K_p value is set according to the table. The K_p value is set to three decimals.
6. The critical period T_d, is defined as the period of the oscillations produced by the PID-regulator with proportional gain equal to critical gain. The T_d value is read as an integer (whole seconds). Tuned values for T_d and T_i are set according to the table. The tuned values are rounded to two decimals.
7. In general, the regulator used is a PI-regulator, where T_d is set to zero.
8. If desired, rate of convergence or stability may be improved by scaling the regulator parameters. This is done by multiplying K_p, $1/T_i$ and T_d with a common factor, c. Thus, the proportional term is multiplied with c, and the integral and derivative terms are multiplied with c^2.

A.2. Matlab Code

The complete Matlab code is included in the following sections.

main.m

```
%
%  Transient AUSMV scheme

clear;

% Geometry data/ Must be specified
welldepthmd = 3000;
nobox = 25;
% nobox = 64;
nofluxes = nobox+1;
dx = welldepthmd/nobox;   % Bokslengde
% dt= 0.0125; % Tidsteg må reguleres i forhold til valgt bokslenge og
CFL krav.
dt= 0.025;
dtdx = dt/dx;
time = 0;
endtime = 1200; % Lengde på simulering i sekund
nosteps = (endtime-time)/dt;
timebetweensavingtimedata = 5;
nostepsbeforesavingtimedata = timebetweensavingtimedata/dt;


% Slip parameters of gas/can be adjusted vg = Kxvmix+s for vertical,
% assume no-slip for horizontal. vg=((k-1)cos(ang)+1)xvmix+scos(ang)
k = 1.2;
s = 0.5;
% k=1; %No-slip
% s=0; %No-slip

% Viscosities (Pa*s)
viscl = 0.05;
viscg = 0.000005;

% Density parameters

% liquid density at stc and speed of sound in liquid. Viss vi skal inn
% med en mud i stedet for vann må vi endre her.
  dstc = 1500.0;
  pstc = 100000.0;
  al = 1000;
  t1 = dstc-pstc/(al*al);
% Ideal gas law constant
  rt = 100000;

% Gravity acceleration
  grav = 9.81;

% Kick schedule (on/off)
  kickschedule=0;
```

```
% SCR schedule (on/off)
  SCRschedule=0;

% BOP Well status (open = 1, closed = 0). BOP is situated at surface.
  bop = 0;

% Choke status (open = 1, closed = 0)
  choke = 1;

% High resolution recorder [on/off, start time, stop time]
hrrecord= [0, 0,570];

% Fricion recorder (on/off)
frictionrecord=0;

% Pit gain [on/off, start time]
influxrecord=[0,200];


%Choke regulator (on/off)
regulator=0;


% Geometry of circulation system. Lengths given in number of segments.
The
% change in cross-section occurs at the segment midpoint below.
  waterdepth=4;%-1/2 Length of chokeline and riser
  bhalength=2; %-1/2 Length of BHA
  ohlength=3; %-1/2 Length of open hole
  kop=22; %kick off point below segment #kop
  eob=10; %end of build above segment #eob
  bhinclination=0*pi()/2; %inclination measured in rad in the lower
segments

% Failsafe status (open = 1, closed = 0)
  failsafe = 0; % Velger om sirkulasjon foregår gjennom chokeline(1)
eller riser(0). Kan ikkje opererast etter at simuleringa er
initialisert.

  if failsafe == 0
   for i = nobox-waterdepth+1:nobox % DP x Riser
    do(i) = 0.476; % 18 3/4"
    di(i) = 0.127; % 5"
    areal(i+1) = 3.14/4*(do(i)*do(i)- di(i)*di(i));
    arear(i) = 3.14/4*(do(i)*do(i)- di(i)*di(i));
    area(i) = 3.14/4*(do(i)*do(i)- di(i)*di(i));
   end
  elseif failsafe == 1
   for i = nobox-waterdepth+1:nobox % Chokeline
    do(i) = 0.0762; % 3"
    di(i) = 0.0;
    areal(i+1) = 3.14/4*(do(i)*do(i)- di(i)*di(i));
    arear(i) = 3.14/4*(do(i)*do(i)- di(i)*di(i));
    area(i) = 3.14/4*(do(i)*do(i)- di(i)*di(i));
   end
  end
   for i = max(bhalength,ohlength)+1:nobox-waterdepth % DP x Cased hole
```

```
    do(i) = 0.32; % 13 3/8" OD - 2*wall thickness
    di(i) = 0.127; % 5"
    areal(i+1) = 3.14/4*(do(i)*do(i)- di(i)*di(i));
    arear(i) = 3.14/4*(do(i)*do(i)- di(i)*di(i));
    area(i) = 3.14/4*(do(i)*do(i)- di(i)*di(i));
   end
   for i=bhalength+1:ohlength % DP x Open hole
    do(i) = 0.311; % 12 1/4"
    di(i) = 0.127; % 5"
    areal(i+1) = 3.14/4*(do(i)*do(i)- di(i)*di(i));
    arear(i) = 3.14/4*(do(i)*do(i)- di(i)*di(i));
    area(i) = 3.14/4*(do(i)*do(i)- di(i)*di(i));
   end
   for i=ohlength+1:bhalength % BHA x Cased hole
    do(i) = 0.32; % 13 3/8" OD - 2*wall thickness
    di(i)=0.2159; % 8 1/2"
    areal(i+1) = 3.14/4*(do(1)*do(1)- di(1)*di(1));
    arear(i) = 3.14/4*(do(1)*do(1)- di(1)*di(1));
    area(i) = 3.14/4*(do(i)*do(i)- di(i)*di(i));
   end
   for i=1:min(bhalength,ohlength) % BHA x Open hole
    do(i)=0.311; % 12 1/4"
    di(i)=0.2159; % 8 1/2"
    areal(i+1) = 3.14/4*(do(1)*do(1)- di(1)*di(1));
    arear(i) = 3.14/4*(do(1)*do(1)- di(1)*di(1));
    area(i) = 3.14/4*(do(i)*do(i)- di(i)*di(i));
   end
   areal(1)=arear(1);
   areal (nobox+1)=[];
   welldepthtvd=0;
%   load hzpf475t570shutindata.mat;

do(1:nobox)=0.1;
di(1:nobox)=0;
areal(1:nobox)=pi()/4*do.*do;
arear(1:nobox)=areal(1:nobox);
area(1:nobox)=areal(1:nobox);

    for i = 1:nobox
        if i<=eob
            ang(i)=bhinclination;
        elseif i>eob && i<kop
            ang(i)=bhinclination*(1-(i-eob)/(kop-eob));
        else
            ang(i)=0;
        end
        welldepthtvd=welldepthtvd+dx*cos(ang(i));
        dl(i) = dstc;
        dlo(i)= dl(i);
        dg(i)= 1.0;
        dgo(i)=dg(i);
        vl(i) = 0.0;
        vlo(i)= 0.0;
        vg(i)= 0.0;
        vgo(i)= 0.0;
        p(i) = 100000.0;
        po(i) = p(i);
        eg(i)= 1.0;
```

```
        ego(i)=eg(i);
        ev(i)=1-eg(i);
        evo(i)=ev(i);

        vg(i)=0.0;
        vgo(i)=0.0;
        vl(i)=0.0;
        vlo(i)=0.0;

        vgr(i)=0.0;
        vgor(i)= 0.0;
        vgl(i)= 0.0;
        vgol(i)= 0.0;

        vlr(i)=0.0;
        vlor(i)=0.0;
        vll(i)=0.0;
        vlol(i)=0.0;

       qv(i,1)=dl(i)*ev(i)*(areal(i)+arear(i))*0.5;
       qvo(i,1)=qv(i,1);

       qv(i,2)=dg(i)*eg(i)*(areal(i)+arear(i))*0.5;
       qvo(i,2)=qv(i,2);

       qv(i,3)=(qv(i,1)*vl(i)+qv(i,2)*vg(i))*(areal(i)+arear(i))*0.5;
       qvo(i,3)=qv(i,3);

    end

% Intialize fluxes

for i = 1:nofluxes
  for j =1:3
   flc(i,j)=0.0;
   fgc(i,j)=0.0;
   fp(i,j)= 0.0;
  end
end



%  Main program. Here we will progress in time. First som
intializations
hrcounter=1; % Refererer til high resolution pressure recorder.
chokecounter=0; % Refererer til choke regulator;
int=0; % Refererer til choke regulator.
deriv=0; % Refererer til choke regulator.
eo=0; % Refererer til choke regulator.
countsteps = 0;
counter=0;
printcounter = 1;
pressureoutlet=pstc;
inletliqmassrate=0;
inletgasmassrate=0;
pdp(printcounter)=pstc;
pbot(printcounter) = pstc;
pchoke(printcounter)= p(nobox)+(p(nobox)-p(nobox-1))/2;
```

```
if
ohlength>0&&ohlength<nobox,pshoe(printcounter)=(p(ohlength)+p(ohlength+
1))/2;end % Linear interpolation.
if waterdepth>0,pseabed(printcounter) = (p(nobox-waterdepth)+p(nobox-
waterdepth+1))/2;end % Linear interpolation.
liquidmassrateout(printcounter) = 0;
gasmassrateout(printcounter)=0;
timeplot(printcounter)=time;
if influxrecord(1)==1,
pitgain(printcounter)=0;influxvolume(printcounter)=0;influxmass(printco
unter)=0;end
if frictionrecord==1
dpds(printcounter)=0;
dpann(printcounter)=0;
dpriser(printcounter)=0;
dpcl(printcounter)=0;
dpbit(printcounter)=0;
end



for i = 1:nosteps
   countsteps=countsteps+1;
   counter=counter+1;
   time = time+dt;
if time<250, pressureoutlet=1e5;
elseif time<=251, pressureoutlet=(1+10(time-250))e5;
elseif time>251, pressureoutlet=11e5; end
% First of all a dirty trick is used in order to make the well
vertical.
% The pipe was initialised for a horisontal case. However, for a
vertical
% case we would need a steady state solver. Since the programmer in
this
% case is quite lazy, he rather chose to adjust the gravity constant g
from
% zero to 9.81 m/s2 during 100 seconds (corresponds to hoisting the
well
% from a horisontal postion to vertical case.

       if (time <= 100)
         g = grav*time/100;
       else
         g = grav;
       end

% Horisontal case.
        g = 0.0;

% Then a section where we check the boundary conditions.
% Operational changes must be changed here since it is here we
"control"
% the changes (e.g inflow rates, BOP status etc).

% First specify the outlet pressure (either open to atmosphere or a
choke
% pressure. Initially we are circ to shaker which have atmospheric
% pressure.
```

```
% % Implementation of choke model.
% if time<150
%     pressureoutlet=pstc;
% else
%
qmix=(vlo(nobox)*evo(nobox)+vgo(nobox)*ego(nobox))*(areal(nobox)+arear(
nobox))/2;
%     cchoke=1.91;
%     chokevalve=0.8;
%     deltaP= (densmix*qmix^2/(cchoke*chokevalve)^2;
%     pressureoutlet=pstc+ deltaP;
% end


% Then specify the inlet rates. Interpolates so that we have smooth
rate
% changes. The rates is in kg/s. The outlet pressure is in Pascal.
% Assume dowhole reservoir pressure equal to 400 bars which gives a gas
% density downhole of approx 400 kg/m3 (ideal gas law).
% Pumprate. Given in lpm. Converted to downhole rate in kg/s by
% using mud density is constant.

% Kick schedule
if kickschedule==1
    formationpressure=475*1e5;
   killrate = 1000;  %lpm
   mudratekilling = killrate/(60*1000)*dstc;
   kicksize = 4 ; % Volume of kick in m3 at downhole cond (same as pit
gain)
   kickmass = kicksize*400; % Convert this volume to mass (kg)at
downhole cond
   kickinflowtime = 60; %+10 s ramp up && 10 s ramp down. how fast the
kick enters in seconds
%    kickmassrate = kickmass/(kickinflowtime+10); % Gas rate into well
in kg/s
   kickmassrate=10;
   kickstart=200;
   BOPstart=325;
   BOPstengetid=45;
   killstart=580+110;

% Please note that if you change the influx time, you also have to
adjust
% the timeintervall for taking the kick accordingly so you get the
correct
% kick size. (Note that the integrated area of outlet gasrate in kg/s
should
% be the same as the integrated inlet rate (principle of mass
conservation)
% Please also note that we let the pump rate be zero while taking the
kick, i.e.
% we could look upon this as a swabbed kick.

% Please also note how we use linear interpolation when changing
% flowvariables (ramp the upp gradully, if you turn them on
immediately,
```

```
% you create a pressure pulse that can cause major problems (water
hammering
% effect)
if time>15000,bop=0;end

   if (time < kickstart)
 % Well is hoisted
     inletliqmassrate = 0;
     inletgasmassrate = 0;

    % Drilled kick
   elseif ((time>kickstart) && (time<=kickstart+10))
  %  Kick is started to be taken
     inletliqmassrate = 0;
     inletgasmassrate = min(kickmassrate*(time-
kickstart)/10,kickmassrate*(bhp^2-formationpressure^2)/(staticbhp^2-
formationpressure^2));
   elseif (time>kickstart+10)%&&(time<=kickstart+kickinflowtime+10)
  % The kick is taken
     inletliqmassrate = 0;
     inletgasmassrate = kickmassrate*(bhp^2-
formationpressure^2)/(staticbhp^2-formationpressure^2);
   elseif (time>=BOPstart+BOPstengetid)&& (time<=killstart)
  % BOP, closed, bop = 0.
      inletgasmassrate = max(0,kickmassrate*(bhp-
formationpressure)/(staticbhp-formationpressure));
      bop = 0;
      psavecsg = p(nobox)+(p(nobox)-p(nobox-1))/2; % Tar vare på
innestengningstrykket SICP
      psavebhp = bhp;
   elseif (time> killstart)&& (time<=killstart+10)
  % Choke åpnes, pumperates rampes opp
     inletliqmassrate = mudratekilling*(time-killstart)/10;
%      inletgasmassrate = max(0,kickmassrate*(bhp-
formationpressure)/(staticbhp-formationpressure));
     inletgasmassrate = 0;
     choke = 1.0;
     pressureoutlet = psavecsg; % Choketrykk settes lik SICP
   elseif (time>killstart+10)
  % Sirkulerer kicket ut. Må endre choketrykk (variablene
pressureoutlet nedenfor)
     inletliqmassrate = mudratekilling;
%      inletgasmassrate = max(0,kickmassrate*(bhp-
formationpressure)/(staticbhp-formationpressure));
     inletgasmassrate = 0;

    % Swabbed kick.
%    elseif ((time>kickstart) && (time<=kickstart+10))
%   %  Kick is started to be taken
%      inletliqmassrate = 0;
%      inletgasmassrate = kickmassrate*(time-kickstart)/10;
%    elseif ((time>kickstart+10)&&(time<=kickstart+kickinflowtime+10))
%   % The kick is taken
%      inletliqmassrate = 0;
%      inletgasmassrate = kickmassrate;
%    elseif
((time>kickstart+kickinflowtime+10)&&(time<=kickstart+kickinflowtime+20
))
```

```
%   % The kick is seasing to be taken
%      inletliqmassrate = 0;
%      inletgasmassrate = kickmassrate-kickmassrate*(time-210-
kickinflowtime)/10.0;
%    elseif ((time > BOPstart)&&(time<=BOPstart+BOPstengetid))
%   % Well open, wait upon closing BOP!
%      inletliqmassrate = 0;
%      inletgasmassrate = 0;
%    elseif (time>=BOPstart+BOPstengetid)%&& (time<=killstart)
%   % BOP, closed, bop = 0.
%      inletliqmassrate = 0;
%      inletgasmassrate = 0;
%      bop = 0;
%      psavecsg = p(nobox); % Tar vare på innestengningstrykket SICP
%      psavebhp = bhp; % Tar vare på BHP ved shut-in


   end
end

%   SCR schedule
if SCRschedule==1
if time<500
    inletliqmassrate=0;
    inletgasmassrate=0;
    pressureoutlet=pstc;
    v0=vl;
elseif time<510
    inletliqmassrate=((time-500)/10*600)*dstc/60000;
    inletgasmassrate=0;
    pressureoutlet=pstc;
elseif time<750
    inletliqmassrate=600*dstc/60000;
    inletgasmassrate=0;
    pressureoutlet=pstc;
    v600=vl;
elseif time<760
    inletliqmassrate=(600+(time-750)/10*200)*dstc/60000;
    inletgasmassrate=0;
    pressureoutlet=pstc;
elseif time<1000
    inletliqmassrate=800*dstc/60000;
    inletgasmassrate=0;
    pressureoutlet=pstc;
    v800=vl;
elseif time<1010
    inletliqmassrate=(800+(time-1000)/10*200)*dstc/60000;
    inletgasmassrate=0;
    pressureoutlet=pstc;
else
    inletliqmassrate=1000*dstc/60000;
    inletgasmassrate=0;
    pressureoutlet=pstc;
    v1000=vl;
end
end
```

```
  % Choke regulator. Basert på PID. Styrer BHP ved å endre choketrykk,
ie
  % pressureoutlet.
   if (time>510)&&regulator==1&&choke==1
%      setp=psavebhp; % Det ønskede bunnhullstrykket.
%      setp=480*1e5; % Det ønskede bunnhullstrykket.
     setp=93*1e5; %ICP=81 bar
     kp=33.75e-4; % Propersjonalforsterkning. Bestemmes ved Ziegler-
Nichols.
     ti=47.5; % Integraltid. Bestemmes ved Ziegler-Nichols.
     td=0 ; % Derivattid. Bestemmes ved Ziegler-Nichols.
     coeff=0.6; % For skalering av regulatorparametrar.
     sampletime = dt; % Sekund mellom trykksample. Heiltal multiplisert
med dt.

     if chokecounter==0
%          e = setp-bhp;
         e = setp-dpp;
         pressureoutlet=psavecsg;
         eo=e;
         eoo=e;
     elseif chokecounter>=sampletime/dt
%          e = setp-bhp;
         e = setp-dpp;
         int=int+(e*sampletime);
         deriv=(e-eo)/sampletime;

%          pressureoutlet =
psavecsg+coeff*kp*e+coeff^2*kp/ti*int+coeff^2*kp*td*deriv; % 0)
%          pressureoutlet = pressureoutlet+coeff*kp*(e-
eo)+coeff^2*kp*sampletime/ti*e+coeff^2*kp*td/sampletime*(e-2*eo+eoo)+;
% 1)
         pressureoutlet =
pressureoutlet+coeff.*kp*e+coeff.*coeff.*kp/ti*int+coeff.*coeff.*kp*td*
deriv; % New Approach)
         eoo=eo;
         eo=e;
         chokecounter=0;
     end
          if pressureoutlet<pstc
              pressureoutlet=pstc; % Ambient pressure.
          elseif pressureoutlet>103600000
              pressureoutlet=103600000; % Choke valve pressure rating.
          end

     chokecounter=chokecounter+1;
   end

%    if (time<=10)
%      inletliqmassrate = mudratekilling*time/10;
%      inletgasmassrate = 0;
%    elseif ((time>10)&&(time<=500))
%        inletliqmassrate=mudratekilling;
%        inletgamassrate=0;
%    elseif ((time>500)&&(time<=510))
%        inletliqmassrate=mudratekilling-mudratekilling*(time-500)/10;
%        inletgasmassrate=0;
%     else
```

```
%        inletliqmassrate=0;
%        inletgasmassrate=0;
%    end


% Based on these boundary values combined with use of extrapolations
techniques
% for the remaining unknowns at the boundaries, we will define the mass
and
% momentum fluxes at the boundaries (inlet and outlet of pipe). Disse
treng
% ikke endres

% inlet fluxes first.

     flc(1,1)= inletliqmassrate/areal(1);
     flc(1,2)= 0.0;
     flc(1,3)= flc(1,1)*vlo(1);

     fgc(1,1)= 0.0;
     fgc(1,2)= inletgasmassrate/areal(1);
     fgc(1,3)= fgc(1,2)*vgo(1);

     fp(1,1)= 0.0;
     fp(1,2)= 0.0;
     fp(1,3)= po(1)+0.5*(po(1)-po(2));


%     end

% Outlet fluxes (open && closed conditions)

    if (bop>0.01)
% randkrav når brønnen er åpen initielt
        flc(nofluxes,1)= dlo(nobox)*evo(nobox)*vlo(nobox);
        flc(nofluxes,2)= 0.0;
        flc(nofluxes,3)= flc(nofluxes,1)*vlo(nobox);

        fgc(nofluxes,1)= 0.0;
        fgc(nofluxes,2)= dgo(nobox)*ego(nobox)*vgo(nobox);
        fgc(nofluxes,3)= fgc(nofluxes,2)*vgo(nobox);

        fp(nofluxes,1)= 0.0;
        fp(nofluxes,2)= 0.0;
        fp(nofluxes,3)= pstc; % Atmospheric pressure.
    else
% randkrav som slår inn når brønnen er stengt eller etter
% at den blir åpnet igjen.

        if (choke == 0.0)
         flc(nofluxes,1)= 0.0;
         flc(nofluxes,2)= 0.0;
         flc(nofluxes,3)= 0.0;

         fgc(nofluxes,1)= 0.0;
         fgc(nofluxes,2)= 0.0;
         fgc(nofluxes,3)= 0.0;
```

```
         fp(nofluxes,1)=0.0;
         fp(nofluxes,2)=0.0;
         fp(nofluxes,3)= po(nobox)-0.5*(po(nobox-1)-po(nobox));

        else

         flc(nofluxes,1)= dlo(nobox)*evo(nobox)*vlo(nobox);
         flc(nofluxes,2)= 0.0;
         flc(nofluxes,3)= flc(nofluxes,1)*vlo(nobox);

         fgc(nofluxes,1)= 0.0;
         fgc(nofluxes,2)= dgo(nobox)*ego(nobox)*vgo(nobox);
         fgc(nofluxes,3)= fgc(nofluxes,2)*vgo(nobox);

         fp(nofluxes,1)= 0.0;
         fp(nofluxes,2)= 0.0;
         fp(nofluxes,3)= pressureoutlet;  % Her hentes choketrykket
spes lengre oppe


        end

    end

% Now we will find the fluxes between the different cells. Treng ikke
% endres

     for j = 2:nofluxes-1
      cl = csound(ego(j-1),po(j-1),dlo(j-1),k);
      cr = csound(ego(j),po(j),dlo(j),k);
      c = max(cl,cr);
      pll = psip(vlor(j-1),c,evo(j));
      plr = psim(vlol(j),c,evo(j-1));
      pgl = psip(vgor(j-1),c,ego(j));
      pgr = psim(vgol(j),c,ego(j-1));
      vmixr = vlol(j)*evo(j)+vgol(j)*ego(j);
      vmixl = vlor(j-1)*evo(j-1)+vgor(j-1)*ego(j-1);

      pl = pp(vmixl,c);
      pr = pm(vmixr,c);
      mll= evo(j-1)*dlo(j-1);
      mlr= evo(j)*dlo(j);
      mgl= ego(j-1)*dgo(j-1);
      mgr= ego(j)*dgo(j);

      flc(j,1)= mll*pll+mlr*plr;
      flc(j,2)= 0.0;
      flc(j,3)= mll*pll*vlor(j-1)+mlr*plr*vlol(j);

      fgc(j,1)=0.0;
      fgc(j,2)= mgl*pgl+mgr*pgr;
      fgc(j,3)= mgl*pgl*vgor(j-1)+mgr*pgr*vgol(j);

      fp(j,1)= 0.0;
      fp(j,2)= 0.0;
      fp(j,3)= pl*po(j-1)+pr*po(j);
     end
```

```
% Fluxes have now been calculated. we will Now update the conservative
% variables in each of the numerical cells. First liquid mass, then gas
% mass and finally momemtum equation. Her kan det kun være aktuelt
% å forandre friksjonsmodellen!

     for j=1:nobox
      vmixfric = vlo(j)*evo(j)+vgo(j)*ego(j);
      viscmix =  viscl*evo(j)+viscg*ego(j);
      densmix = dlo(j)*evo(j)+dgo(j)*ego(j);
      a2 = arear(j);
      a1 = areal(j);
      avg = (a2+a1)*0.5;

% De to første ligningene er bevaring av masse for de to fasene.
      qv(j,1)=qvo(j,1)-dtdx*((a2*flc(j+1,1)-a1*flc(j,1))...
                            +(a2*fgc(j+1,1)-a1*fgc(j,1))...
                            +(avg*fp(j+1,1)-avg*fp(j,1)));

      qv(j,2)=qvo(j,2)-dtdx*((a2*flc(j+1,2)-a1*flc(j,2))...
                            +(a2*fgc(j+1,2)-a1*fgc(j,2))...
                            +(avg*fp(j+1,2)-avg*fp(j,2)));

     qv(j,3)=qvo(j,3)-dtdx*((a2*flc(j+1,3)-a1*flc(j,3))...
                            +(a2*fgc(j+1,3)-a1*fgc(j,3))...
                            +(avg*fp(j+1,3)-avg*fp(j,3)))...
                     -
dt*avg*(dpfric(vlo(j),vgo(j),evo(j),ego(j),dlo(j),dgo(j),po(j),do(j),di
(j),viscl,viscg,dstc)+g*densmix*cos(ang(j)));

%       qv(j,3)=qvo(j,3)-dtdx*((a2*flc(j+1,3)-a1*flc(j,3))...
%                              +(a2*fgc(j+1,3)-a1*fgc(j,3))...
%                              +(avg*fp(j+1,3)-avg*fp(j,3)))...
%                      -dt*avg*(32*vmixfric*viscmix/((do(j)-
di(j))*(do(j)-di(j)))+g*densmix);
% Merk den siste lign er moment der friksjon, hydrostatisk grad inngår.
Her ganget
% jeg friksjonen med 10 for å drepe pulsene. Vi kan prøve å få inn en
mer
% realistisk friksjonsmodell. Se nyttpaper!
     end

% Section where we find the physical variables (pressures, densities
etc)
% from the conservative variables. Some tricks to ensure stability.
Treng
% ikke endres. (sjekk viss vi endrer fra vann til mud)


     for j=1:nobox

      qv(j,1)= qv(j,1)/(areal(j)+arear(j))*2.0;
      qv(j,2)= qv(j,2)/(areal(j)+arear(j))*2.0;

      if (qv(j,1)<0.00000001)
        qv(j,1)=0.0;
      end
```

```
      if (qv(j,2)< 0.00000001)
        qv(j,2)=0.0000001;
      end


      a = 1/(al*al);
      b = t1-qv(j,1)-rt*qv(j,2)/(al*al);
      c = -1.0*t1*rt*qv(j,2);

      p(j)=(-b+sqrt(b*b-4*a*c))/(2*a);
      dl(j)= dstc + (p(j)-pstc)/(al*al);
      dg(j) = p(j)/rt;
      eg(j)= qv(j,2)/dg(j);
      ev(j)=1-eg(j);

      qv(j,1)=qv(j,1)*(areal(j)+arear(j))/2.0;
      qv(j,2)=qv(j,2)*(areal(j)+arear(j))/2.0;


      bhp=p(1)+(p(1)-p(2))/2; % True Bottomhole Pressure. Obtained by
linear extrapolation.

% Drillpipe pressure function. A trick is used in order to get the
% hydrostatic pressure on the drillstring side equal to the hydrostatic
pressure in the annulus.
% The frictional pressure loss is modelled regarding the drillstring as
one single segment.
if time<100
    dpp=pressureoutlet;
    dsfriction=0;
    bitloss=0;
    staticbhp= 44839864; %3000m/1,5sg BHP after initial oscillations
are damped. Has to be changed if density is changed. Corresponds with
the sum of the pressure exerted by a static column of 1.5 sg (at sc) of
compressible mud and the atmospheric pressure.
%     staticbhp= 2.9966*1e7; %3000m/1,0sg
    hydrostatic=staticbhp-pstc;
    meandens=hydrostatic/(grav*welldepthtvd);
else

dsfriction=dpfric(inletliqmassrate/(meandens*0.008),0,1,0,meandens,0,(d
pp+bhp)/2,0.1,0,viscl,0,dstc)*welldepthmd;
    bitloss=1/(2*meandens-dstc)*(inletliqmassrate/(5.82e-4*0.95))^2;
    dpp=bhp-hydrostatic+dsfriction+bitloss;
end


% Part where we interpolate in the slip parameters to avoid
% singularities. In the transition to one-phase gas flow, we need to
% have a smooth transition to no-slip conditions.

      xint = (eg(j)-0.75)/0.25;
      k0 = k;
      s0 = s;
      if ((eg(j)>=0.75) && (eg(j)<=1.0))
        k0 =1.0*xint+k*(1-xint);
        s0 = 0.0*xint+s*(1-xint);
      end
```

```
      if (eg(j)>=0.999999)
        k1 = 1.0;
        s1 = 0.0;
      else
        k1 = (1-k0*eg(j))/(1-eg(j));
        s1 = -1.0*s0*eg(j)/(1-eg(j));
      end
%      help1 = dl(j)*ev(j)*k1+dg(j)*eg(j)*k0;
%      help2 = dl(j)*ev(j)*s1+dg(j)*eg(j)*s0;

%      vmixhelp = (qv(j,3)-help2)/help1;
%      vg(j)=k0*vmixhelp+s0;
%      vl(j)=k1*vmixhelp+s1;
      help1 = qv(j,3)/(dl(j)*ev(j)+dg(j)*eg(j));

      vll(j)= help1/areal(j);
      vlr(j)= help1/arear(j);
      vgl(j)= vll(j);
      vgr(j)= vlr(j);


%     Test slip parameters && areachange!

      help1 = dl(j)*ev(j)*k1+dg(j)*eg(j)*k0;
      help2 = dl(j)*ev(j)*s1+dg(j)*eg(j)*s0;

      vmixhelpl = (qv(j,3)/areal(j)-help2)/help1;
      vgl(j)=((k0-1)*cos(ang(j))+1)*vmixhelpl+s0*cos(ang(j));
      vll(j)=((k1-1)*cos(ang(j))+1)*vmixhelpl+s1*cos(ang(j));

      vmixhelpr = (qv(j,3)/arear(j)-help2)/help1;
      vgr(j)=((k0-1)*cos(ang(j))+1)*vmixhelpr+s0*cos(ang(j));
      vlr(j)=((k1-1)*cos(ang(j))+1)*vmixhelpr+s1*cos(ang(j));

%   Averaging velocities.

      vl(j)= 0.5*(vll(j)+vlr(j));
      vg(j)= 0.5*(vgl(j)+vgr(j));

    end



% Old values are now set equal to new values in order to prepare
% computation of next time level. Treng ikke endres
    for j = 1:nobox
     po(j)=p(j);
     dlo(j)=dl(j);
     dgo(j)=dg(j);
     vlo(j)=vl(j);
     vgo(j)=vg(j);
     ego(j)=eg(j);
     evo(j)=ev(j);

     vlor(j)=vlr(j);
     vlol(j)=vll(j);
     vgor(j)=vgr(j);
```

```
     vgol(j)=vgl(j);

      for m =1:3
       qvo(j,m)=qv(j,m);
      end
    end


% Section where we save some timedependent variables in arrays.
% e.g. the bottomhole pressure. They will be saved for certain
% timeintervalls defined in the start of the program in order to ensure
% that the arrays do not get to long! Pass på at casingskotrykk hentes
fra
% rett boks.


%   High resolution pressure recorder. Records the pressure in every
%   segment at every timestep.
%   Results my be presented as a surface plot by: 'mesh
(xaxis,yaxis,prec);',
%   where xaxis is the time axis, yaxis is the segment # and prec is
the
%   recorded pressure.
    if hrrecord (1)==1 &&(time>=hrrecord(2)) && (time<=hrrecord(3))
        for i=1:nobox
        prec(i,hrcounter)=p(i)./pstc;
        egrec(i,hrcounter)=eg(i);
        end
        dpprec(hrcounter)=dpp;
        bhprec(hrcounter)=bhp;
        xaxis(hrcounter)=time;
        yaxis=(1:1:nobox);
        hrcounter =hrcounter+1;
    end

  if rem(time,100)<dt
      egplot(round(time/100),:)=eg;
  end


  if (counter>=nostepsbeforesavingtimedata)
    printcounter=printcounter+1;
    time
    pdp(printcounter) = dpp;
    pbot(printcounter)= bhp;
    pchoke(printcounter)=p(nobox)+(p(nobox)-p(nobox-1))/2;
    if
ohlength>0&&ohlength<nobox,pshoe(printcounter)=(p(ohlength)+p(ohlength+
1))/2;end % Linear interpolation.
    if waterdepth>0,pseabed(printcounter) = (p(nobox-
waterdepth)+p(nobox-waterdepth+1))/2;end % Linear interpolation.

liquidmassrateout(printcounter)=dl(nobox)*ev(nobox)*vl(nobox)*arear(nob
ox);

gasmassrateout(printcounter)=dg(nobox)*eg(nobox)*vg(nobox)*arear(nobox)
;
    timeplot(printcounter)=time;
```

```
    counter = 0;
    if
time>=influxrecord(2)&&influxrecord(1)==1&&((bop==1&&choke==0)||(bop==0
&&choke==1)||(bop==1&&choke==1))
        pitgain(printcounter)=pitgain(printcounter-
1)+(liquidmassrateout(printcounter)-
inletliqmassrate)*timebetweensavingtimedata/dstc;
        influxvolume(printcounter)=sum(eg.*(areal+area)/2)*dx;
        influxmass(printcounter)=influxmass(printcounter-
1)+inletgasmassrate*timebetweensavingtimedata;
    elseif influxrecord(1)==1
        pitgain(printcounter)=pitgain(printcounter-1)+(0-
inletliqmassrate/dstc)*timebetweensavingtimedata;
        influxvolume(printcounter)=sum(eg.*(areal+area)/2)*dx;
        influxmass(printcounter)=influxmass(printcounter-
1)+inletgasmassrate*timebetweensavingtimedata;
    end

    if frictionrecord==1
    dpds(printcounter)=dsfriction;
    dpbit(printcounter)=bitloss;

    dpann(printcounter)=0;
    dpriser(printcounter)=0;
    dpcl(printcounter)=0;
    for j=1:nobox-waterdepth

dpann(printcounter)=dpann(printcounter)+dpfric(vlo(j),vgo(j),evo(j),ego
(j),dlo(j),dgo(j),po(j),do(j),di(j),viscl,viscg,dstc)*dx;
    end
    for j=nobox-waterdepth+1:nobox
         if failsafe==1

dpcl(printcounter)=dpcl(printcounter)+dpfric(vlo(j),vgo(j),evo(j),ego(j
),dlo(j),dgo(j),po(j),do(j),di(j),viscl,viscg,dstc)*dx;
         elseif failsafe==0

dpriser(printcounter)=dpriser(printcounter)+dpfric(vlo(j),vgo(j),evo(j)
,ego(j),dlo(j),dgo(j),po(j),do(j),di(j),viscl,viscg,dstc)*dx;
         end
    end
    end
  end
  end

% end of stepping forward in time.

% Printing of results section


countsteps

plot(timeplot,pbot/1e5);
```

dpfric.m

```
function friclossgrad =
dpfric(vlo,vgo,evo,ego,dlo,dgo,pressure,do,di,viscl,viscg,dstc)

%friclossgrad =
%dpfric(vlo,vgo,evo,ego,dlo,dgo,pressure,do,di,viscl,viscg,dstc)
% Works for two phase flow. The one phase flow model is used but
mixture
 % values are introduced.

 rhol = rholiq(pressure,dstc);
 rhog = rogas(pressure);
 vmixfric = vlo*evo+vgo*ego;
 viscmix =  viscl*evo+viscg*ego;
 densmix = dlo*evo+dgo*ego;

 % Calculate mix reynolds number
 Re = ((densmix*abs(vmixfric)*(do-di))/viscmix);

 % Calculate friction factor. For Re > 3000, the flow is turbulent.
 % For Re < 2000, the flow is laminar. Interpolate in between.

 if (Re<0.001)
   f=0.0;
 else
  if (Re >= 3000)
   f = 0.052*Re^(-0.19);
  elseif ( (Re<3000) & (Re > 2000))
   f1 = 24/Re;
   f2 = 0.052*Re^(-0.19);
   xint = (Re-2000)/1000.0;
   f = (1.0-xint)*f1+xint*f2;
  else
   f = 24/Re;
  end
 end

  friclossgrad = ((2*f*densmix*vmixfric*abs(vmixfric))/(do-di));

end
```

csound.m

```
function mixsoundvelocity = csound(gvo,po,dlo,k)
% Note that at this time k is set to 1.0 (should maybe be
% included below

temp= gvo*dlo*(1.0-gvo);
a=1;
if (temp < 0.01)
  temp = 0.01;
end

cexpr = sqrt(po/temp);

if (gvo <= 0.5)
 mixsoundvelocity = min(cexpr,1000);
else
 mixsoundvelocity = min(cexpr,316);
end
```

rogas.m

```
function rhog = rogas(pressure)

%Simple gas density model. Temperature is neglected.
% rhogas = pressure / (velocity of sound in the gas phase)^2 = pressure
/
% rT -->

  rhog = pressure/100000.0;
```

rholiq.m

```
function [rhol] = rholiq(pressure,dstc)
%Simple model for liquid density
p0 = 100000.0; % Assumed

rhol = dstc + (pressure-p0)/(1000.0*1000.0);
end
```

psip.m

```
function pmvalue = psip(v,c,alpha)


  if (abs(v)<=c)
    pmvalue = alpha*(v+c)*(v+c)/(4*c)+(1-alpha)*(v+abs(v))/2;
  else
    pmvalue = 0.5*(v+abs(v));
  end
end
```

psim.m

```
function pmvalue = psim(v,c,alpha)


  if (abs(v)<=c)
    pmvalue = -1.0*alpha*(v-c)*(v-c)/(4*c)+(1-alpha)*(v-abs(v))/2;
  else
    pmvalue = 0.5*(v-abs(v));
  end
end
```

pp.m

```
function pmvalue = pp(v,c)

  if (abs(v)<=c)
    pmvalue = (v+c)*(v+c)/(4*c)*(2.0-v/c)/c;
  else
    pmvalue = 0.5*(v+abs(v))/v;
  end
end
```

pm.m

```
function pmvalue = pm(v,c)


  if (abs(v)<=c)
    pmvalue = -1.0*(v-c)*(v-c)/(4*c)*(-2.0-v/c)/c;
  else
    pmvalue = 0.5*(v-abs(v))/v;
  end
end
```